SLAMMING OF A SHIP'S STRUCTURAL MODEL BACKED WITH DAMPING MATERIAL

by
LT. JOHN T. GARDNER, JR., USN
LT. CLYDE C. MORRIS, USN

May 1965

Thesis Supervisor: J. HARVEY EVANS

SLAMMING OF A SHIP'S STRUCTURAL MODEL BACKED WITH DAMPING MATERIAL

by

JOHN T. GARDNER, JR., LIEUTENANT, UNITED STATES NAVY
// B.S., U. S. NAVAL ACADEMY
(1958)

CLYDE C. MORRIS, LIEUTENANT, UNITED STATES NAVY
B.S., U. S. NAVAL ACADEMY
(1958)

SUBMITTED IN PARTIAL FULFILLMENT OF THE REQUIREMENTS

FOR THE DEGREE OF NAVAL ENGINEER

AND THE DEGREE OF

MASTER OF SCIENCE IN NAVAL ARCHITECTURE

AND MARINE ENGINEERING

at the

MASSACHUSETTS INSTITUTE OF TECHNOLOGY

May 1965

SLAMMING OF A SHIP'S STRUCTURAL MODEL BACKED WITH DAMPING MATERIAL

by

JOHN T. GARDNER, JR., LIEUTENANT, UNITED STATES NAVY
B.S., U.S. NAVAL ACADEMY
(1958)

CLYDE C. MORRIS, LIEUTENANT, UNITED STATES NAVY
B.S., U.S. NAVAL ACADEMY
(1958)

SUBMITTED IN PARTIAL FULFILLMENT OF THE REQUIREMENTS

FOR THE DEGREE OF NAVAL ENGINEER

AND THE DEGREE OF

MASTER OF SCIENCE IN NAVAL ARCHITECTURE

AND MARINE ENGINEERING

at the

MASSACHUSETTS INSTITUTE OF TECHNOLOGY

May 1965

Signature of Authors: _____

Department of Naval Architecture and
Marine Engineering, 21 May 1965

Certified by: _____

Professor of Naval Architecture
Thesis Supervisor

Accepted by: _____

Chairman, Departmental Committee on
Graduate Students

SLAMMING OF A SHIP'S STRUCTURAL MODEL BACKED WITH DAMPING MATERIAL

by

John T. Gardner, Jr., U.S.N.

and

Clyde C. Morris, U.S.N.

Submitted to the Department of Naval Architecture and Marine Engineering 21 May 1965 in partial fulfillment of the requirements for the Master of Science degree in Naval Architecture and Marine Engineering and the professional degree, Naval Engineer.

ABSTRACT

Two 1/4 structurally scaled models representing the area of a ship's bottom shown most susceptible to slamming damage were backed with damping material. In order to determine the effectiveness of the damping material in reducing slamming damage, each model was given ten controlled test drops into water to simulate the effects of repeated slamming.

The damping materials tested were a polyvinyl chloride-polyvinyl acetate, the best known low frequency damping material suitable for shipboard use, and ML-D2, a polyamide-epoxy aluminum oxide filled material.

The models were instrumented to give time history plots of pressure, strain, velocity, and deflection of the model bottom shell plating and stiffeners. These data along with direct offset measurements of model deformation were compared with data from a similarly tested unbacked model. The results showed that the model damage occurred during the first half cycle of model vibration (a period of approximately 10 milliseconds) and the damping material was unable to dissipate enough energy during this time interval to perform substantial damage reduction. The damping materials did not prevent the tripping of the stiffeners.

A full analysis of the effects of damping was not possible because the variations in deformation resulting from the use of the damping materials were of the same order of magnitude as the variation of deformation experienced in controlled test drops of an unbacked model.

Damping materials are not recommended for shipboard use in slamming damage reduction on the basis of these tests.

Thesis Advisor: J. Harvey Evans

Title: Professor of Naval Architecture

ACKNOWLEDGMENTS

The authors wish to express their gratitude to Professor J. Harvey Evans, Department of Naval Architecture and Marine Engineering, Massachusetts Institute of Technology, for his supervision and continuing interest in this subject, to Dr. Alfred H. Keil, Technical Director, David Taylor Model Basin, and Dr. Heinrich M. Schauer, Head, Underwater Explosions Research Division, David Taylor Model Basin, for their interest and cooperation, to James W. Church, Head, Performance Evaluation Branch, David Taylor Model Basin, for his advice and encouragement, and to Mr. Elso Elsarelli, Engineering and Test Section, Underwater Explosions Research Division, David Taylor Model Basin, for his assistance and outstanding liaison during the testing phase of this experiment.

The models were built at the Norfolk Naval Shipyard under the supervision of the Underwater Explosions Research Division, David Taylor Model Basin. Testing was conducted by the Underwater Explosions Research Division, David Taylor Model Basin, under the direction of the authors. This project was funded by the Structural Mechanics Laboratory, David Taylor Model Basin.

TABLE OF CONTENTS

LIST OF FIGURES

NOTATION

B = Maximum beam of a ship

C = Damping coefficient

C_o = Critical damping coefficient

E_2 = Young's modulus of damping material

E_2^* = Complex Young's modulus of damping material

E_2' = Real part of complex Young's modulus

E_2'' = Imaginary part of complex Young's modulus

e_2 = Relative Young's modulus = E_2/E_1

H_1 = Shell plating thickness

H_2 = Damping material thickness

h_2 = Relative thickness of damping material = H_2/H_1

L = Length between perpendiculars of a ship

W_1 = Weight of shell plating

W_2 = Weight of damping material

η = Loss factor of a composite plate

η_2 = Loss factor of damping material

$\eta_2 E_2$ = Loss modulus of damping material

$\eta_2 e_2$ = Relative loss modulus of damping material

γ_2 = Density of damping material

ϕ = Phase angle

I. INTRODUCTION

The emergence of the forefoot of a vessel from the sea and its impacting on returning to the sea is known as slamming. The vessel experiences a whipping motion of the hull and in many cases local damage at the impacting area. This phenomenon has been a problem for study by naval architects for many years.[1,2]* The economic effect of slamming manifests itself in costly repairs, overdesign, and a loss of revenue caused by reduced operating speeds in heavy weather.[3] Although there have been many solutions proposed for this problem, slamming damage remains a continuing problem today. Recent investigations have given insight as to the factors that contribute most towards the probability of a slam,[4] the effect of forebody shape on slamming,[5,6] the hydrodynamic aspects of slamming[7] and the structural response of the vessel to slamming.[8-10] These investigations do not solve the slamming problem, but they do lead to an understanding of the basic fundamentals involved in the slamming problem.

Slamming damage can be repaired, but its magnitude cannot be predicted. This implies that we cannot design a vessel to withstand a certain predicted magnitude of slam loading, but instead we must overdesign to some degree if we are to insure relative freedom from damage. Most certainly, factors such as judicious use of course and speed changes, and the forebody shape can reduce the probability of a slam. However, it can be stated that there will always be conditions of sea state, ships speed and loading that will produce impact forces large enough to result in slamming damage. Under these conditions the structural aspects of the problem become of greatest importance.

---

*Numbers in brackets refer to bibliography.

With the above thoughts in mind, the authors set out to investigate the effectiveness of a damping material, applied to the bottom shell plating of a vessel, in reducing local slamming damage. A previous investigation[11] indicated that a damping material applied to the bottom shell plating in a damping weight to plate weight ratio of approximately 5:1 produced a substantial reduction of slamming damage. The authors feel that a damping material applied in this ratio is an impractical solution to the problem. However, it is felt if damping is a major factor in damage reduction similar results could be obtained with lessor amounts of material. An advantage of this approach to a solution is the ease with which the treatment can be installed and the flexibility the designer has in its use. It could be installed in ships presently in service after slamming damage has been repaired to prevent further damage or to new construction as a safety factor.

II. EXPERIMENTATION

A. General: The objectives of this investigation were

a) To determine if a practical application of a damping material was an effective means of preventing or reducing slamming damage.

b) To determine if there was an optimum thickness of damping material for reducing slamming damage.

c) To compare the effectiveness of two damping materials in reducing slamming damage.

d) To determine which properties of a damping material contributed most towards damage reduction.

In order to accomplish these objectives three identical models were constructed, MG 1, MG 2 and MG 3. These models were essentially identical to those used in two previous investigations[11,12] conducted at the Underwater Explosions Research Division (UERD) of the David Taylor Model Basin. This investigation, therefore, benefited from the large amount of data and experience gained in the previous tests of this type of model. An additional benefit derived from using this type model was that data obtained from model KG 1, an unbacked model that had been repeatedly dropped from a height of 10 feet, could be used as the control model for the present investigation.

The damping material selected for the investigation was a polyvinylchloride-polyvinylacetate as specified in military specification MIL-P-23653A and hereafter referred to as PVC-PVA. This material was selected because it was the best available low frequency damping material suitable for shipboard use. (See theory) A high frequency damping material, ML-D2 (MIL-P-22581) the

material found to reduce slamming damage when applied in large amounts, [11] was used to compare its effectiveness with that of PVC-PVA.

B. Model Details:

Each model was of 1/4 scale and represented the bottom of a Coast Guard cutter from .25L to .35L and from .25B starboard to .25B port as shown in Figure 1. This location was chosen because it has been shown to be the area

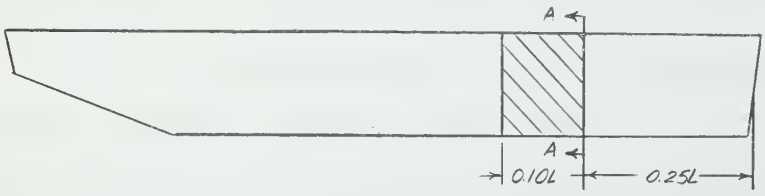

Section AA

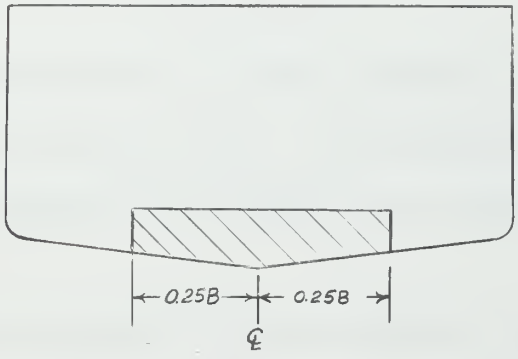

FIG. 1

where maximum slamming damage occurs. [13] The over-all dimensions of the model were 90 inches by 78.8 inches by 11.5 inches. The model had a constant 10 degree deadrise. It had longitudinal framing with transverse bulkheads and floors that divided the bottom shell plating into 8 inch by 18 inch panels.

This 1/8 inch shell plating was mild steel with an average yield strength of 34,000 psi while the framing and bulkheads were constructed from high tensile steel with an average yield strength of 62,400 psi. The keel of each model was considered rigid enough to separate one side of the model from the other so that each side of a model could serve as an individual plate stiffener combination for testing purposes.

Damping material PVC-PVA was applied in five thicknesses, 1/8, 1/4, 1/2, 3/4 and 1 inch, resulting in damping treatment weight to plate weight ratios of .25, .5, 1, 1.5 and 2. Damping material ML-D2 was applied in a thickness of 1/2 inch, with a treatment weight to plate weight ratio of 1. These thicknesses and weight ratios were felt to be sufficient to demonstrate whether or not the material was an efficient means of preventing or reducing slamming damage.

Model MG-1 was backed with 1 inch of PVC-PVA on the starboard side and with 1/4 inch PVC-PVA on the port side. This model gave an immediate contrast between the results obtained from a moderate and a heavy application of damping material.

Model MG-2 was backed with 1/2 inch PVC-PVA on the starboard side and 1/2 inch of ML-D2 on the port side. This model served to contrast the effectiveness of PVC-PVA and ML-D2 and also served as a point of comparison between the 1 inch and 1/4 inch treatments of PVC-PVA.

Model MG-3 was to be backed with 1/8 inch PVC-PVA on the starboard side and 3/4 inch PVC-PVA on the port side. This model was to serve as a refinement on the data points established by models MG-1 and MG-2. In the event that models MG-1 and MG-2 demonstrated that the damping treatment could not

substantially reduce slamming damage, model MG-3 was not to be tested.

In addition to these models, data from model KG-1 was used as the control model for this investigation. As noted earlier in this paper, model KG-1 was of the same construction as models MG-1, 2 and 3 but had no damping material applied to it. Model KG-1 had been dropped a total of 22 times by UERD from a height of 10 feet and the data obtained from these tests were available to the authors.

In all of the damped models, the damping material was in the form of 1-foot square tiles of the specified thicknesses. The tiles were firmly bonded to the plate in accordance with pertinent U.S. Navy instructions. Chemlock 301, a two-part epoxy adhesive, was used to bond the PVC-PVA tiles to the plate, and ML-D2 adhesive (Philadelphia Resins Company) was used as the ML-D2 bonding agent.

C. Instrumentation:

Instrumentation for models MG 1, 2, and 3 was identical and consisted of mechanical deflection gages (MD), piezo-electric pressure gages (PE), strain gages (ST), accelerometers (AC) and velocity meters (VM) located as shown in Figures 2, 3, and 4. The deflection gages were positioned so as to measure the deflection perpendicular to the plane of the undeformed model. The damping material was cut away from all gage locations in order for the gages to be attached directly to the model.

After each test drop, all gages were rezeroed. In the case of the deflection and strain gages, this established a "zero" deformation at the beginning of each drop. Thus, the time history of these gages indicated only

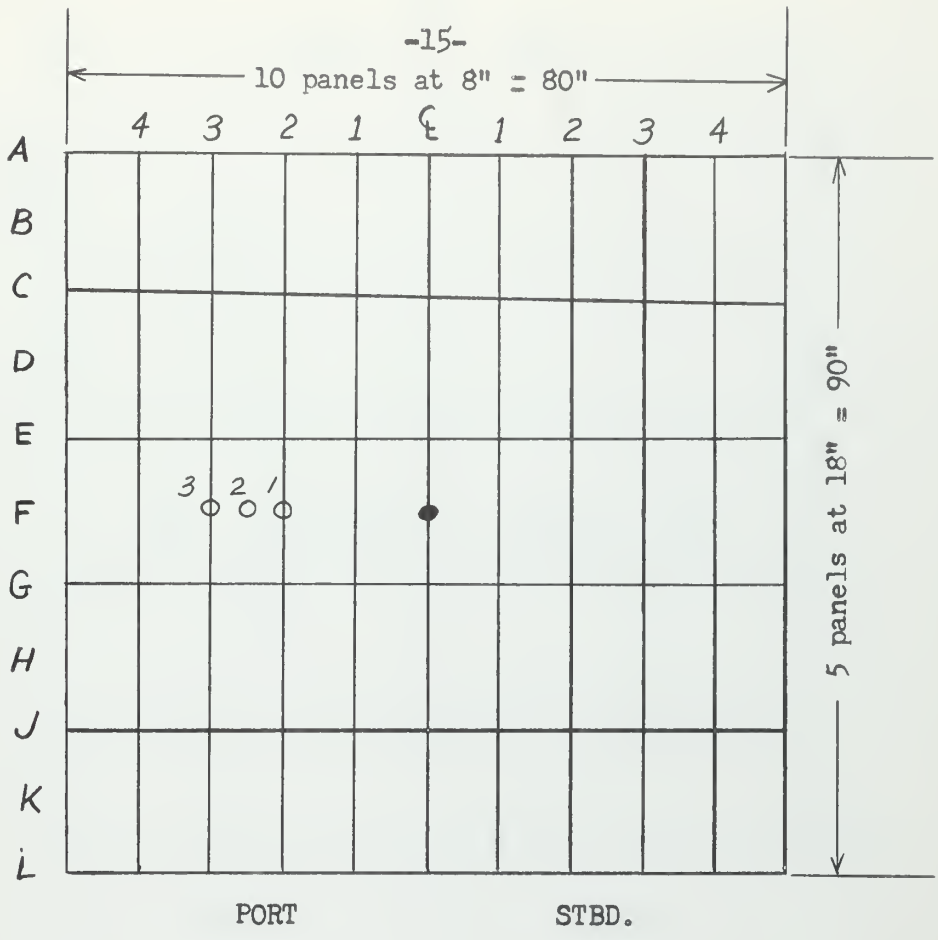

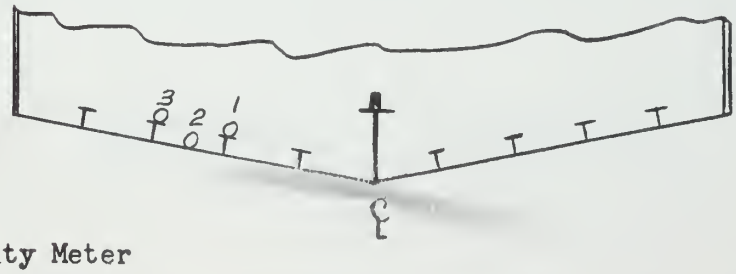

● Velocity Meter

○ Accelerometer

Figure 2
Instrumentation Location, Velocity Meter, Accelerometers

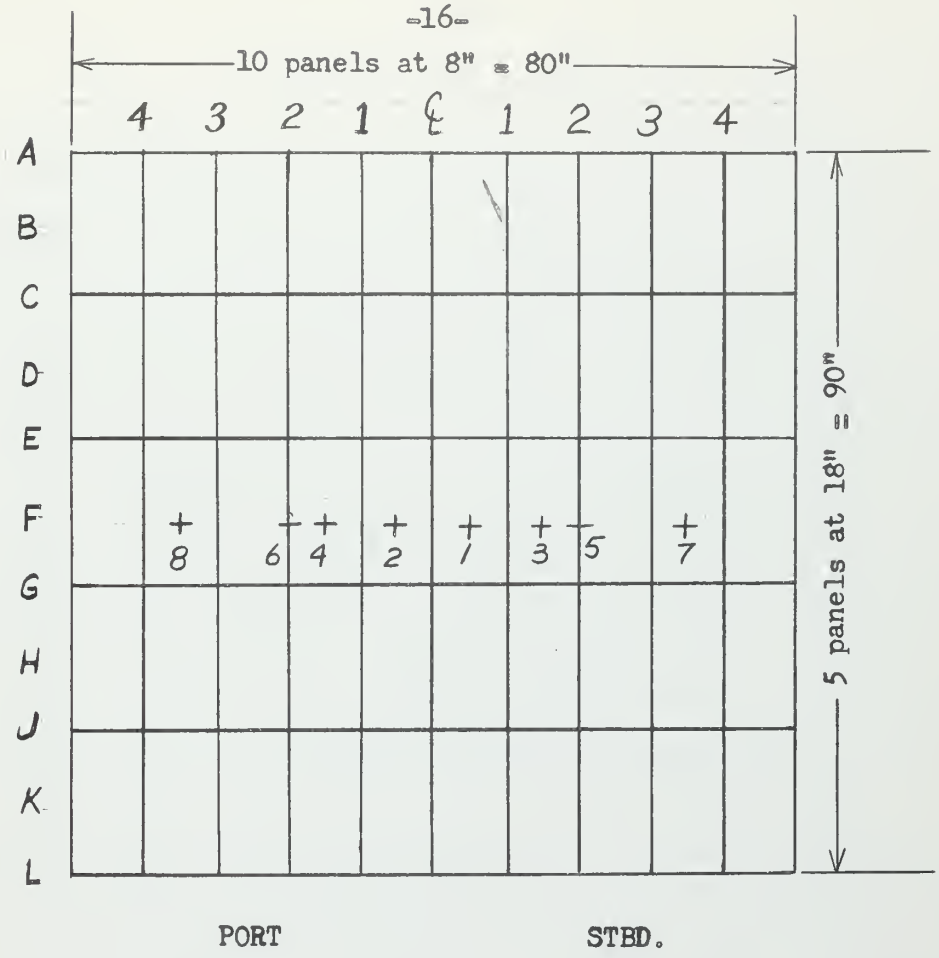

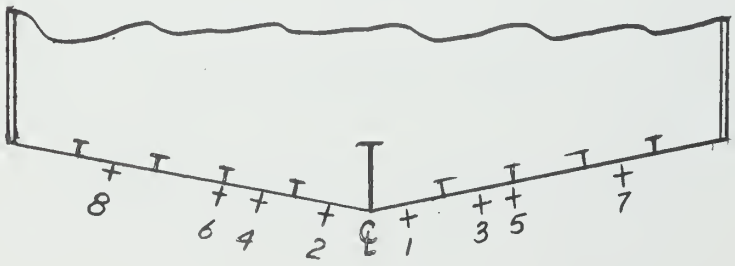

Figure 3
Instrumentation Location, Pressure Gages

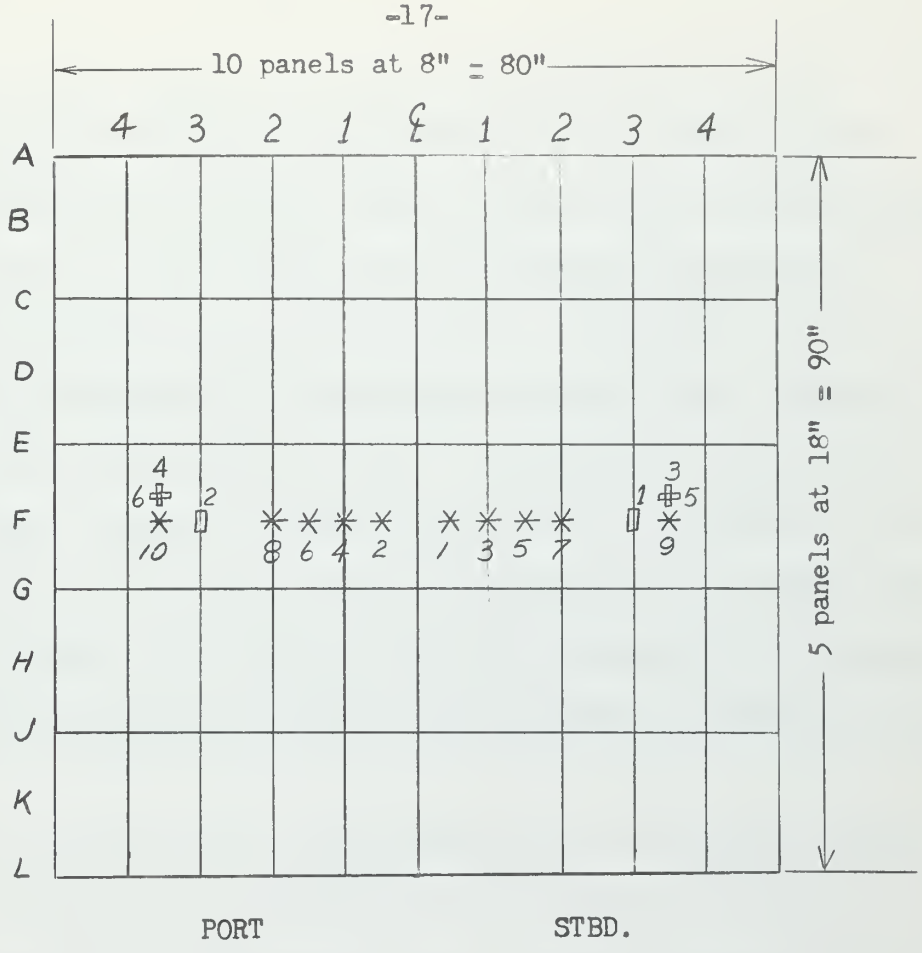

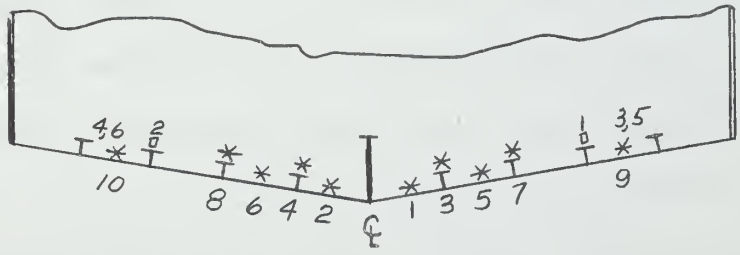

▯ Strain Gage

✳ Mechanical Deflection Gage

Figure 4
Instrumentation Location, Strain Gages, Mechanical Deflection Gages

deflection and strain obtained during an individual drop and they gave no indication of the total set or residual stress existing from the previous drops.

Instrumentation records for each drop were recorded on high speed magnetic tape using the AMPEX FR-114 tape recorder. This system is used extensively in making measurements of underwater explosion tests conducted by UERD and has an over-all response of 10kc. Instrumentation records were turned on by the model tripping a trigger when the keel of the model was six inches from the surface of the water. Data was recorded until the model was lifted clear of the water. This permitted accurate determination of permanent set from MD gages by eliminating the effect of hydrostatic and dynamic loading on the model.

In addition to these dynamic measurements taken of the model response, it was possible to obtain direct measurements of the bottom of the model. These measurements were made by use of jigs that were attached to each end of the model carriage. Wires were tensioned between the two jigs to provide a base line for the measurements (Figure 5). A limitation to this method of taking measurements was that the model had to be removed from the drop rig in order to take the measurements. By use of a second set of jigs that established a base line across line F, the instrumentation line, it was possible to take direct readings of model deformation at line F without removing the model and carriage from the drop rig. In this manner, set deflections obtained from the deflection gages could readily be compared with direct measurements taken at the deflection gage locations.

Figure 5
Technicians Taking Offset Measurements on Model

Figure 6
Model and Carriage Mounted in Drop Rig

D. Procedure:

In order to drop the model it was bolted to the carriage, which in a sense, was an integral part of the model. The carriage formed a rigid base for mounting the deflection gages and added the necessary weight to bring the model up to scale weight of 8900 pounds. The carriage held the model and in conjunction with the guide tracks controlled the drop height and the attitude of the falling model. The guide tracks limited model roll and pitch to 1/2 degree. The guide tracks in turn were mounted on the stern of the UEB-1, which serves as a floating laboratory for UERD tests. The model attached to the carriage is shown in the guide tracks in Figure 6.

Each model was dropped a total of twelve times, data being recorded on each drop. The first two of these drops were from a height of three feet and the next ten drops were from a height of ten feet. The 10 foot drop resulted in a velocity on entering the water of 25.4 feet per second. Drops were made into calm water or water having two to three inch disturbance amplitude. Prior to the first drop and after the last drop a complete set of direct offset readings was taken. During the testing, a set of direct offset readings along line F was obtained after specified drops. These measurements were taken as a backup for deformation measurements obtained from the deflection gages.

III. THEORY

A perfectly elastic material obeys Hook's law without regard to rate of loading, whereas in a viscous fluid, stress is proportional to rate of strain regardless of stress level. Most materials, however, under a certain range of frequencies and temperatures reach a state where the stress effect and strain-rate effect are equally important. These materials are said to be visco-elastic within this range. As the name implies, visco-elastic materials are capable of energy storage (elastic) and energy dissipation (viscous).

Visco-elastic materials dissipate energy through extensional damping and shear motion. This investigation will only be concerned with extensional damping which accounts for the losses when a single layer of damping material is used. (Shear damping is the dominant factor when a damping material is placed between the plate to be damped and a relatively stiff cover plate.)

Visco-elastic materials are composed of long-chain molecules. Deformation of the material may consist of coiling and uncoiling of the chains or of any general change in configeration. These changes are delayed or "retarded" by intermolecular and intra-segmental forces causing the resulting strain to be out of phase with the stress. At low frequency, the delayed response is short compared to the time for stress reversal and near equilibrium is always maintained. As the frequency is increased and/or the temperature is lowered, we reach a point where the internal motions can no longer take place within a stress reversal, the material stiffness (modulus) increases, and the material deforms less and less.[14,15] Dependence of Young's modulus on temperature and frequency can be seen in Figure 7.

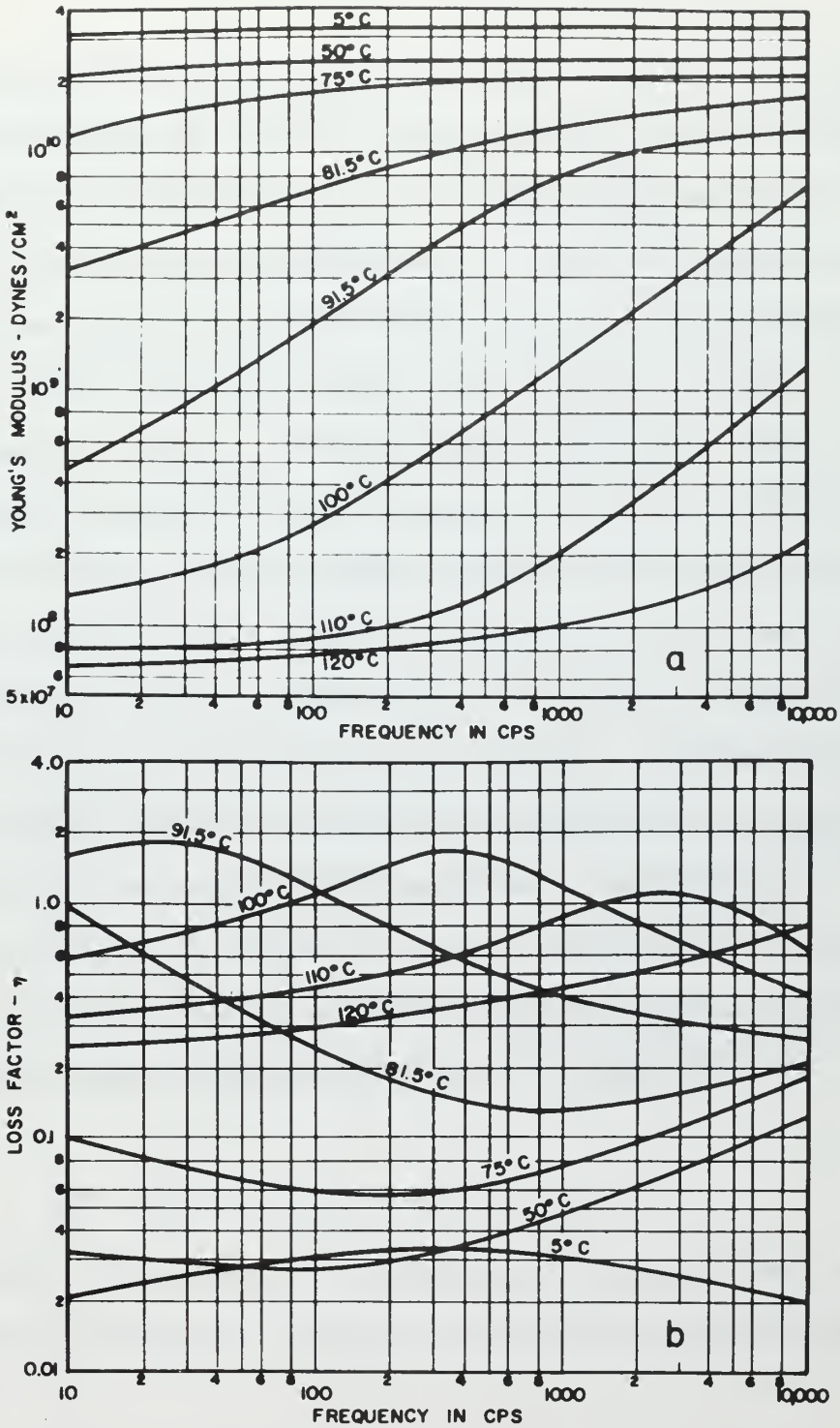

Fig. 7 Frequency and Temperature Dependence of (a) Young's Modulus and (b) Loss Factor of Polyvinylchloride

The phase lag between stress and strain results in energy dissipation because of the displacement of molecular segments against opposing molecular forces. This energy is converted into heat in a dissipative or "lossy" material. Energy loss per cycle is proportional to the strain amplitude and the sine of the phase angle for a given stress amplitude. At low frequency, the phase angle is small and thus the energy loss is small. At higher frequencies, the strain amplitude is small (as explained above) and thus the energy loss is again small. Therefore, maximum energy dissipation occurs at an intermediate range where both phase angle and the strain amplitude are relatively large.[14]

The dynamic properties of a visco-elastic material are a function of frequency and amplitude of stress and/or strain, temperature, loading history, and in general the mean state of stress in the material. For most applications, frequency and temperature are the most significant parameters, and except at very high strains, they are independent of amplitude of vibrations.[15,17] This independence of amplitude permits one to solve equations for visco-elastic damping by solving the equations for an ideal non-lossy material and replacing the Young's modulus, E_2, for extensional damping by the complex elastic modulus, E_2^* in:

$$E_2^* = Ee_2^{j\phi} = E_2' + jE_2'' = E_2'(1 + j\eta_2)$$

where ϕ is the phase angle between the alternating strain and stress, and η_2 is the "loss factor" of the material, so named because of its close relationship to energy loss.

Loss factor can be expressed in terms of the ratio of damping to critical damping for a homogeneous material in the absence of external energy losses by:

$$\eta \equiv \tan \phi = 2C/C_o \quad (\text{when } \eta \leq 0.3). \text{[15]}$$

For single layer extensional damping an approximation of the damping equation is given as:

$$\eta = \frac{\eta_2 e_2 h_2 (3 + 6h_2 + 4h_2^2)}{1 + e_2 h_2 (3 + 6h_2 + 4h_2^2)}$$

where η is the loss factor of the composite plate

η_2 is the loss factor in the damping material

$e_2 = \frac{E_2}{E_1}$ is the relative Young's modulus

$h_2 = H_2/H_1$ is the relative thickness

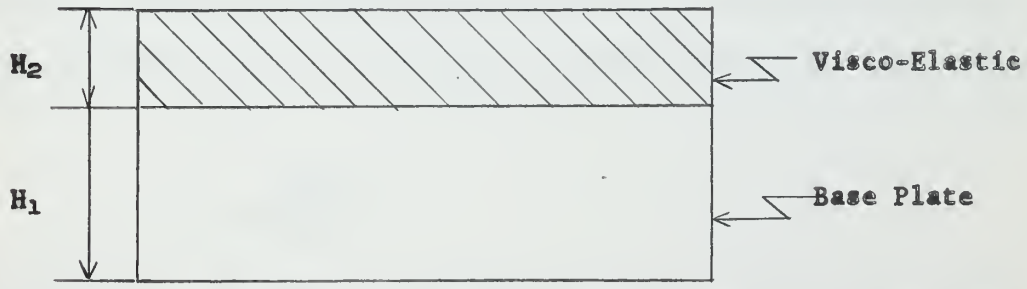

This indicates that η is a function of the loss modulus, $\eta_2 E_2$, and relative thickness of the damping material. The loss factor varies linearly with modulus for moderate damping. It is linear with relative thickness for $h < 1/5$, and a function of the square of the relative thickness for unity

thickness ratio. It is a function of some higher order at higher relative thicknesses until η approaches approximately 40 per cent of η_2 at which time the damping tends to saturate and we reach a region of diminishing returns.[16] See Figure 8. The effect of relative thickness and loss modulus on damping can be seen in Figure 9, for moderate values of relative thickness. The maximum amount of damping which can be expected from a material is limited by the damping characteristics of the material. Ross and Kerwin,[15] using one of the best known damping materials available, with loss modulus of about 10^{10} dynes/cm^2, calculated the loss factor of a composite plate of this material on steel as a function of relative thickness in the form:

$$\eta \leq 0.065\left(\frac{H_2}{H_1}\right)^2$$

for damping materials in the same order of thickness as the plate. This gives an approximate maximum value of η presently attainable.

It has been found for a given weight of damping material, that damping is greatest when $E_2\eta_2/\gamma_2^2$ is a maximum. Thus, using the best known material on this basis, a maximum value of η based on relative weight has been approximated as

$$\eta \leq 4\left(\frac{W_2}{W_1}\right)^2$$

for steel plates.[15] The effect of damping material on steel plate from the above equation can be seen in Figure 10. See Figure 11 for loss factor as a function of relative weight of damping material to base plate. Very little information is available on damping using a relative weight greater than 0.25.

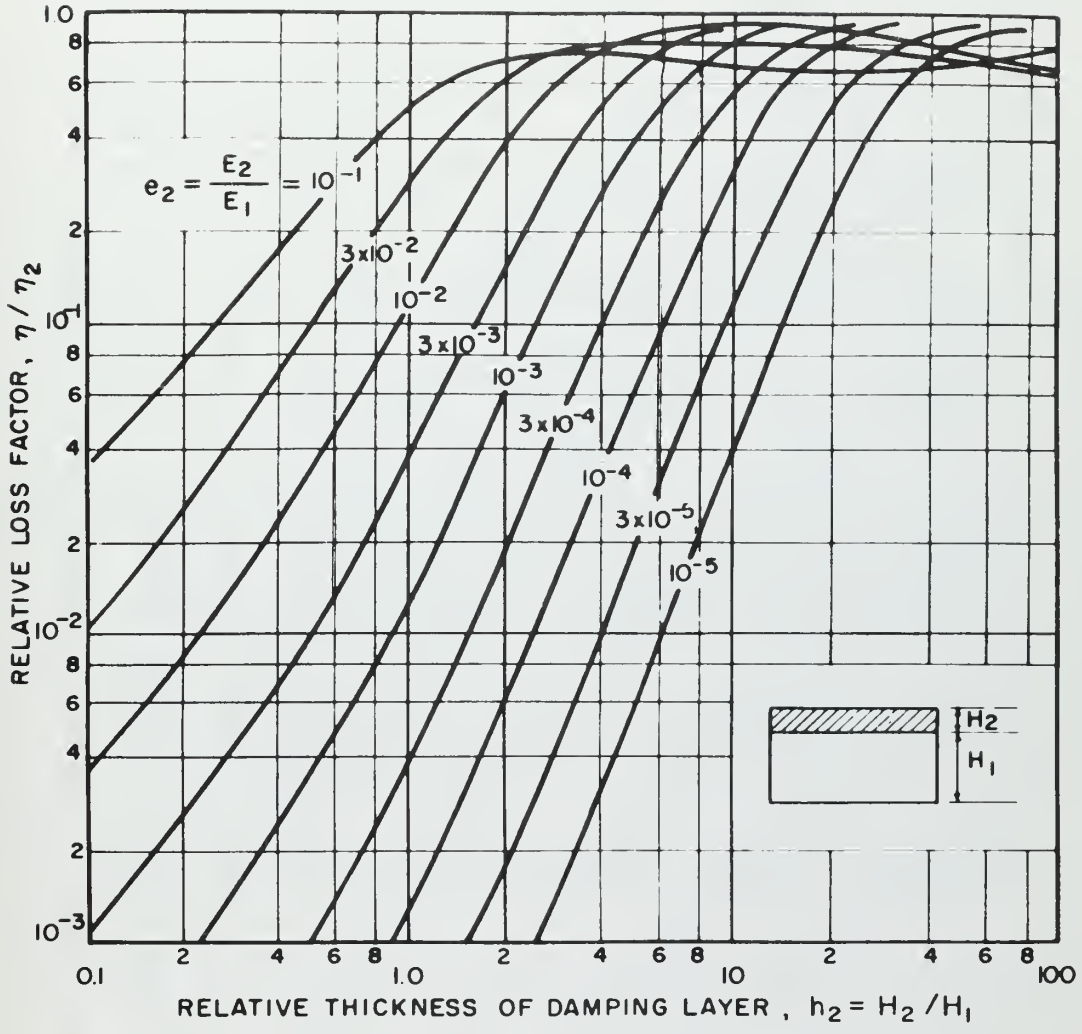

Fig. 8 Relative Damping as a Function of Relative Thickness and Relative Young's Modulus of Homogeneous Damping Layer

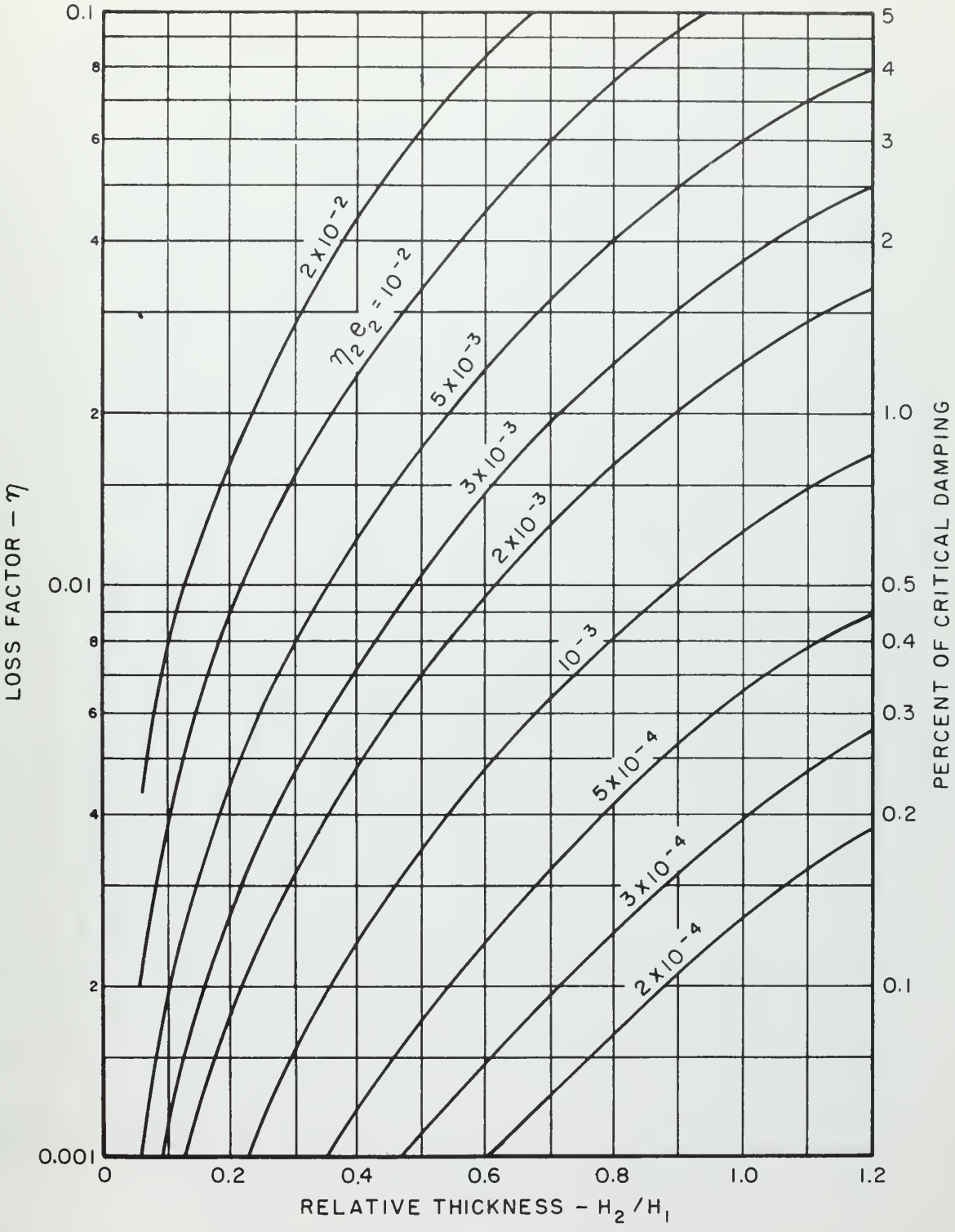

FIG 9 DAMPING OF HOMOGENEOUS TREATMENTS FOR MODERATE THICKNESSES.

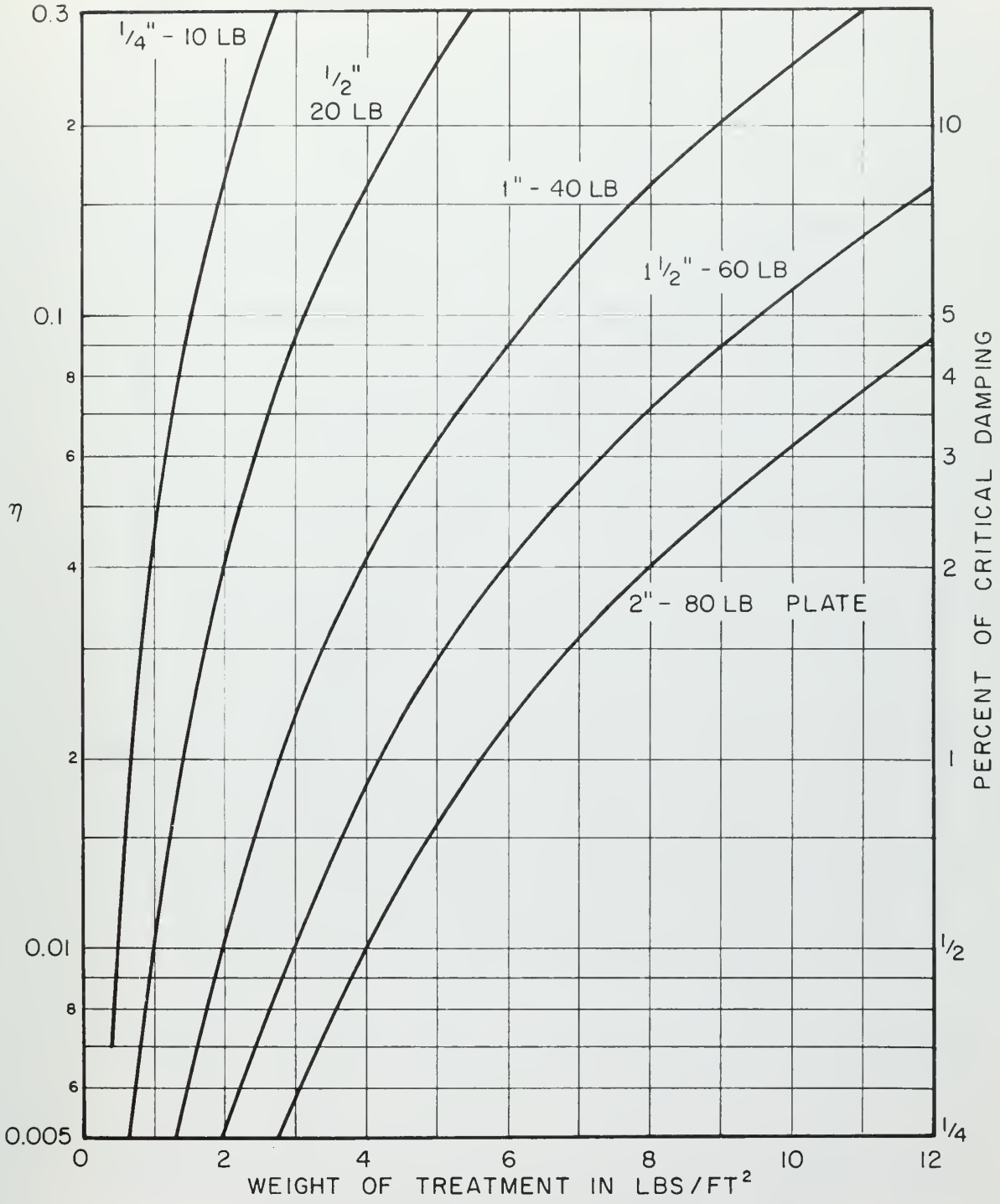

FIG. 10 MAXIMUM HOMOGENEOUS DAMPING FOR FIVE STEEL PLATES.

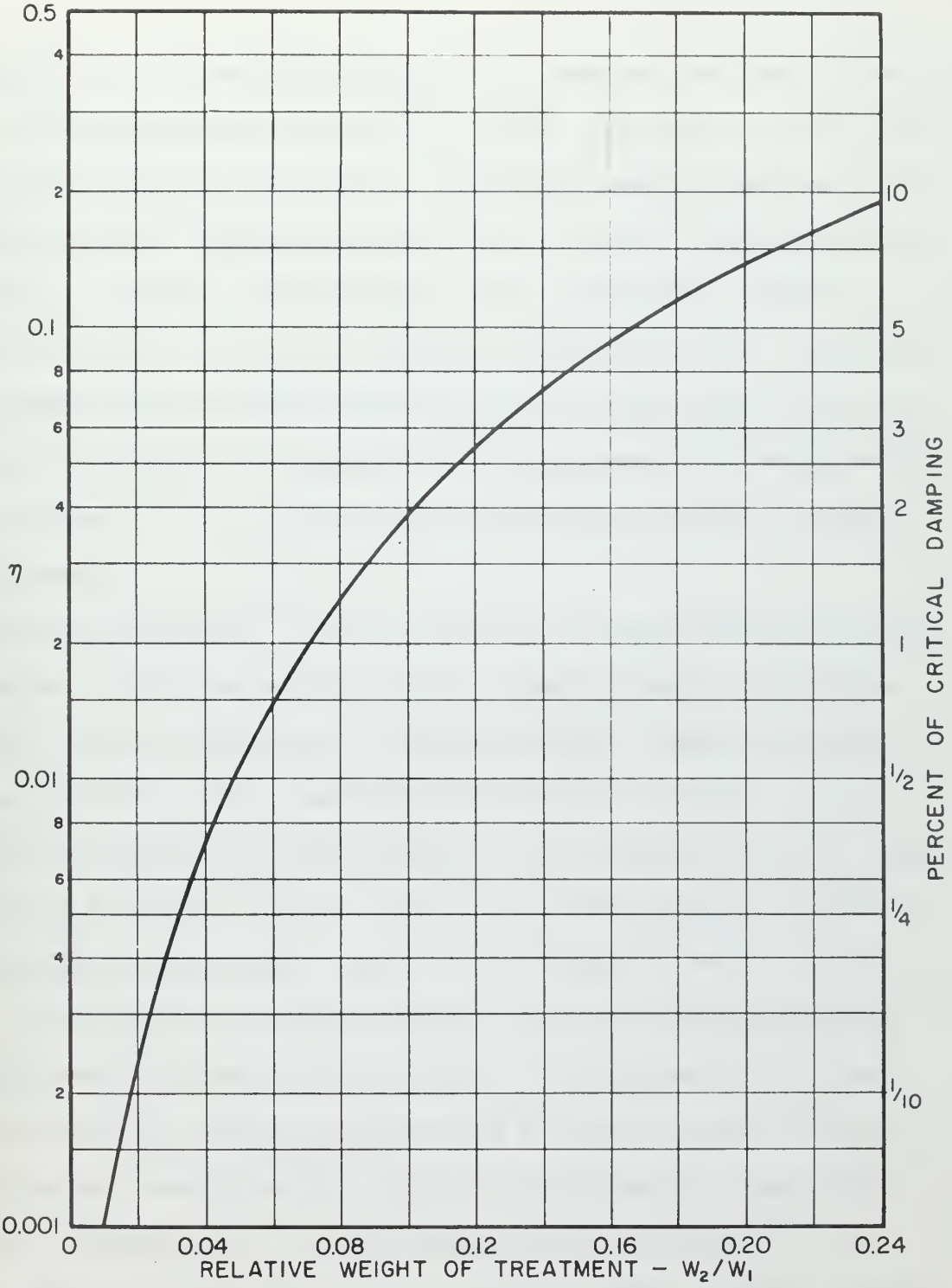

FIG 11 DAMPING AS A FUNCTION OF RELATIVE WEIGHT FOR BEST KNOWN DAMPING MATERIALS.

Shipboard use of damping material for the most part has been limited to reducing sound radiation and self-noise of a ship. Shipboard vibrations have been successfully damped by visco-elastic materials absorbing and dissipating the vibrational energy. The more damping material present, the greater will be the damping. Practical considerations require the damping material to be as light as possible. For effective damping in sound isolation, a compromise has been reached between "damping effectiveness" and weight which calls for a damping material weight to be between 25 and 33 per cent of the weight of the plate to be damped.[18] This limit was not intended to apply to reduction of slamming damage.

A previous experiment[12] was conducted to determine the effectiveness of using various backing materials to reduce slamming damage. Encouraging results were obtained through use of a damping material commonly referred to as ML-D2 and specified in Navy specification Mil-P-22587 (Ships). ML-D2, a sand filled polyamide-epoxy damping material was developed by the U.S. Naval Applied Physics Laboratory, formerly known as the Naval Material Laboratory. It has its maximum damping above 3000 cycles per second as can be seen from Figure 12, and has poor resistance to fuel, water, and accelerated ageing.[18,19] In this experiment, the investigators realized that their use of ML-D2 was excessive, but they had committed themselves to a specified mass of material which resulted in a damping material weight of approximately 5 times plate weight, and a thickness ratio of damping material to plate of 25:1. As a result of their experiment, they recommended without proof a damping material thickness 4 to 6 times plate thickness.

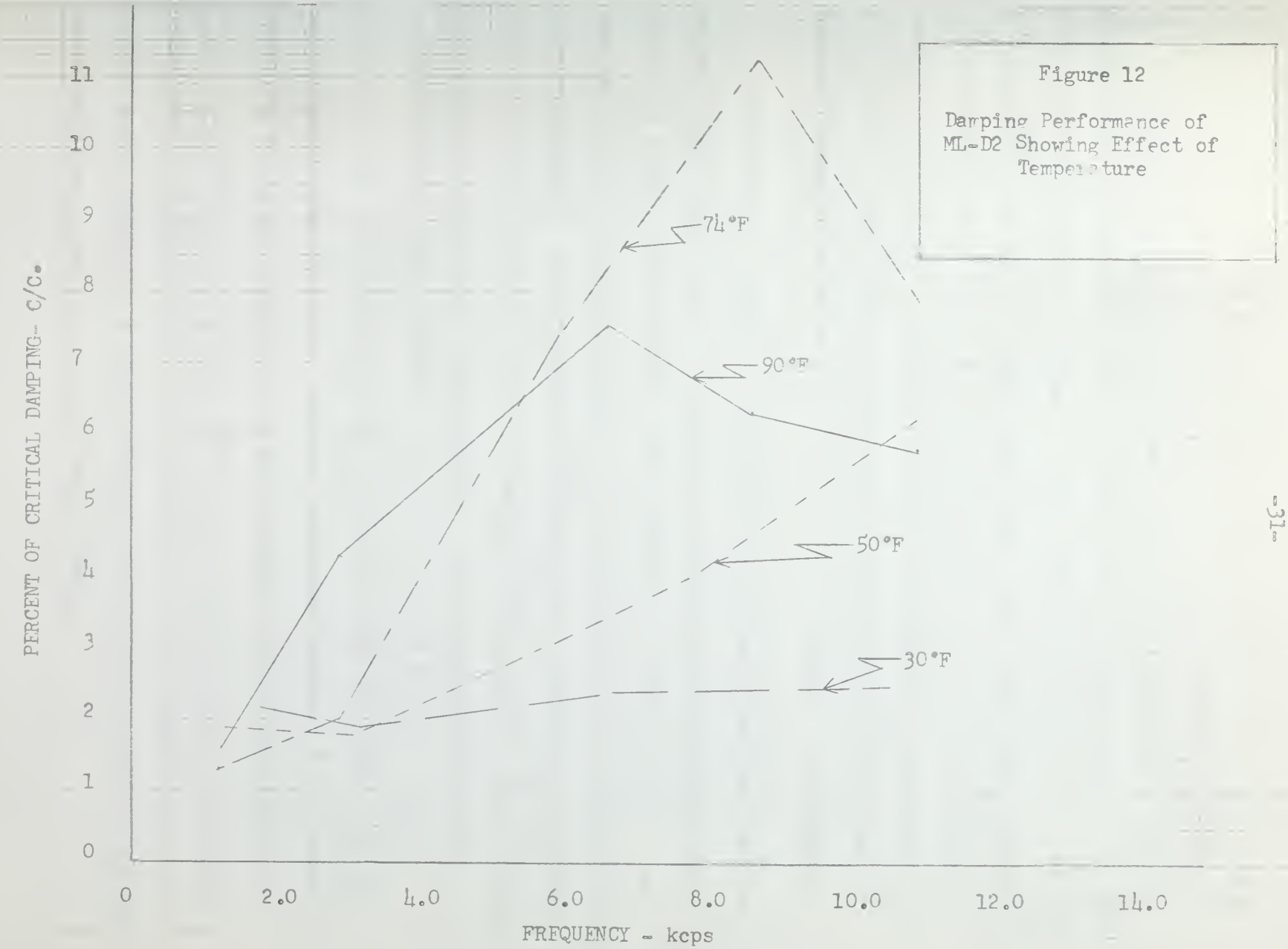

Figure 12

Damping Performance of ML-D2 Showing Effect of Temperature

Reduction in slamming damage as a result of the addition of a damping material can be the result of one or a combination of three effects: (1) added mass, (2) increased plate stiffness, and (3) damping efficiency of the material. If the major contributor to damage reduction is either added mass or increased plate stiffness, this can be done more economically than by use of a damping material. If the major contributor is damping efficiency of the material, we would expect optimum results from the best available materials when applied with a thickness of approximately two times plate thickness. See Figure 9.

In selecting a material, consideration was given to the fact that the unbacked control model (KG-1) vibrated at a frequency of approximately 52 cycles per second, with individual plate frequencies somewhat higher. The material selected for this evaluation was a modification of that specified by Mil-P-23653(Ships). It is graphite filled copolymer of polyvinyl chloride-polyvinyl acetate (PVC-PVA) which was developed under Bureau of Ships contract to dampen frequencies below 3000 cycles per second in light steel plates. Evaluation of this material[20,21] showed it exhibited excellent damping qualities in the frequency range from 50 to 1500 cycles per second, and was not adversely affected by fuel, water or accelerated ageing. It is presently undergoing shipboard evaluation as a sound damping material for submarines. Noting the difference in the loss factor between these materials, especially at the lower frequencies about which the model vibrates, (Figures 12, 13), we would expect PVC-PVA to be more effective than ML-D2, if damping efficiency is a significant factor in reducing slamming damage.

Figure 13

Damping Performance of PVC-PVA Showing Effect of Temperature

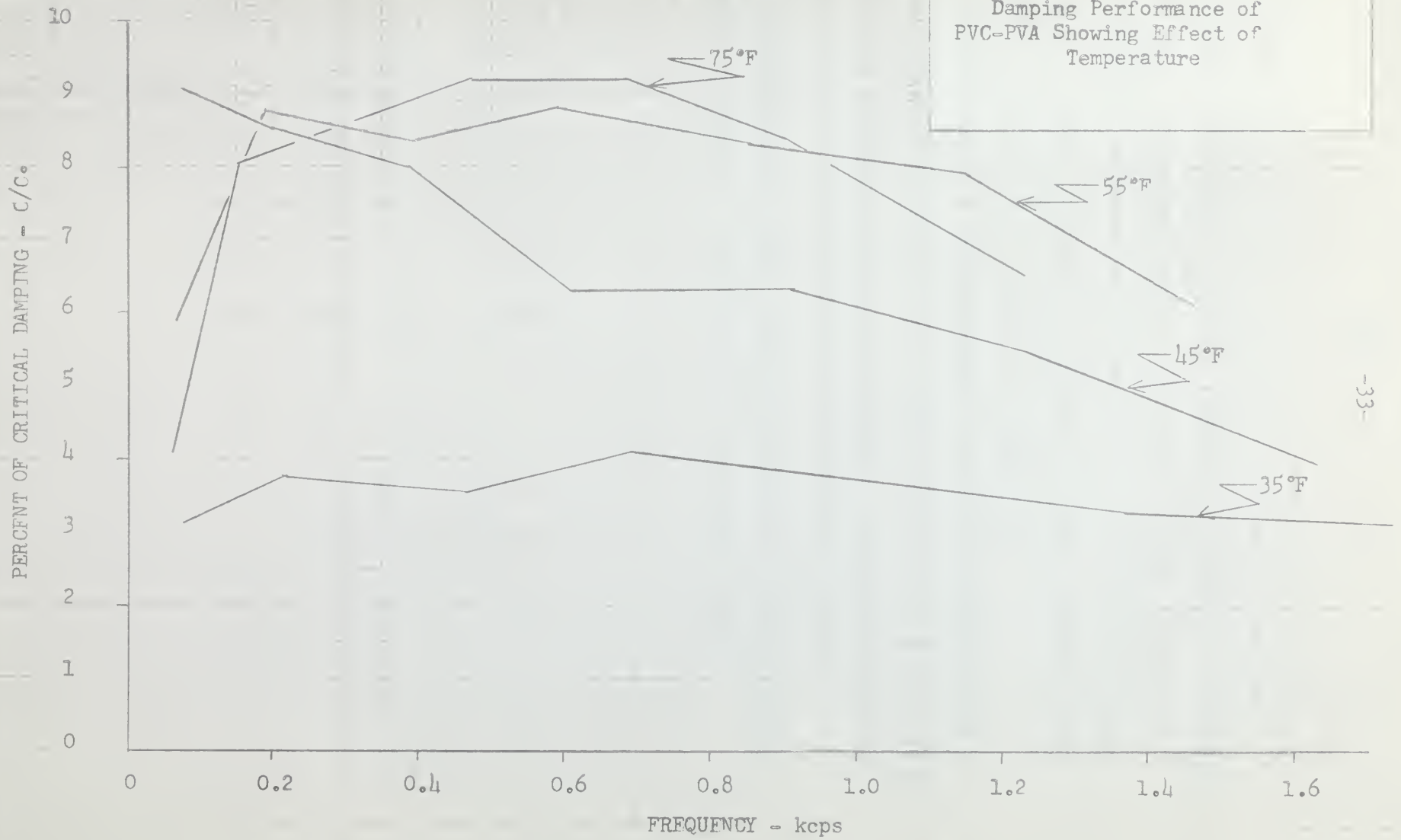

At this time, the Young's modulus and loss modulus have not been determined for PVC-PVA, making it impossible to predict an optimum thickness ratio for maximum damping. With this in mind, we selected a range of thickness ratios of damping material to base plate thickness from 1 to 8, in order to bracket the optimum thickness ratios of other visco-elastic materials with similar characteristics.

Effectiveness of a damping material is found by comparing the damping of a steel bar with that of a similar bar backed with the damping material. The difference between the damping of the two test specimens is the contribution that is attributed to the damping material. A similar comparison will be made between the backed and unbacked models to determine the amount of damping due to the backing material.

IV. RESULTS

Damage resulting from 10-10 foot drops as indicated by mechanical deflection gages and direct offset measurements is shown in the following manner:

1) The accumulative permanent deformation received at each MD gage of models MG 1 and MG 2 is shown in Figures 14-18.

2) The permanent deformation per drop received at each MD gage of model MG 1 and MG 2 is shown in Figures 19-23.

3) The total permanent deformation from direct offset measurements taken at 9 inch intervals in the longitudinal direction and at 4 inches in the transverse direction is shown in Figures 25-30.

4) A comparison of the permanent deformation received in the backed and unbacked models is shown in Figures 24, 25 and 30.

5) Photographs of model MG 1 and MG 2 after testing are shown in Figures 31 and 32 respectively.

Of the 672 recorded time history instrumentation plots, only those plots that supplement the discussion and give the reader some familiarity with the loading and model response are reproduced as results. These are shown as follows:

1) Time history plots of model MG 1 are shown in Figures 33-45.

2) Time history plots of model MG 2 are shown in Figures 46-59.

3) A time history plot of model KG 1 is shown in Figure 60.

The original copies of all data are on file at Underwater Explosives Research Division (UERD) of David Taylor Model Basin. UERD drop identification numbers are shown in Table I.

Offset measurements on model KG 1 were taken after 12-10 foot drops vice 10-10 foot drops. This should be taken into consideration when comparing the results of Figures 25 and 30.

The fundamental frequencies of the models as observed from the deflection time history plots along line F were as follows:

1. Model MG 1 45.8 cps
2. Model MG 2 53.7 cps
3. Model KG 1 51.9 cps

The per cent of critical damping achieved in each model was:

1. Model MG 1 3.10 per cent
2. Model MG 2 3.50 per cent
3. Model KG 1 3.61 per cent

Model MG 3 was not tested.

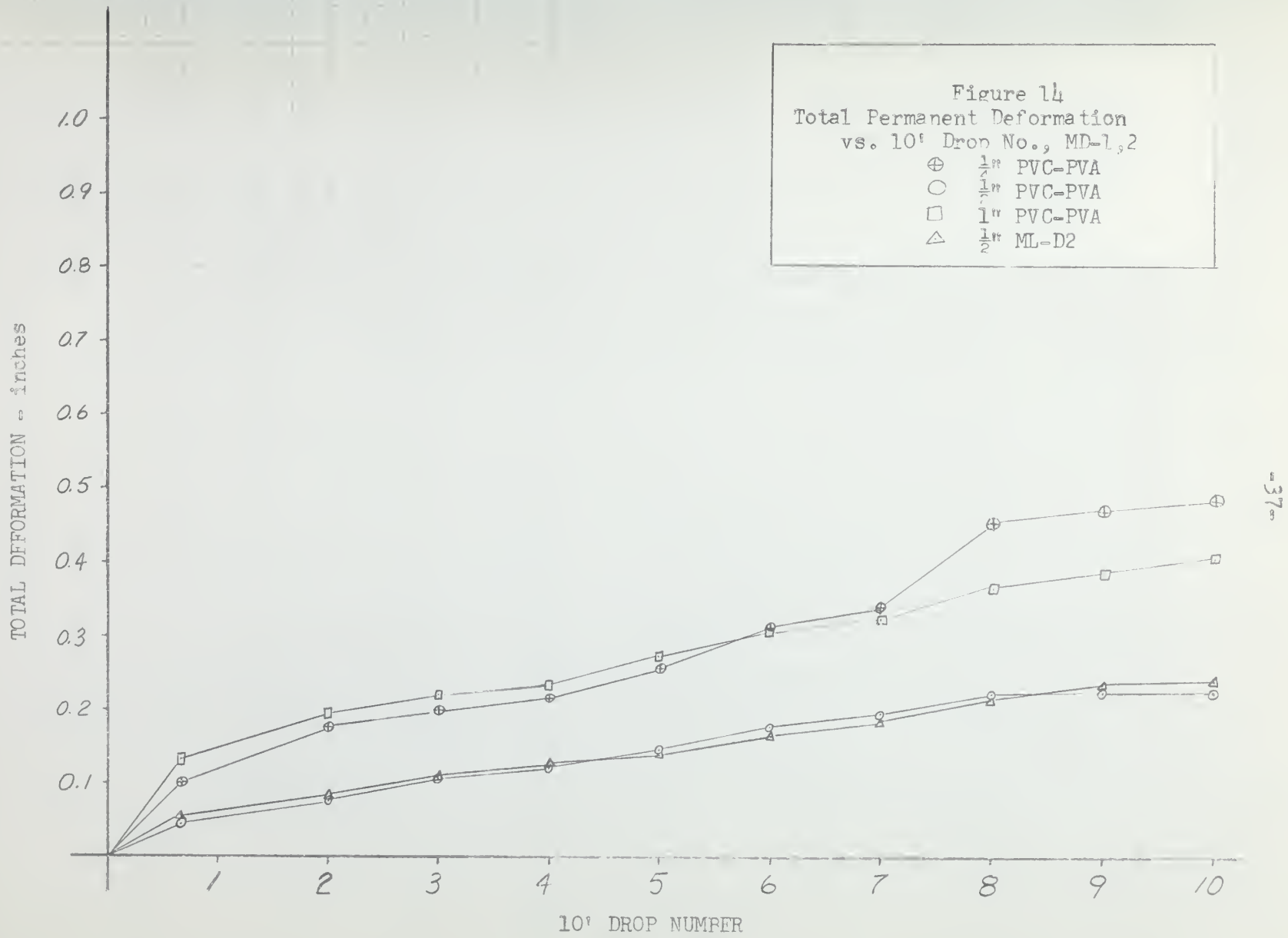
Figure 14
Total Permanent Deformation
vs. 10' Drop No., MD-1,2
½" PVC-PVA
½" PVC-PVA
1" PVC-PVA
½" ML-D2
TOTAL DFORMATION - inches
1.0
0.9
0.8
0.7
0.6
0.5
0.4
0.3
0.2
0.1
1
2
3
4
5
6
7
8
9
10
10' DROP NUMBER

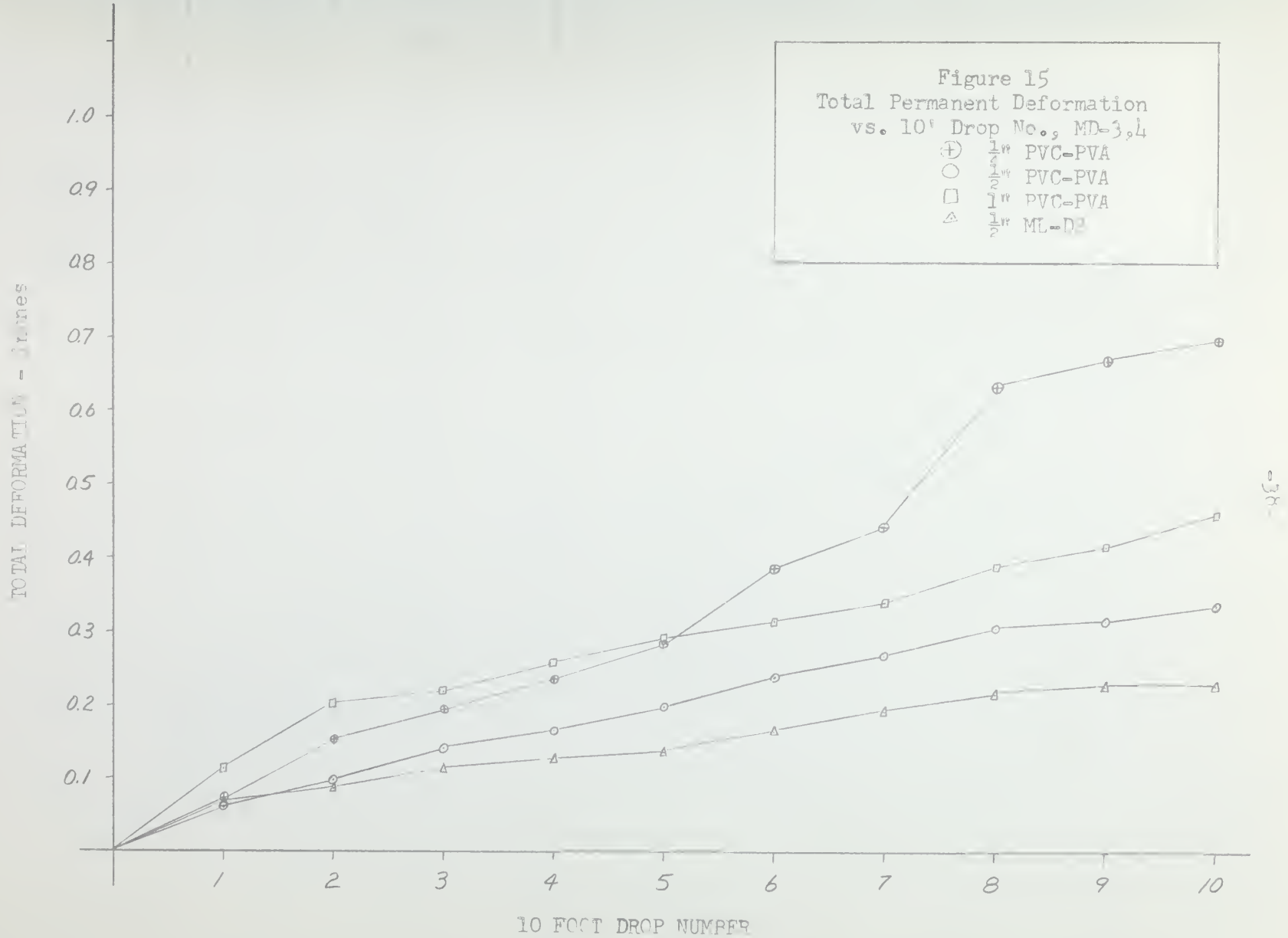
Figure 15
Total Permanent Deformation
vs. 10' Drop No., MD-3,4
1" PVC-PVA
½" PVC-PVA
1" PVC-PVA
½" ML-D2
TOTAL DEFORMATION - Inches
1.0
0.9
0.8
0.7
0.6
0.5
0.4
0.3
0.2
0.1
1
2
3
4
5
6
7
8
9
10
10 FOOT DROP NUMBER

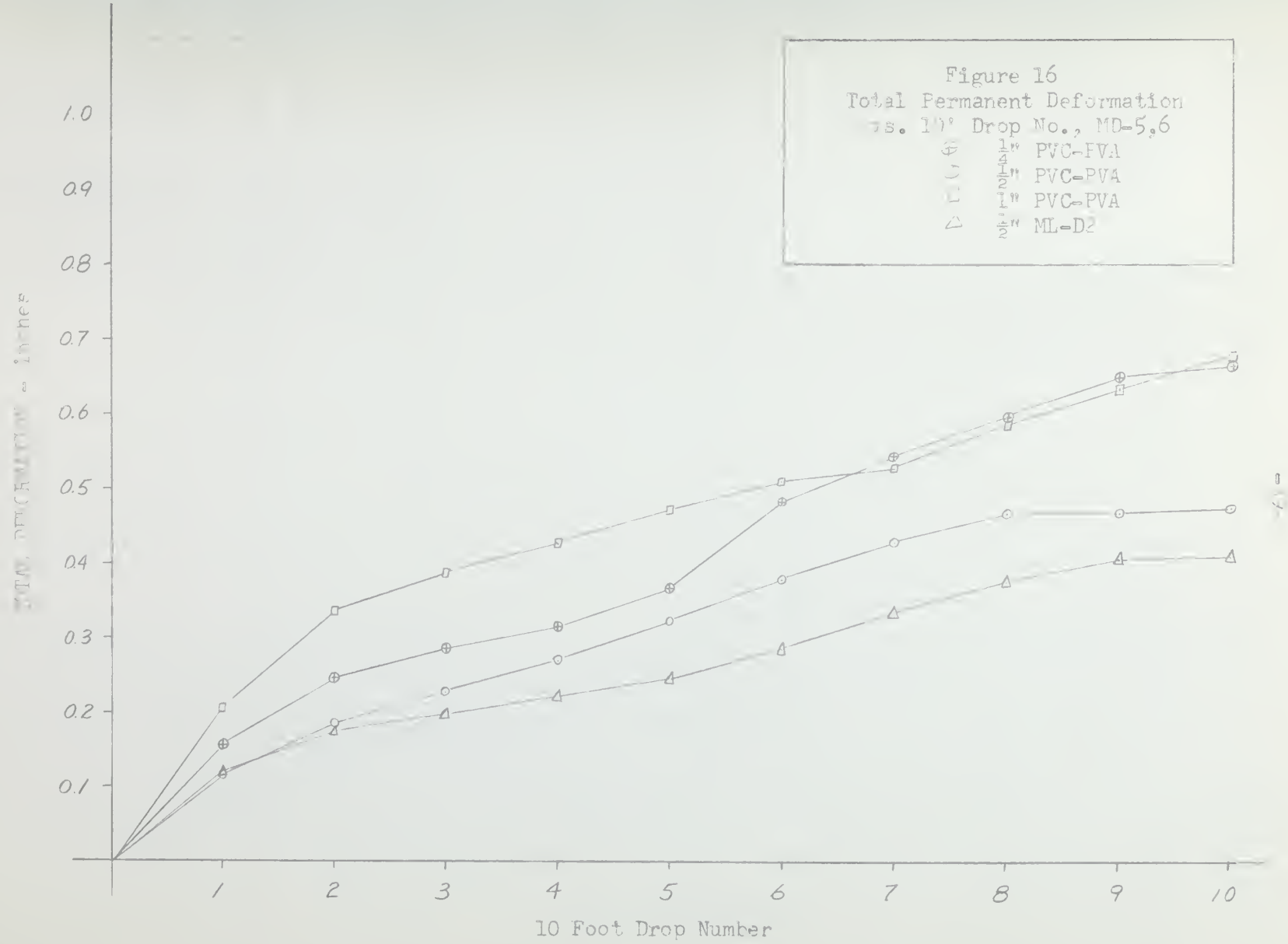
Figure 16
Total Permanent Deformation
vs. 10' Drop No., MD-5,6
¼" PVC-PVA
½" PVC-PVA
1" PVC-PVA
½" ML-D2
1.0
0.9
0.8
0.7
0.6
0.5
0.4
0.3
0.2
0.1
1
2
3
4
5
6
7
8
9
10
10 Foot Drop Number

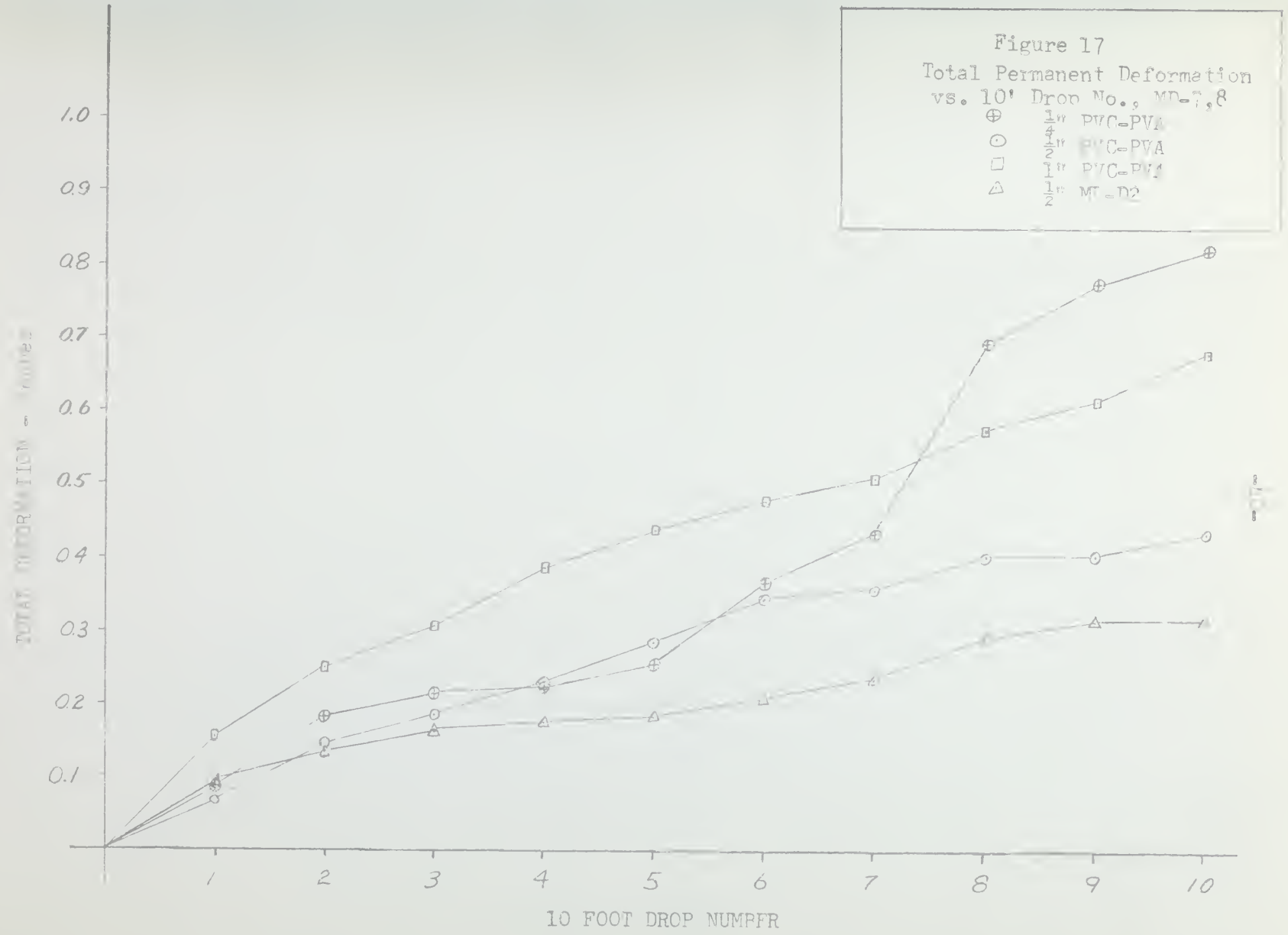
Figure 17
Total Permanent Deformation
vs. 10' Drop No., MD-7,8
1.0
0.9
0.8
0.7
0.6
0.5
0.4
0.3
0.2
0.1
1
2
3
4
5
6
7
8
9
10
10 FOOT DROP NUMBER

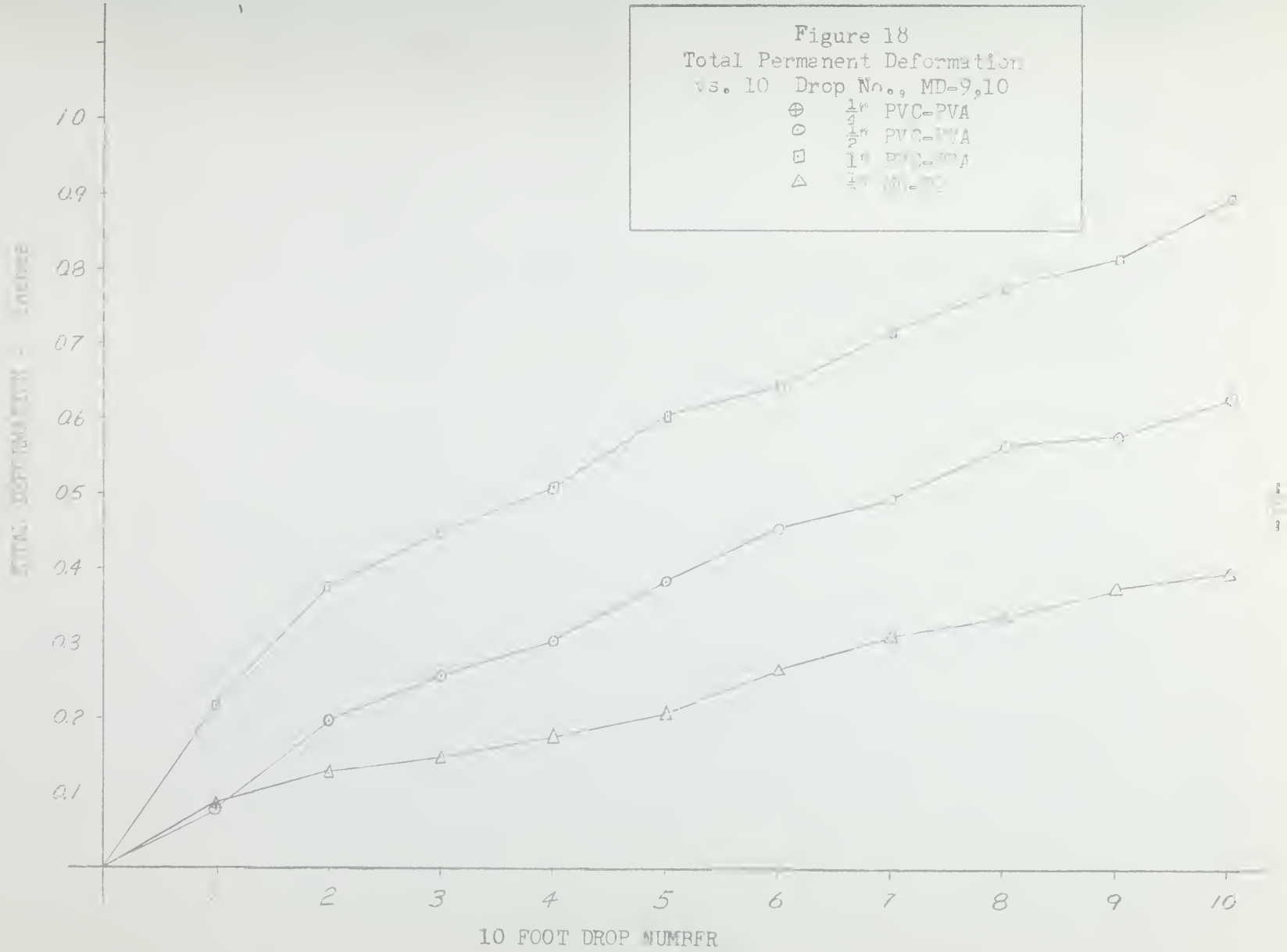
Figure 18
Total Permanent Deformation
vs. 10 Drop No., MD-9,10
⊕ ¼" PVC-PVA
⊙ ½" PVC-PVA
⊡ 1" PVC-PVA
△ ½" MD-9,10
10
0.9
0.8
0.7
0.6
0.5
0.4
0.3
0.2
0.1
2
3
4
5
6
7
8
9
10
10 FOOT DROP NUMBER

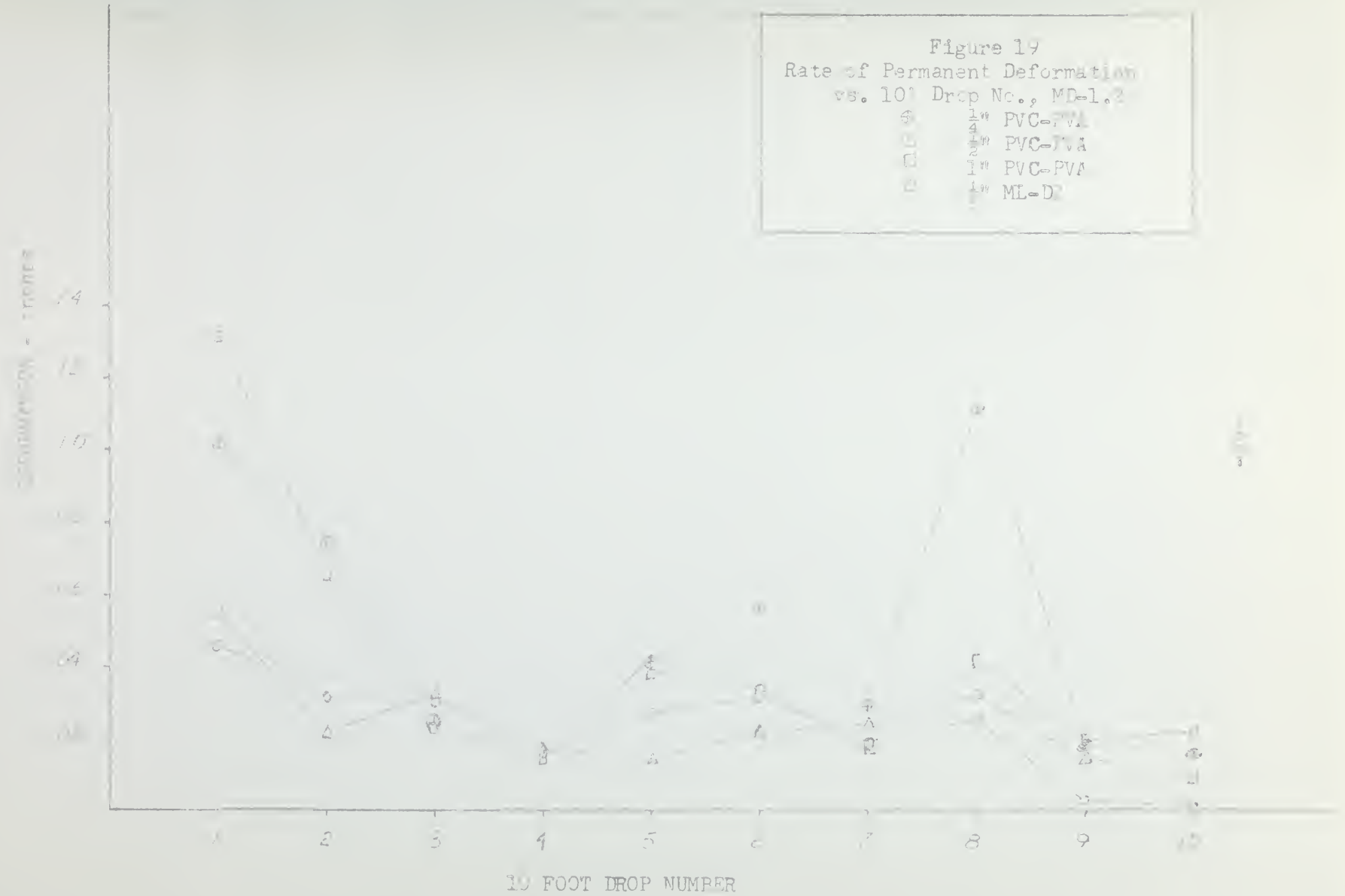
Figure 19
Rate of Permanent Deformation
vs. 10' Drop No., MD-1.2
¼" PVC-PVA
½" PVC-PVA
1" PVC-PVA
¼" ML-D
10 FOOT DROP NUMBER

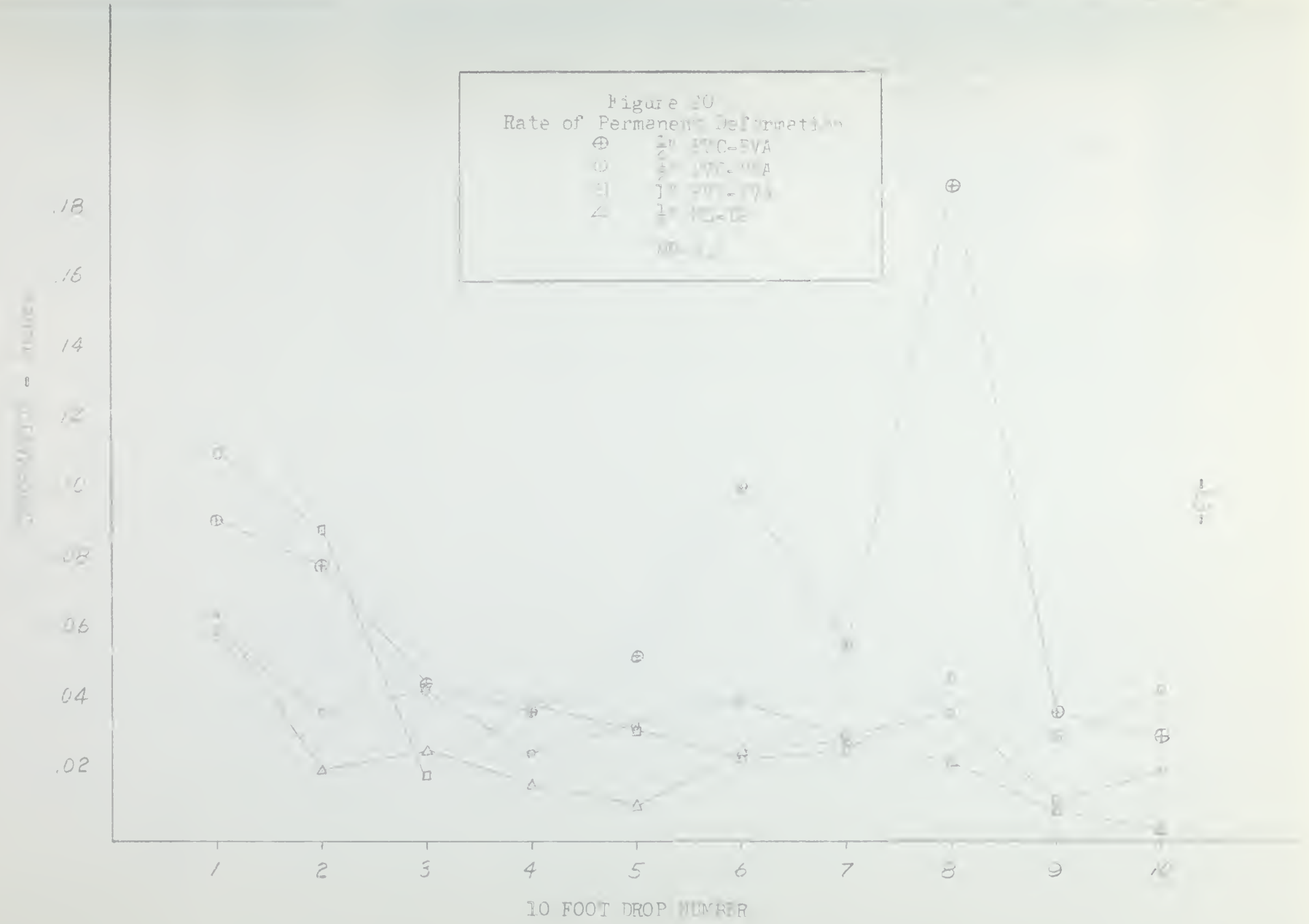
Figure 20
Rate of Permanent Deformation
.18
.16
14
12
.10
.08
.06
.04
.02
1
2
3
4
5
6
7
8
9
10
10 FOOT DROP NUMBER

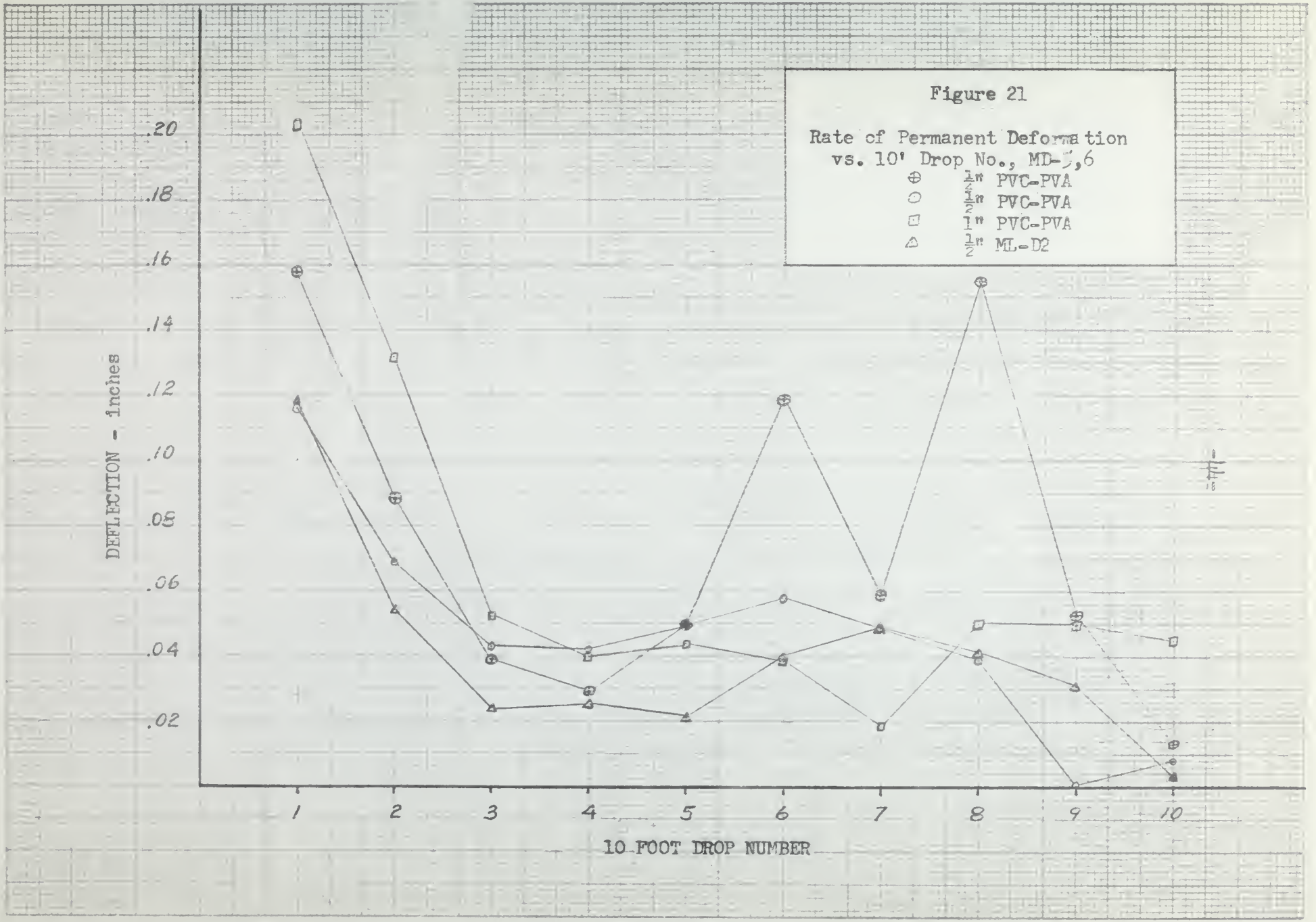
Figure 21
Rate of Permanent Deformation
vs. 10' Drop No., MD-5,6
⊕ ½" PVC-PVA
○ ½" PVC-PVA
□ 1" PVC-PVA
△ ½" ML-D2
DEFLECTION - inches
.20
.18
.16
.14
.12
.10
.08
.06
.04
.02
1
2
3
4
5
6
7
8
9
10
10 FOOT DROP NUMBER

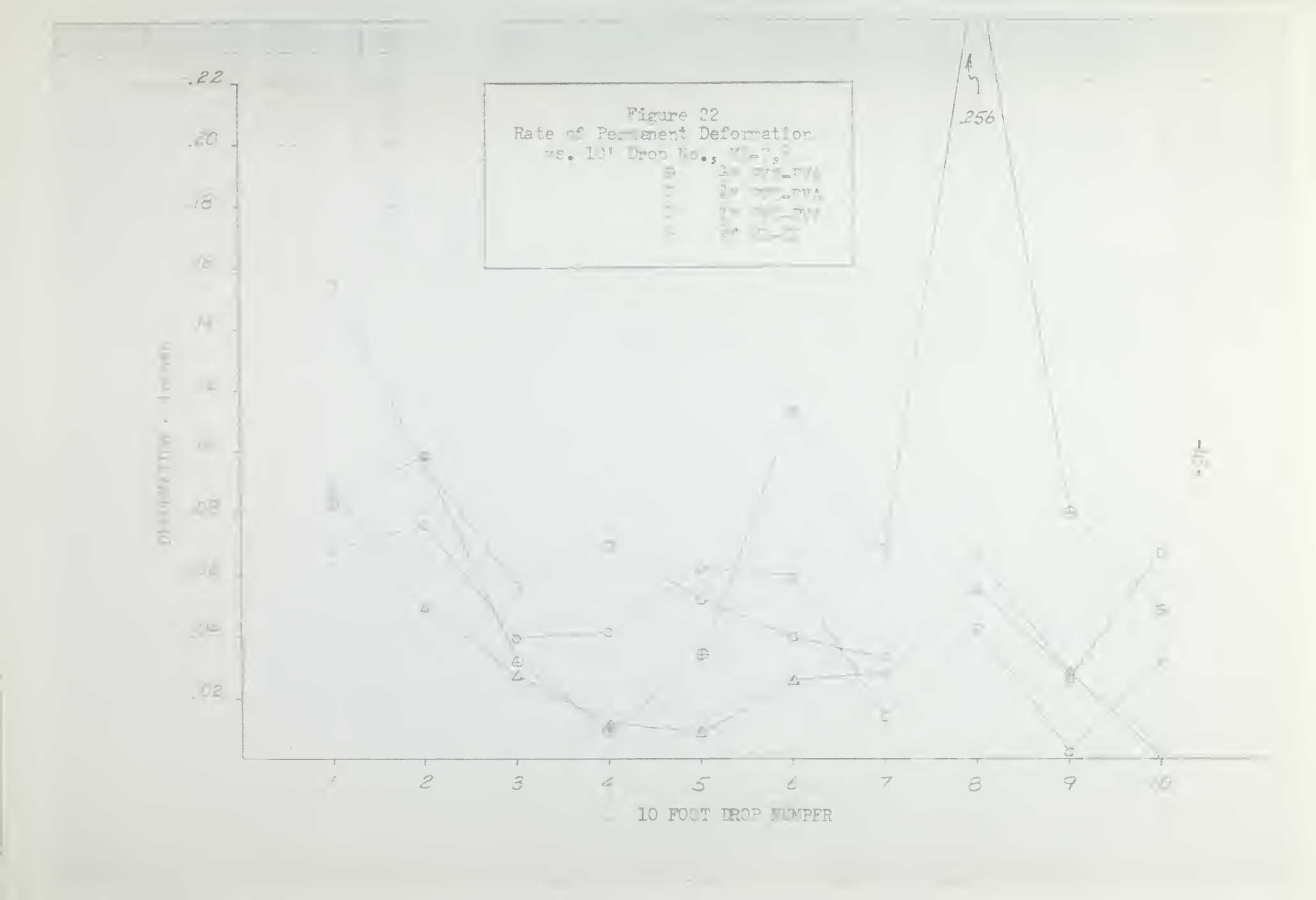
Figure 22
Rate of Permanent Deformation
vs. 10' Drop No., W=7.2
.22
.20
.18
.02
.256
10 FOOT DROP NUMBER

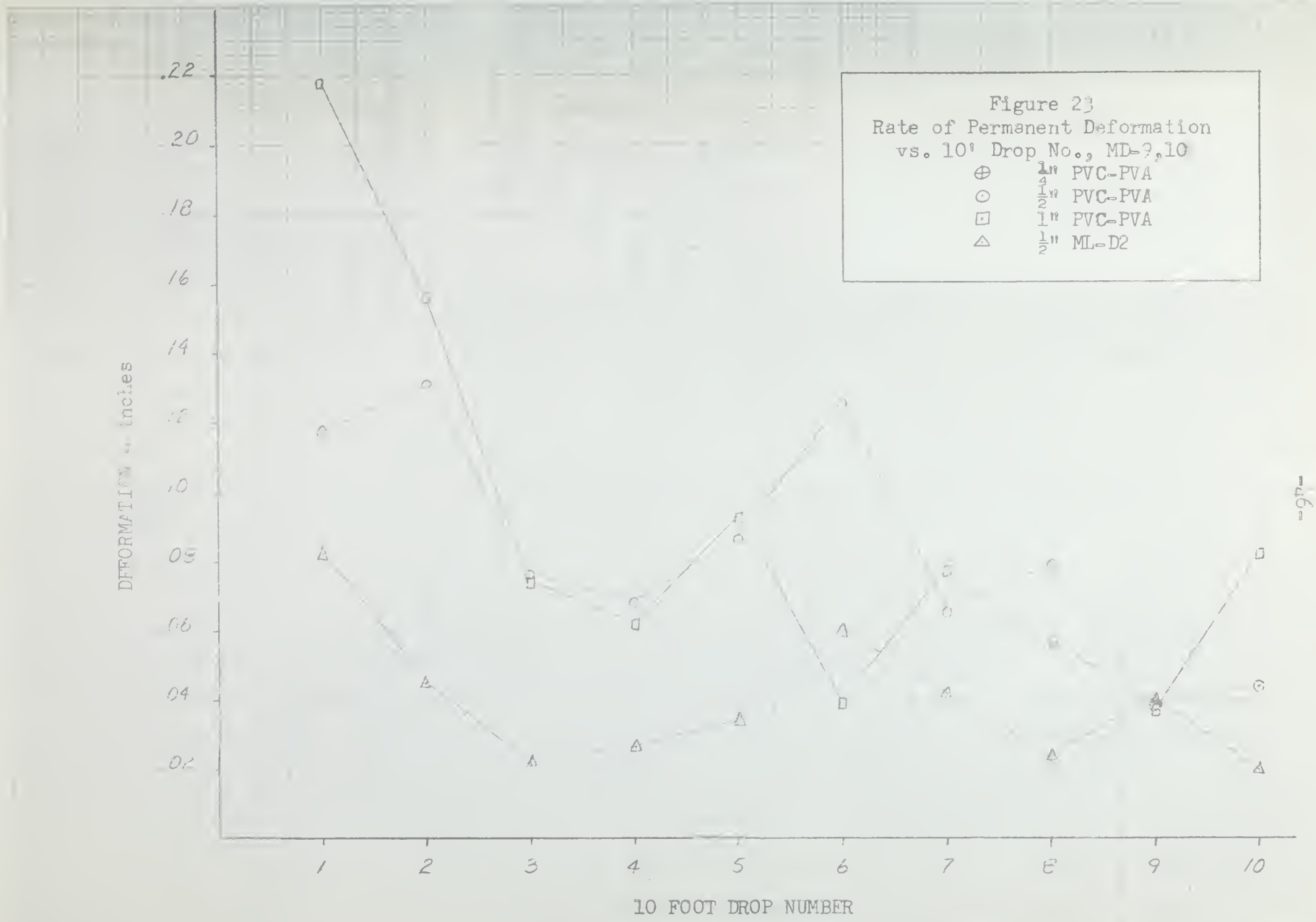
Figure 23
Rate of Permanent Deformation
vs. 10' Drop No., MD-?,10
1" PVC-PVA
½" PVC-PVA
1" PVC-PVA
½" ML-D2
DEFORMATION - Inches
.22
.20
.18
.16
.14
.12
.10
.08
.06
.04
.02
1
2
3
4
5
6
7
8
9
10
10 FOOT DROP NUMBER

Figure 24

Total Permanent Deformation vs. 10' Drop No. for ½" PVC-PVA, and Unbacked Model 12 inches From Keel

⊙ ½" PVC-PVA

• Unbacked Model

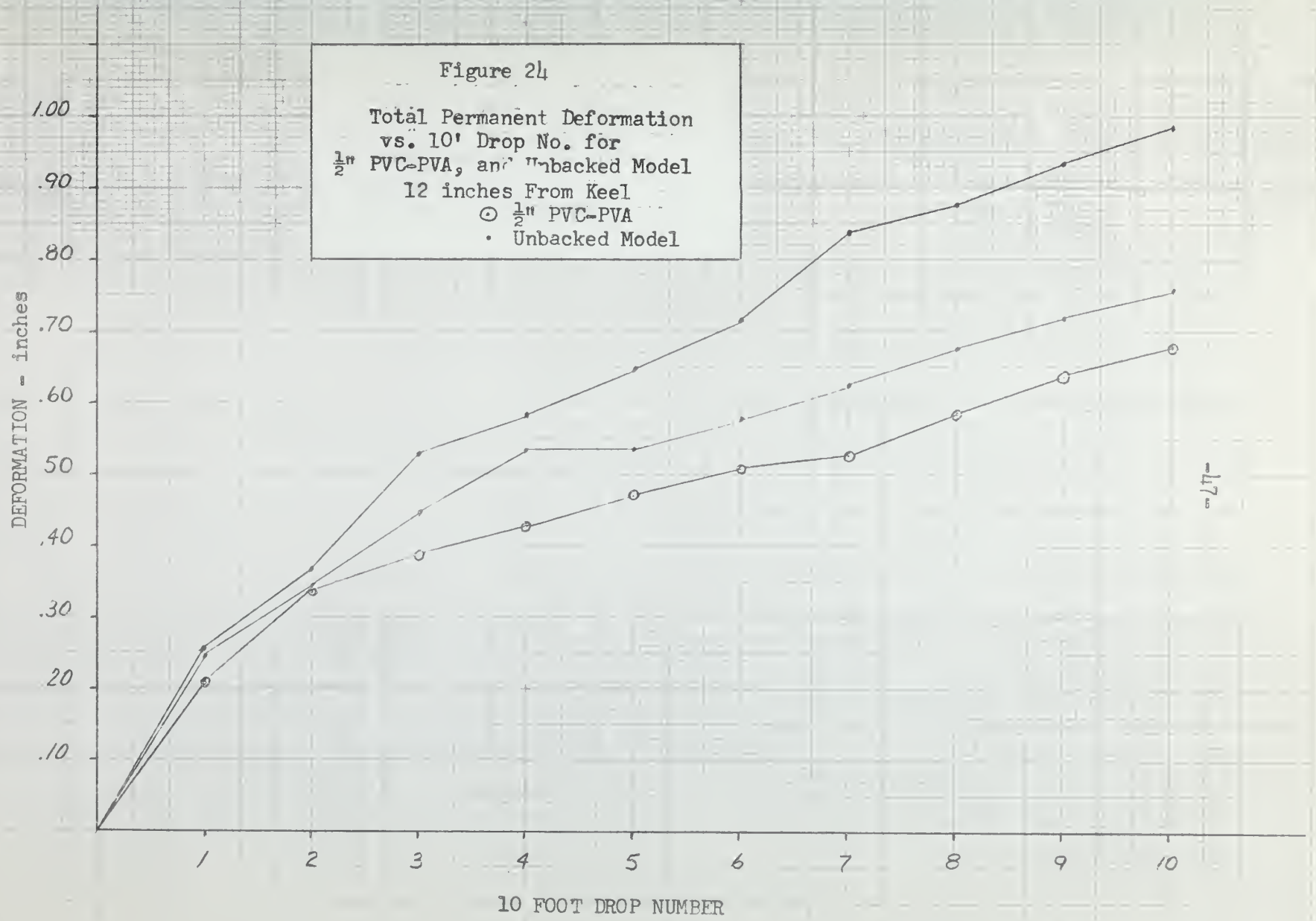

Figure 25

Final Permanent Deformation
Along Keel

- • Model KG 1
- ⊡ Model MG 1
- ⊙ Model MG 2

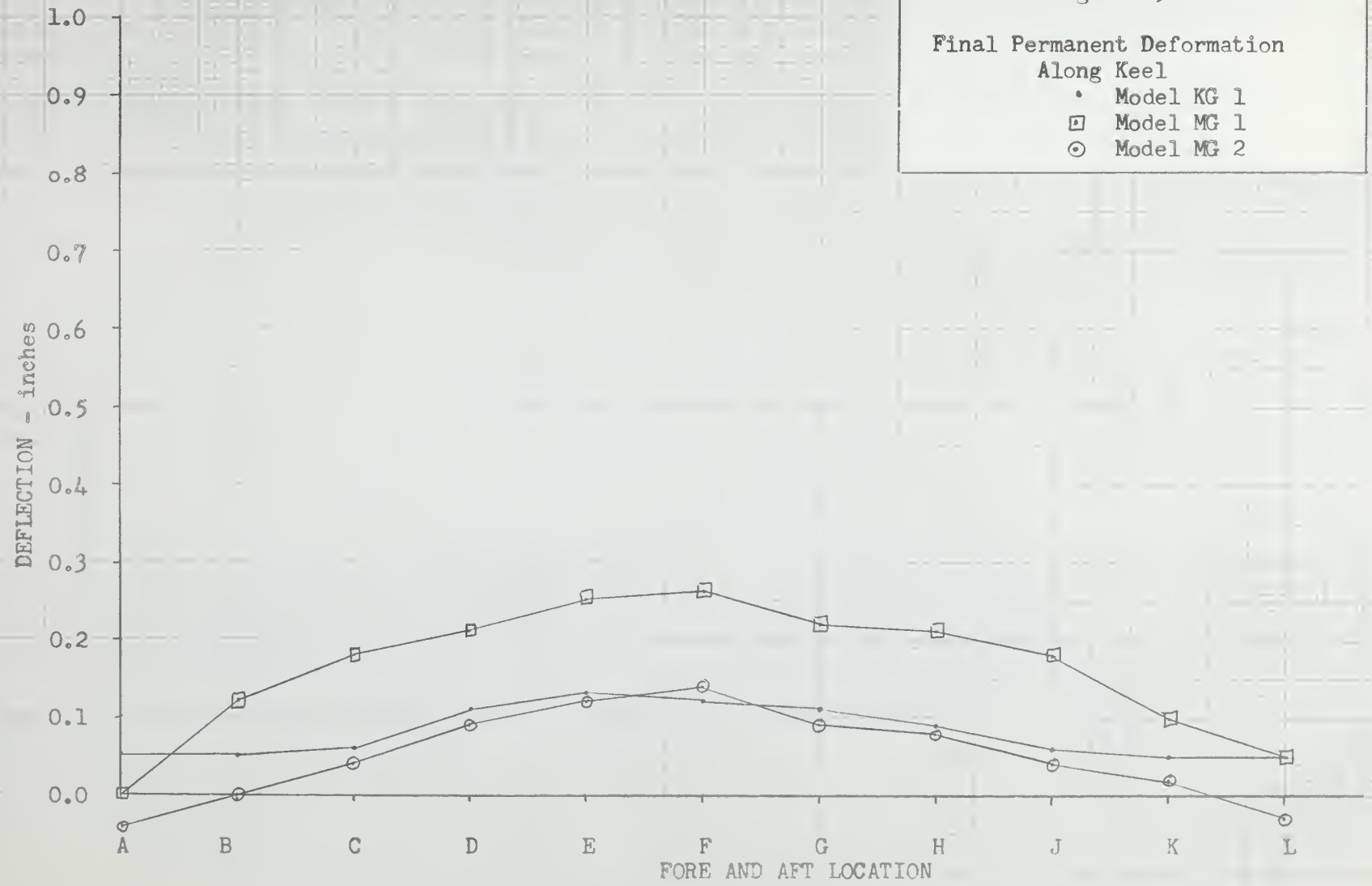

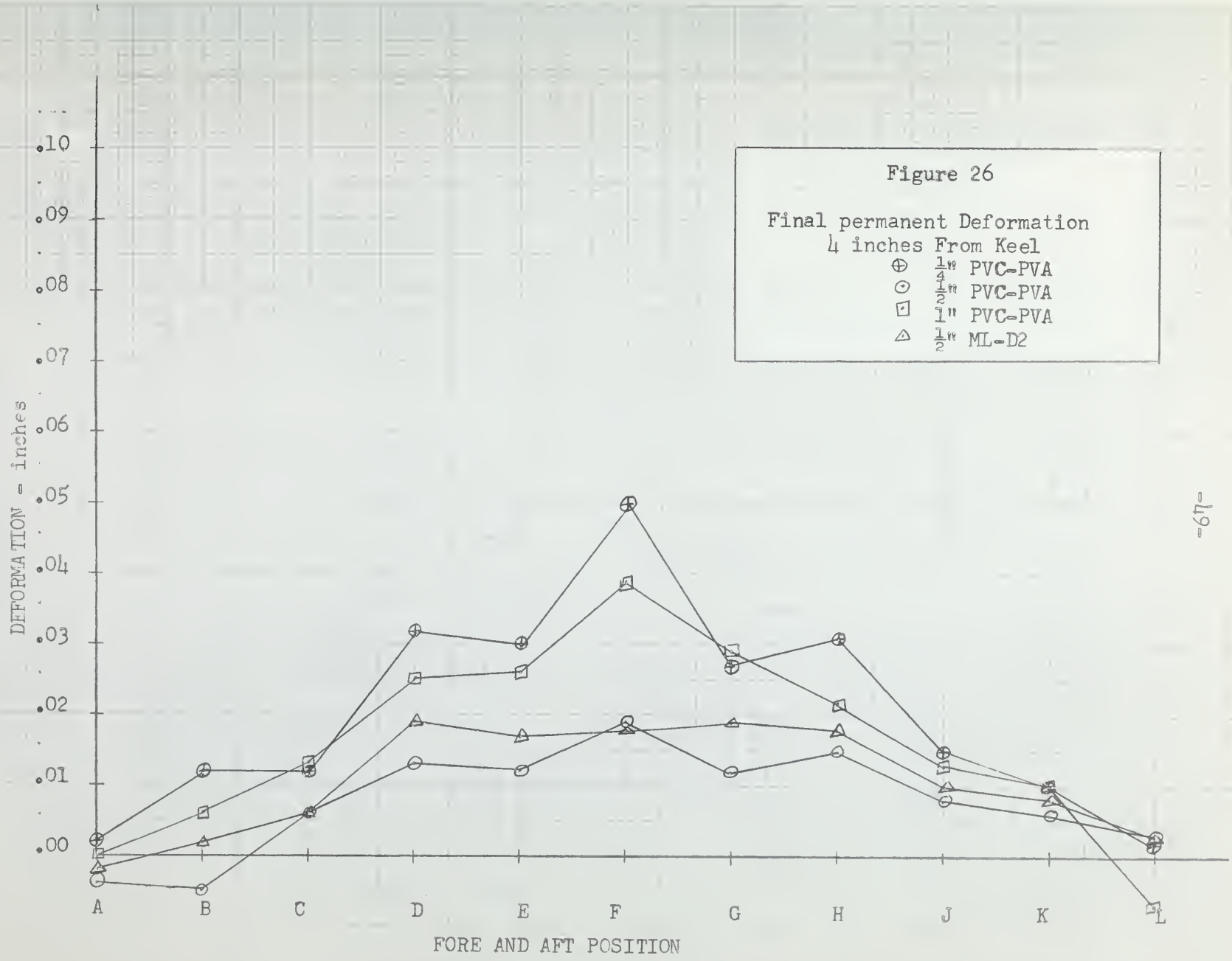
Figure 26
Final permanent Deformation
4 inches From Keel
¼" PVC-PVA
½" PVC-PVA
1" PVC-PVA
½" ML-D2
DEFORMATION - inches
.10
.09
.08
.07
.06
.05
.04
.03
.02
.01
.00
A
B
C
D
E
F
G
H
J
K
L
FORE AND AFT POSITION

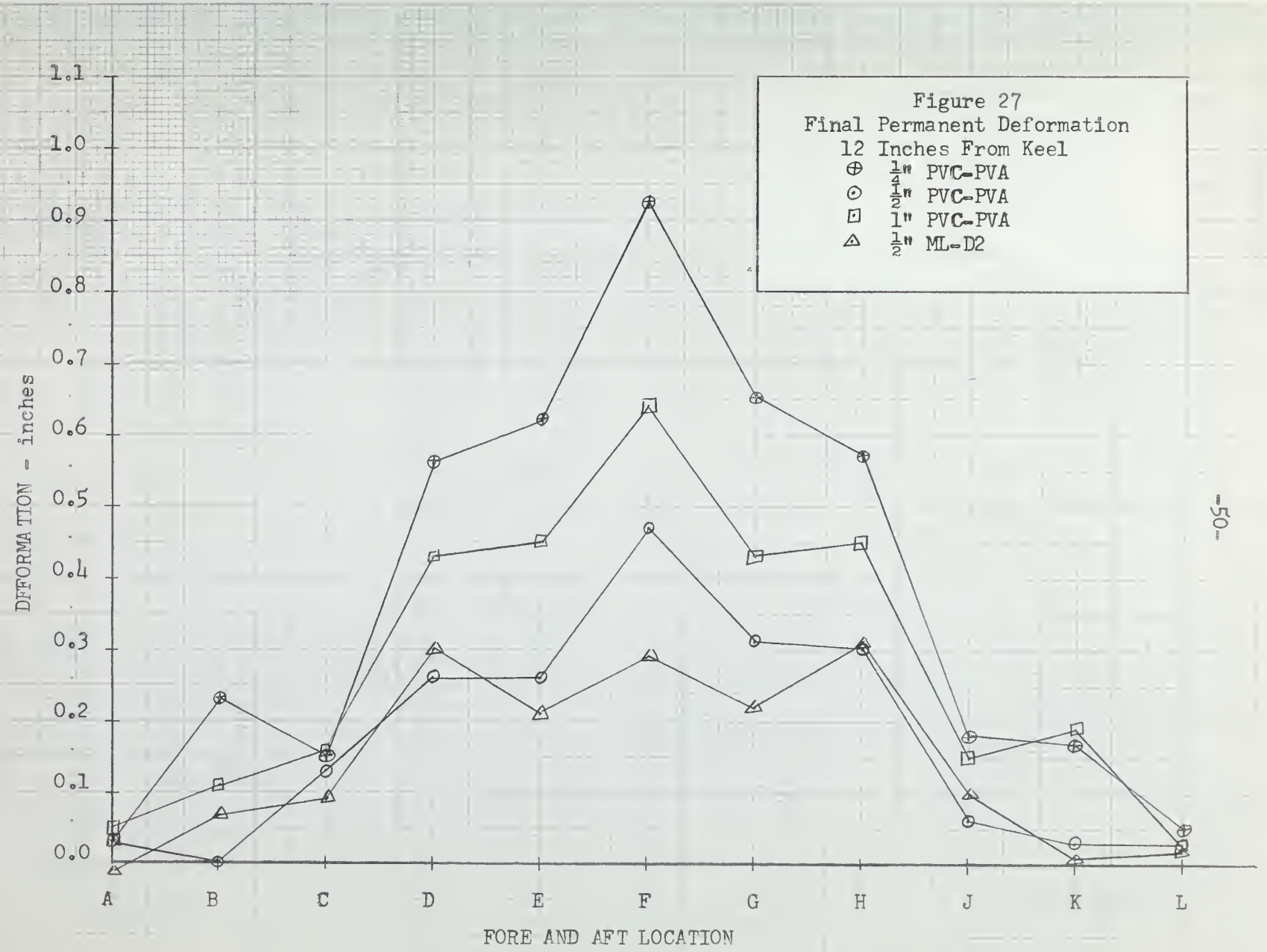
Figure 27
Final Permanent Deformation
12 Inches From Keel
¼" PVC-PVA
½" PVC-PVA
1" PVC-PVA
½" ML-D2
DEFORMATION - inches
1.1
1.0
0.9
0.8
0.7
0.6
0.5
0.4
0.3
0.2
0.1
0.0
A
B
C
D
E
F
G
H
J
K
L
FORE AND AFT LOCATION

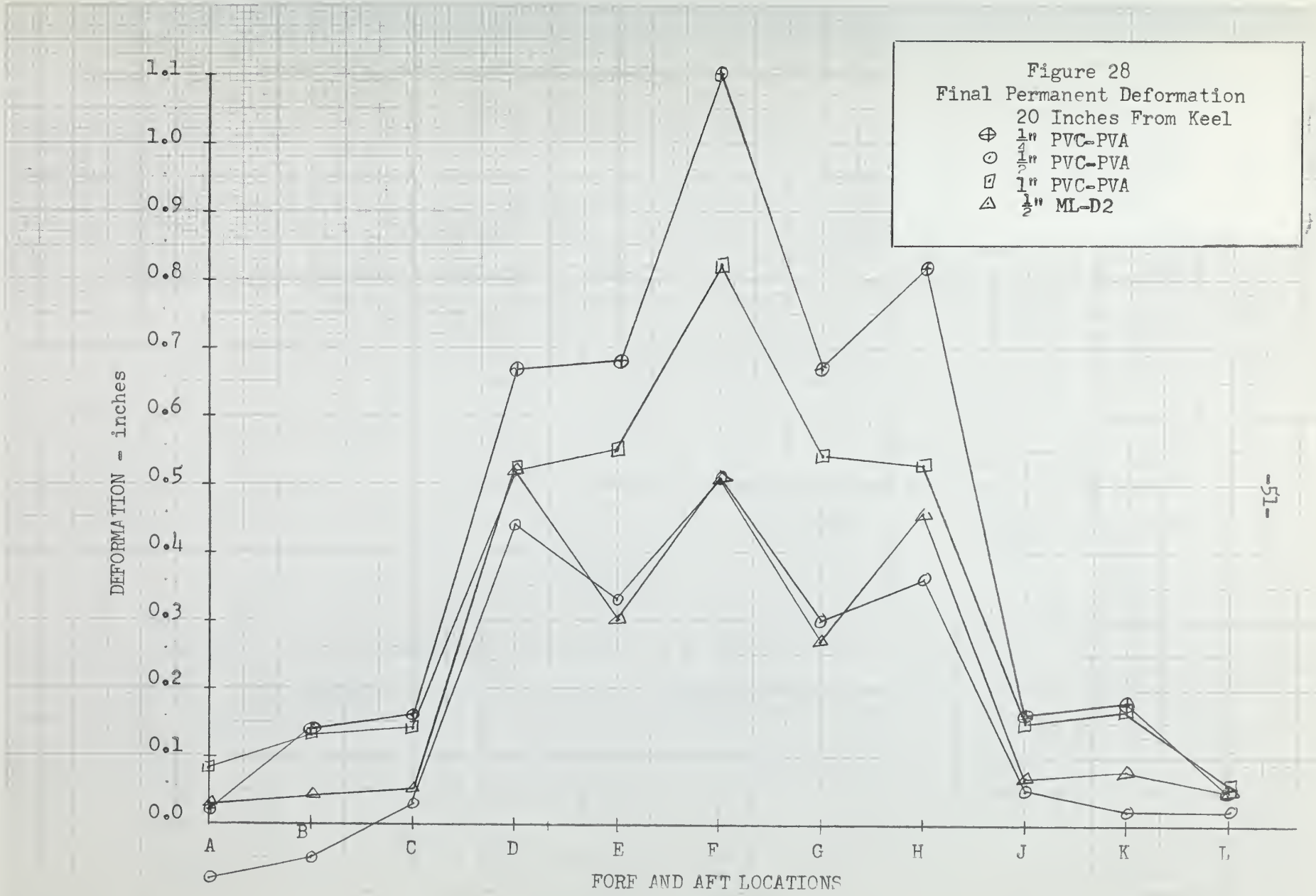
Figure 28
Final Permanent Deformation
20 Inches From Keel
1" PVC-PVA
1" PVC-PVA
1" PVC-PVA
½" ML-D2
DEFORMATION - inches
1.1
1.0
0.9
0.8
0.7
0.6
0.5
0.4
0.3
0.2
0.1
0.0
A
B
C
D
E
F
G
H
J
K
L
FORE AND AFT LOCATIONS

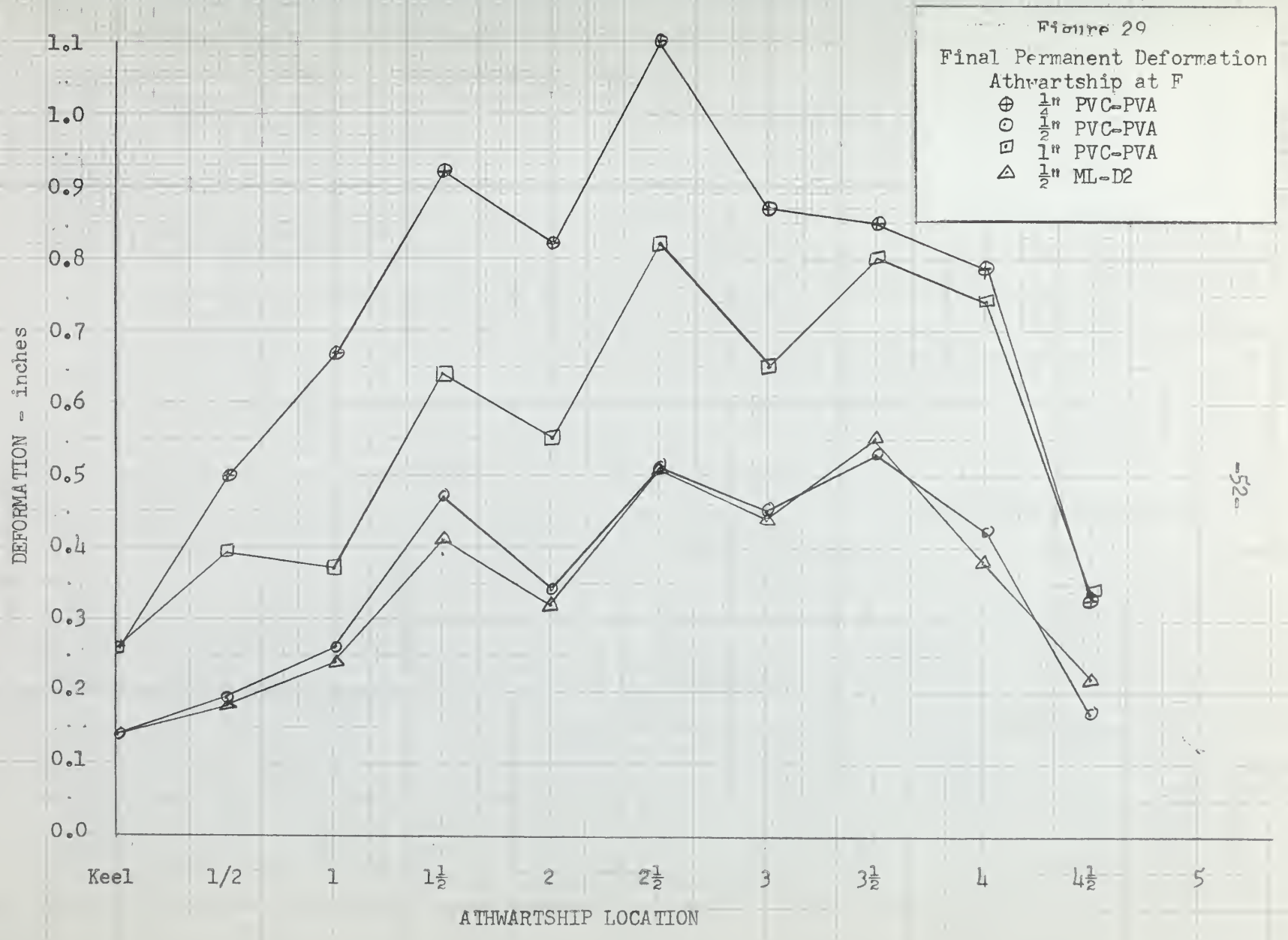
Figure 29
Final Permanent Deformation
Athwartship at F
¼" PVC-PVA
½" PVC-PVA
1" PVC-PVA
½" ML-D2
DEFORMATION - inches
1.1
1.0
0.9
0.8
0.7
0.6
0.5
0.4
0.3
0.2
0.1
0.0
Keel
1/2
1
1½
2
2½
3
3½
4
4½
5
ATHWARTSHIP LOCATION

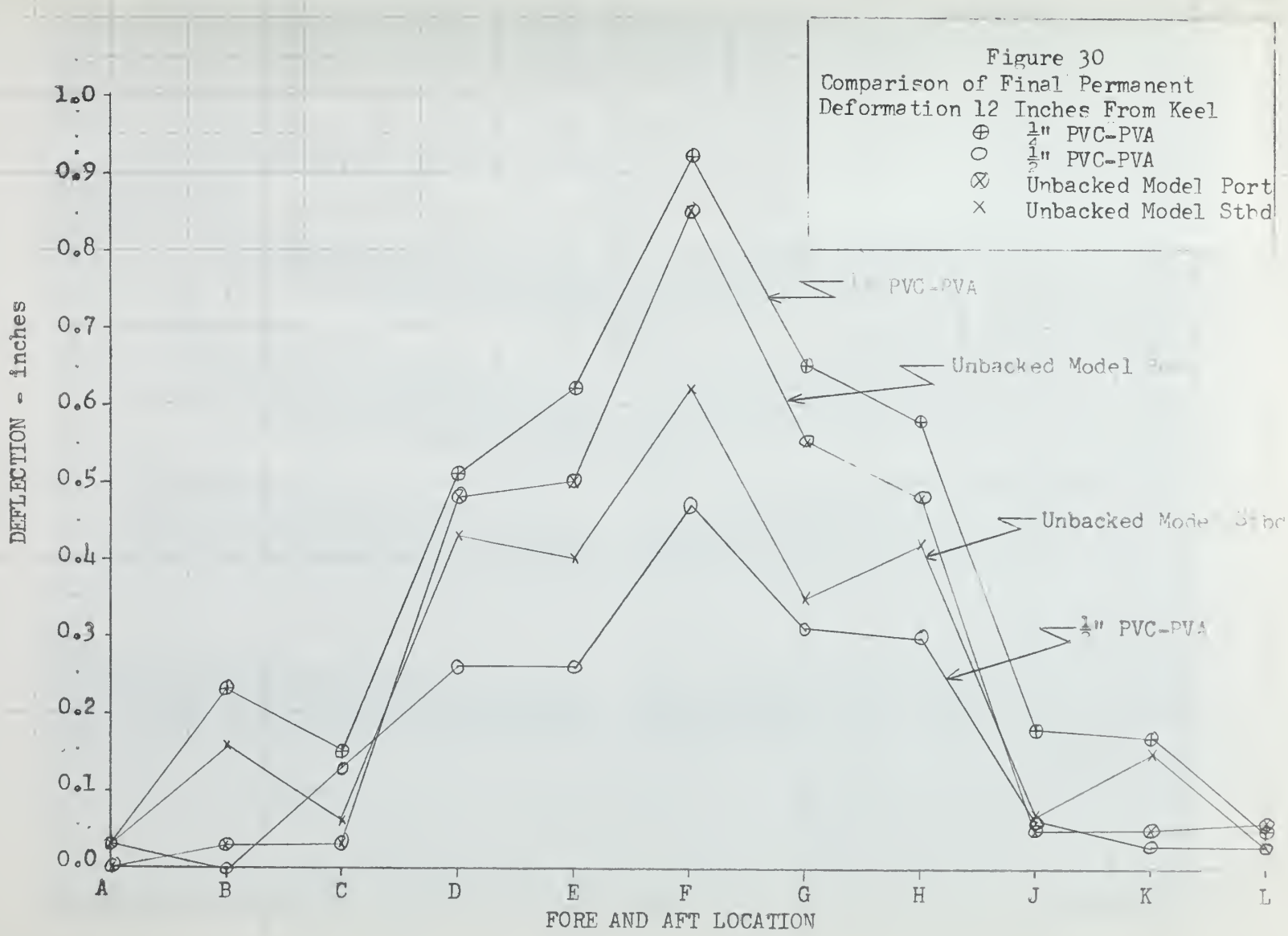
Figure 30
Comparison of Final Permanent
Deformation 12 Inches From Keel
⊕ ¼" PVC-PVA
○ ½" PVC-PVA
⊗ Unbacked Model Port
× Unbacked Model Stbd
PVC-PVA
Unbacked Model
Unbacked Mode
¼" PVC-PVA
DEFLECTION - Inches
1.0
0.9
0.8
0.7
0.6
0.5
0.4
0.3
0.2
0.1
0.0
A
B
C
D
E
F
G
H
J
K
L
FORE AND AFT LOCATION

Figure 31
Model MG 1 After 10-10 Foot Drops

Figure 32
Model MG 2 After 10-10 Foot Drops

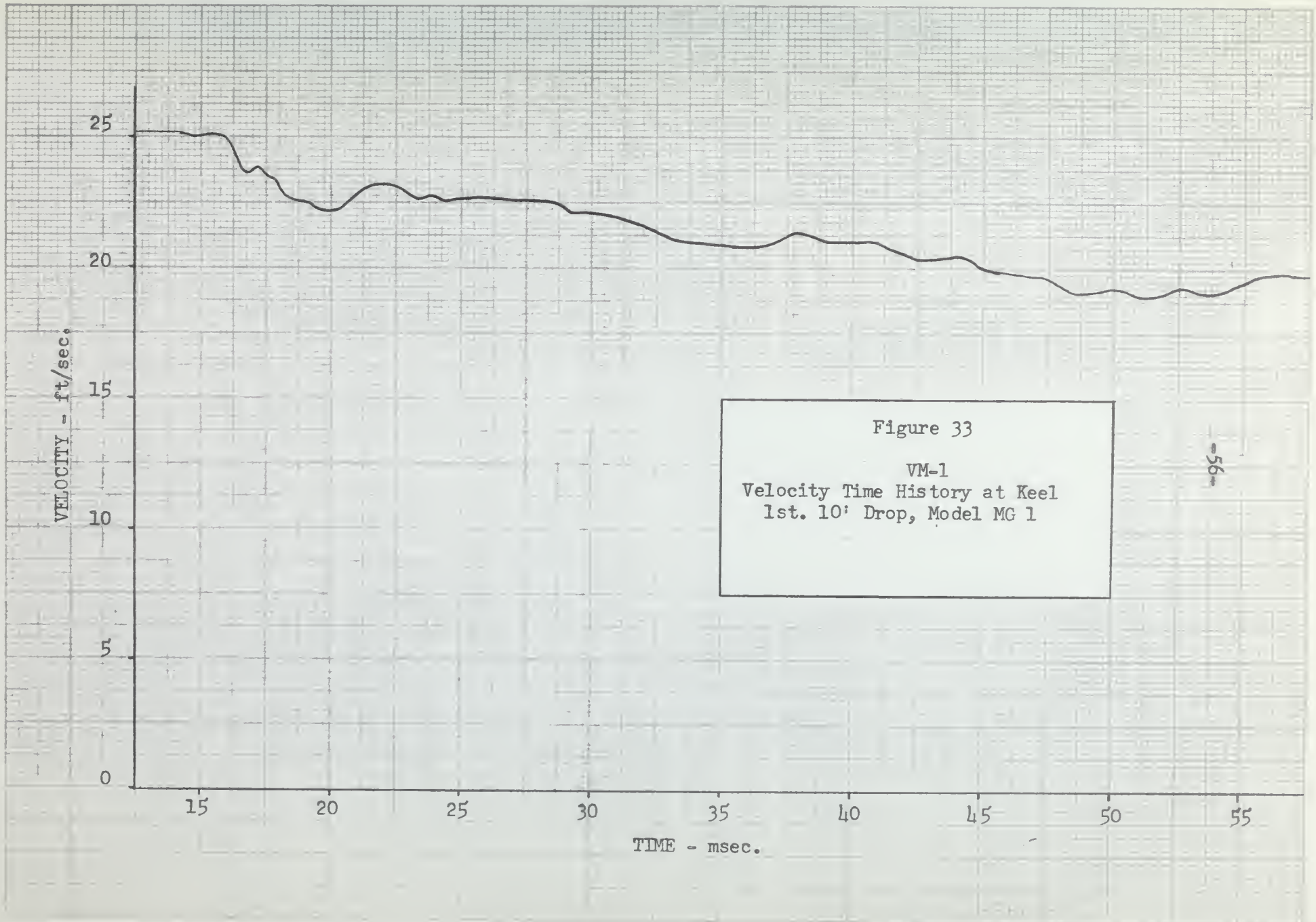

Figure 33

VM-1
Velocity Time History at Keel
1st. 10' Drop, Model MG 1

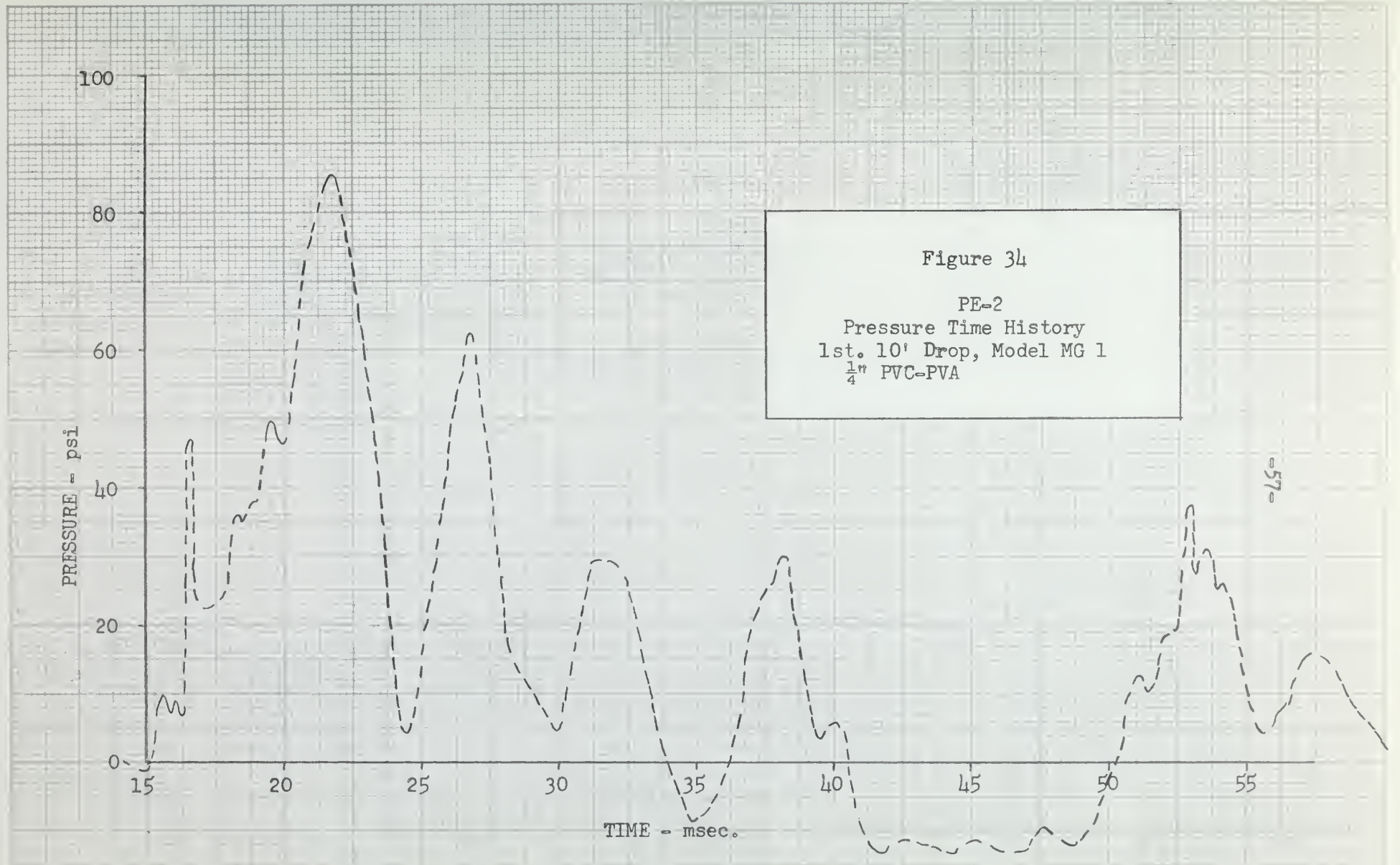

Figure 34

PE-2
Pressure Time History
1st. 10' Drop, Model MG 1
$\frac{1}{4}$" PVC-PVA

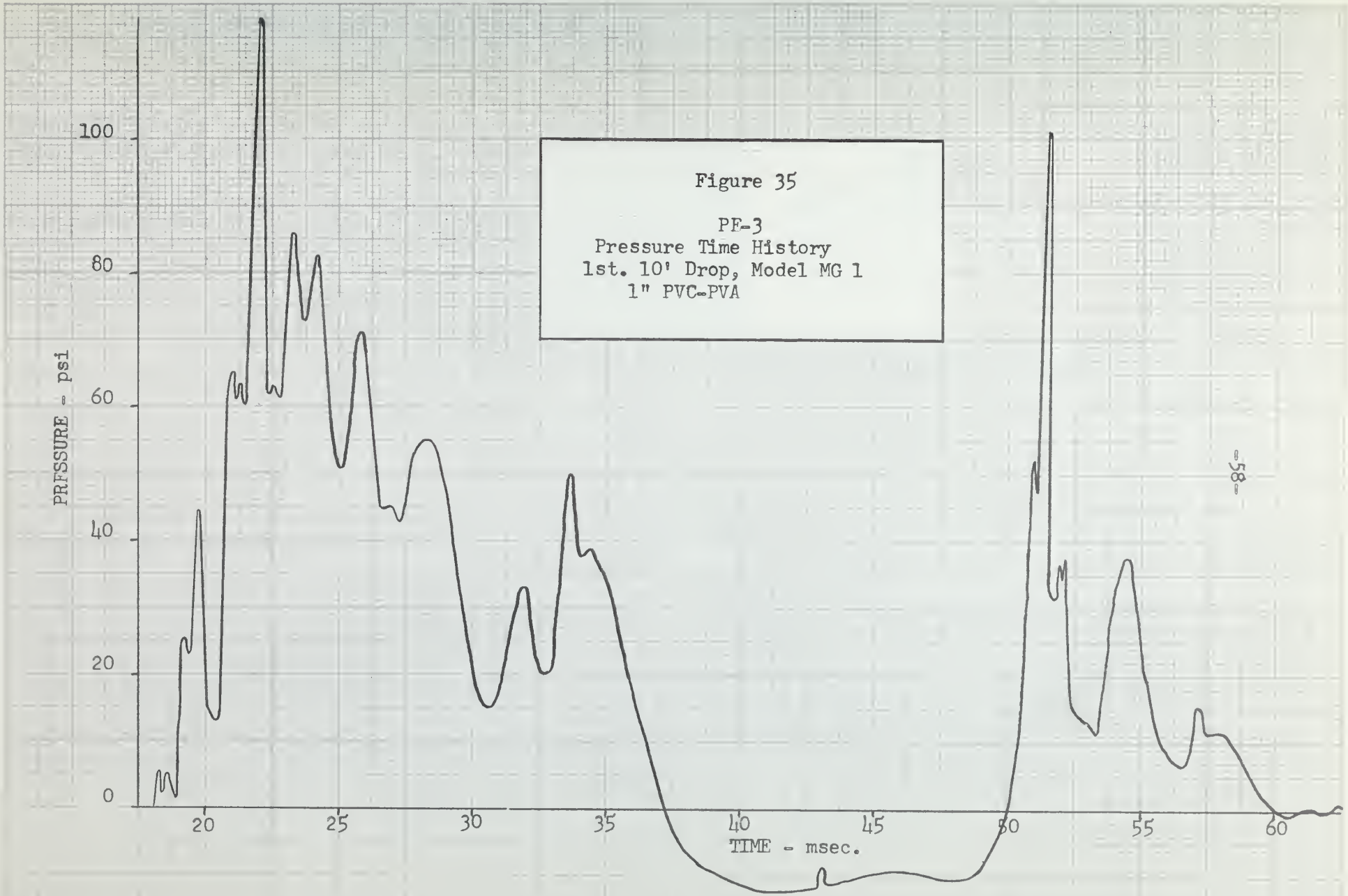

Figure 35

PF-3
Pressure Time History
1st. 10' Drop, Model MG 1
1" PVC-PVA

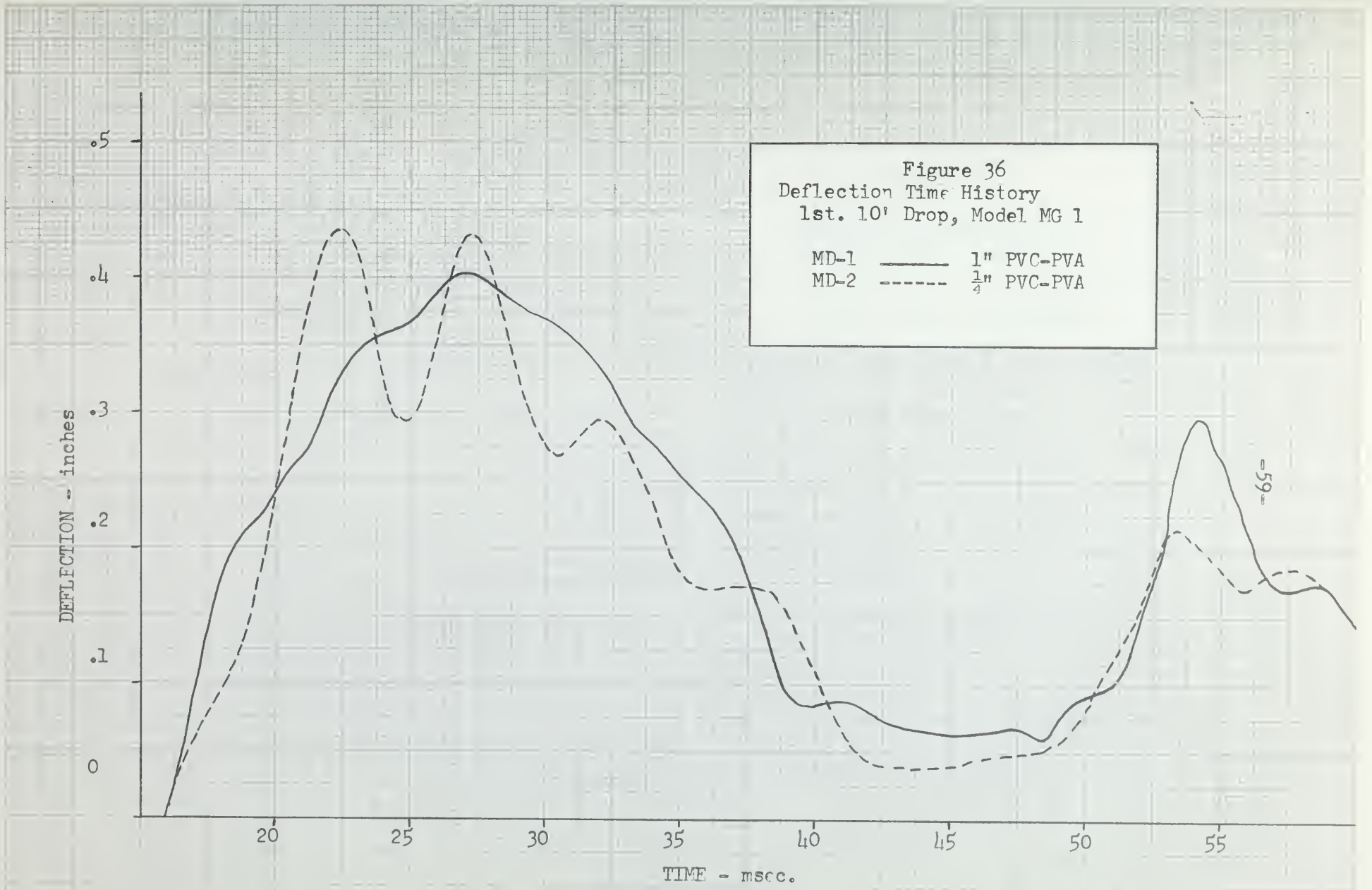
Figure 36
Deflection Time History
1st. 10' Drop, Model MG 1
MD-1 ——— 1" PVC-PVA
MD-2 ------ ¼" PVC-PVA
DEFLECTION - inches
0
.1
.2
.3
.4
.5
20
25
30
35
40
45
50
55
TIME - msec.

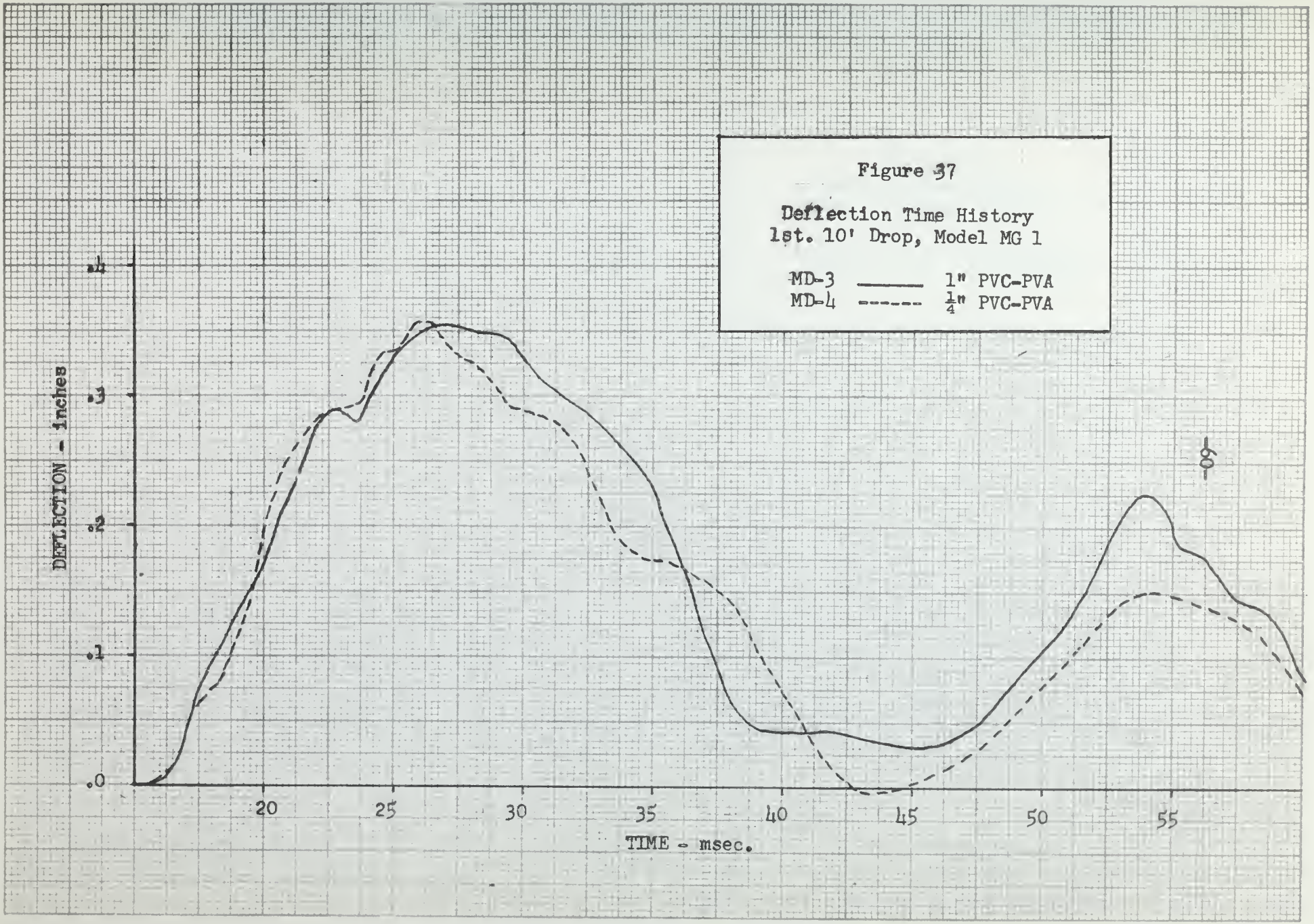
Figure 37
Deflection Time History
1st. 10' Drop, Model MG 1
MD-3 ——— 1" PVC-PVA
MD-4 ------ ¼" PVC-PVA
DEFLECTION - inches
.0
.1
.2
.3
.4
20
25
30
35
40
45
50
55
TIME - msec.

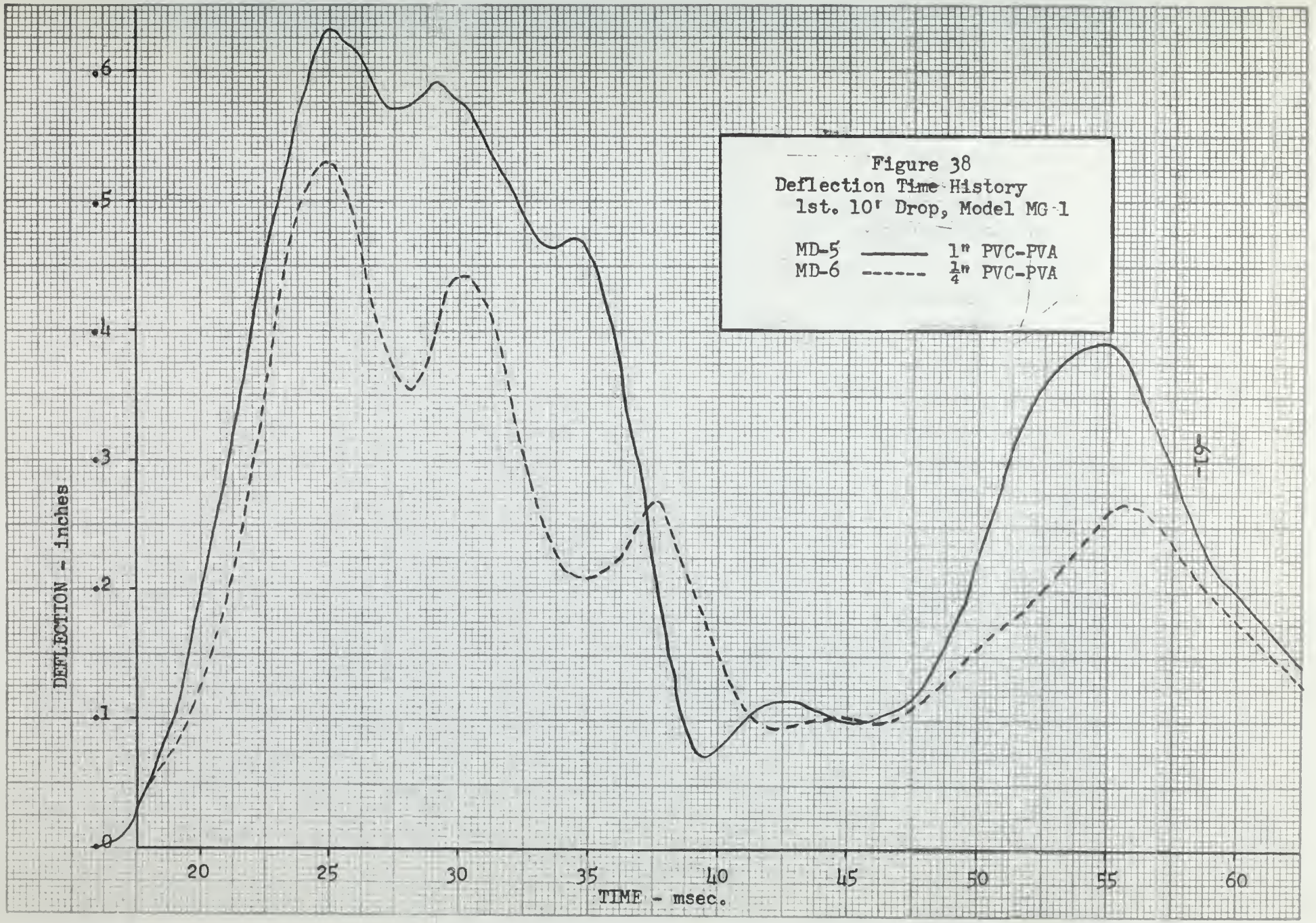
Figure 38
Deflection Time History
1st. 10' Drop, Model MG-1
MD-5 ——— 1" PVC-PVA
MD-6 ------ ¼" PVC-PVA
DEFLECTION - inches
.6
.5
.4
.3
.2
.1
0
20
25
30
35
40
45
50
55
60
TIME - msec.

Figure 39

Strain Time History
1st. 10' Drop, Model MG 1

ST-1 ——— 1" PVC-PVA
ST-2 - - - - - $\frac{1}{4}$" PVC-PVA

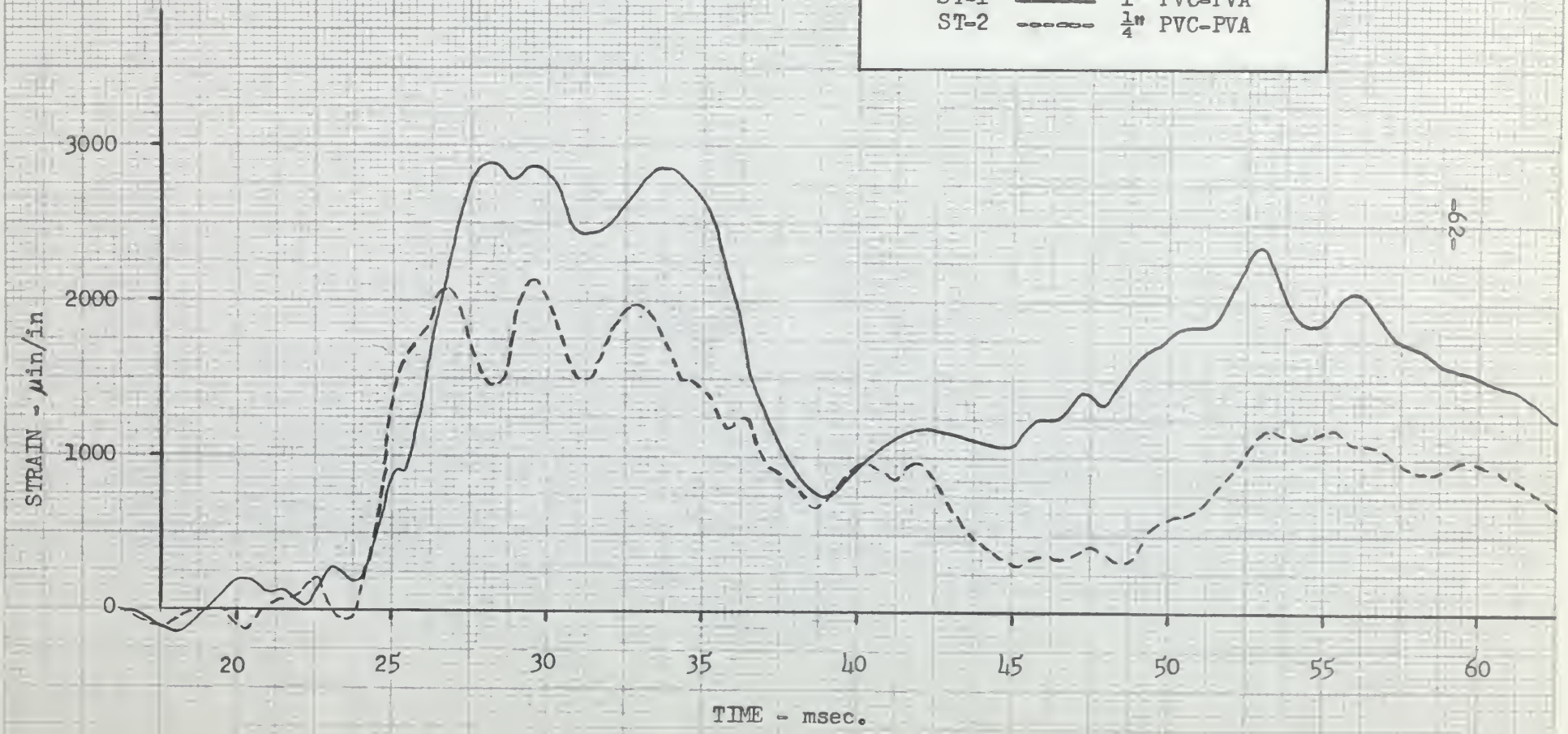

Figure 40

Strain Time History
1st. 10' Drop, Model MG 1

ST-5 ——— 1" PVC-PVA
ST-6 ------ ¼" PVC-PVA

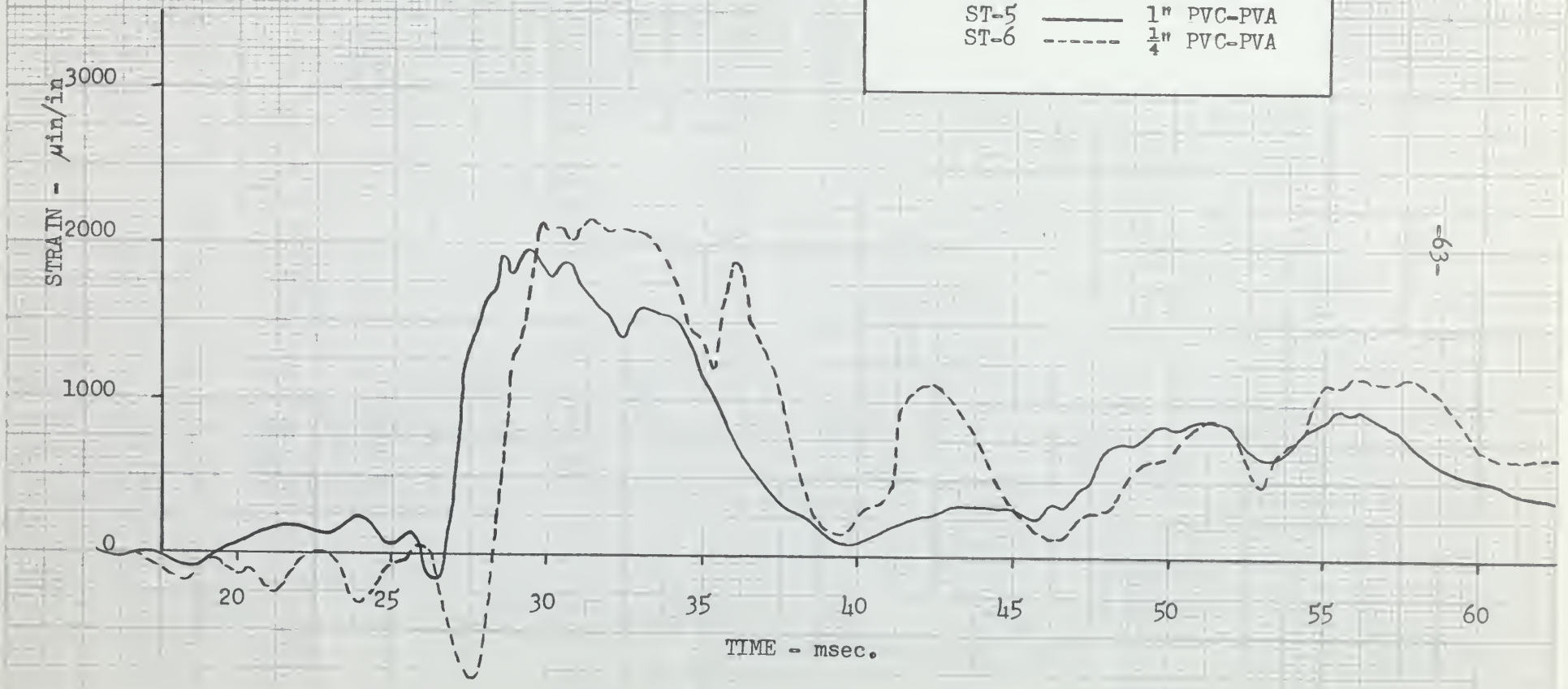

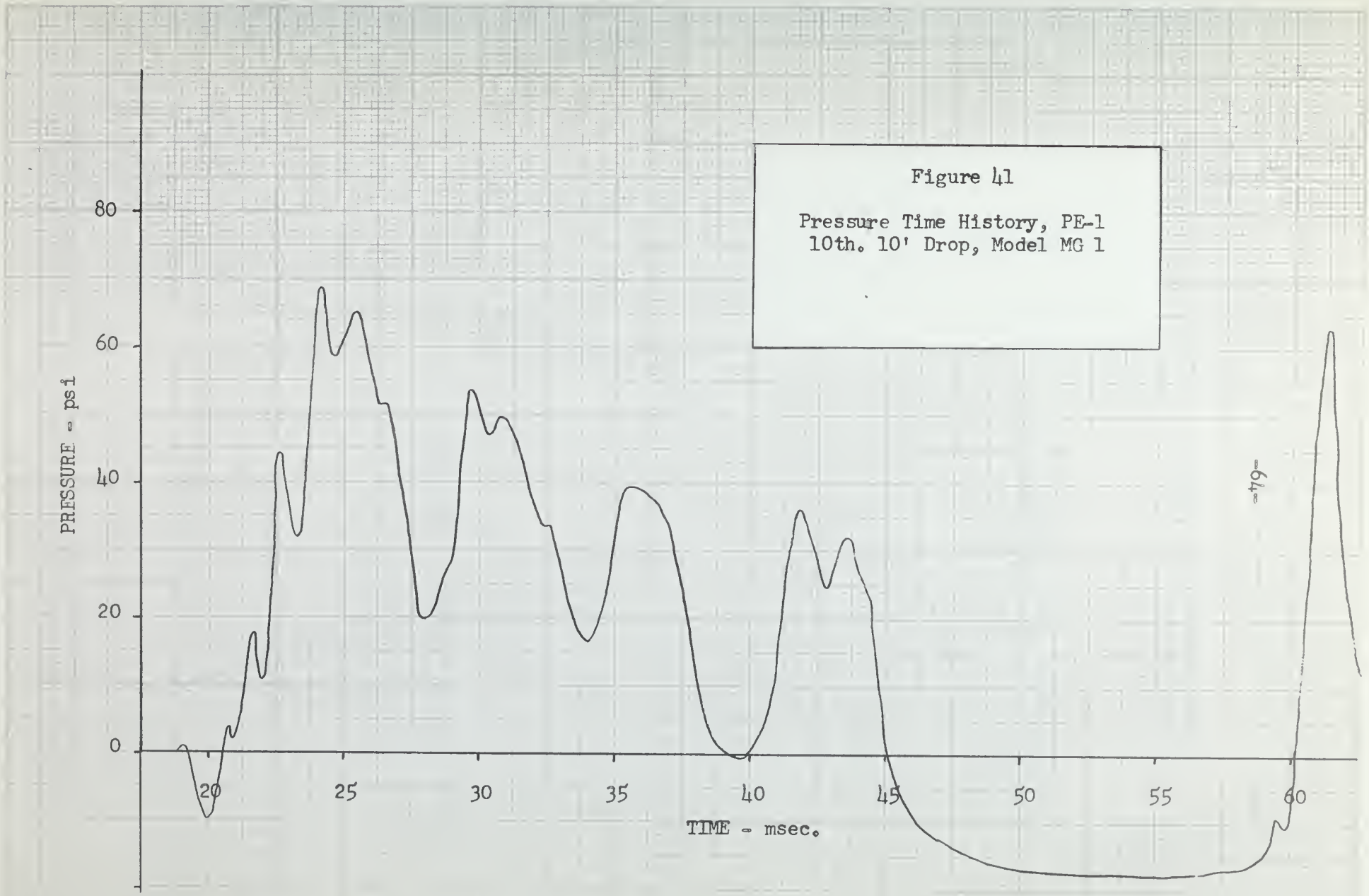
Figure 41
Pressure Time History, PE-1
10th. 10' Drop, Model MG 1
PRESSURE - psi
80
60
40
20
0
20
25
30
35
40
45
50
55
60
TIME - msec.
-64-

Figure 42

Pressure Time History, PE 3
10th. 10' Drop, Model MG 1

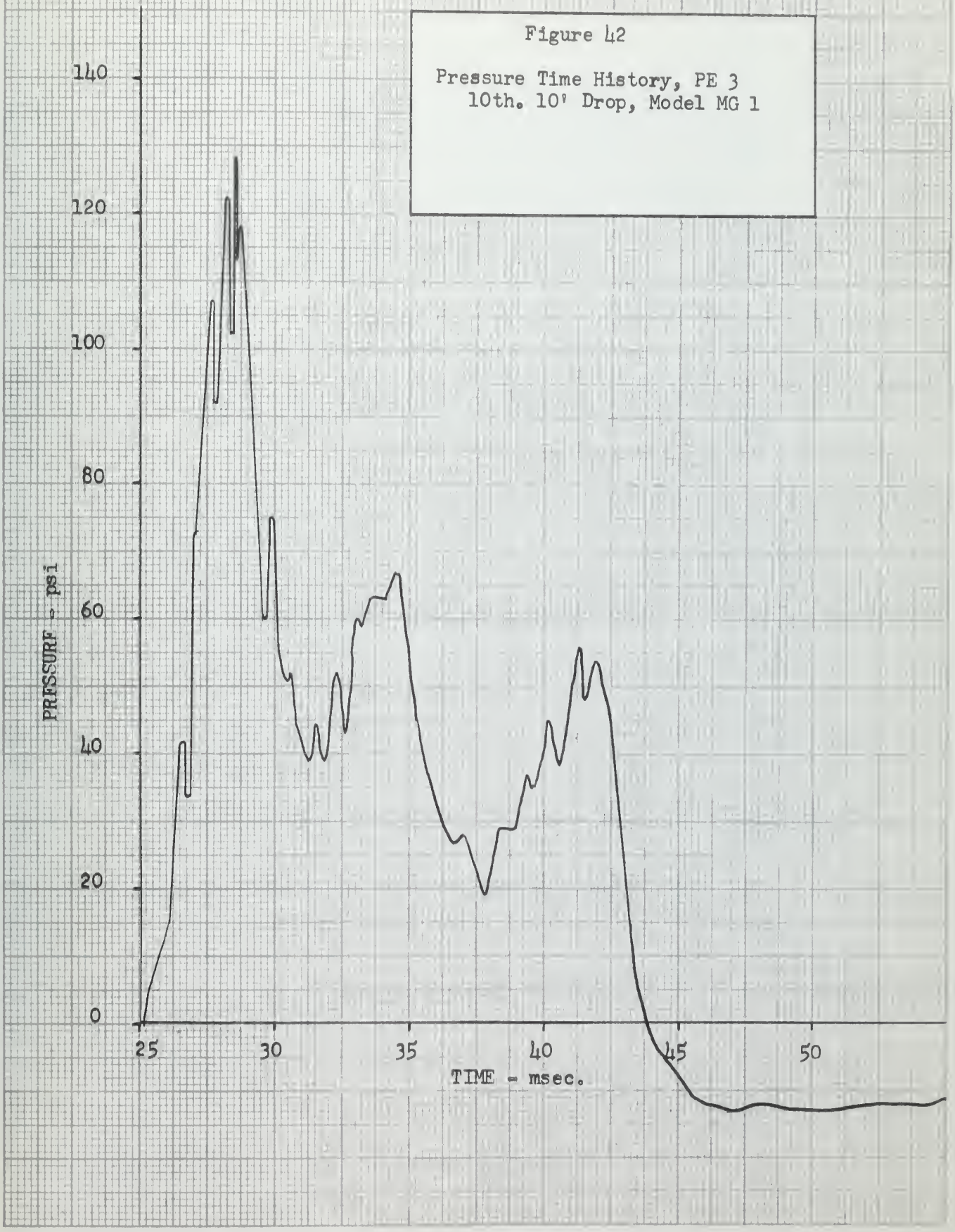

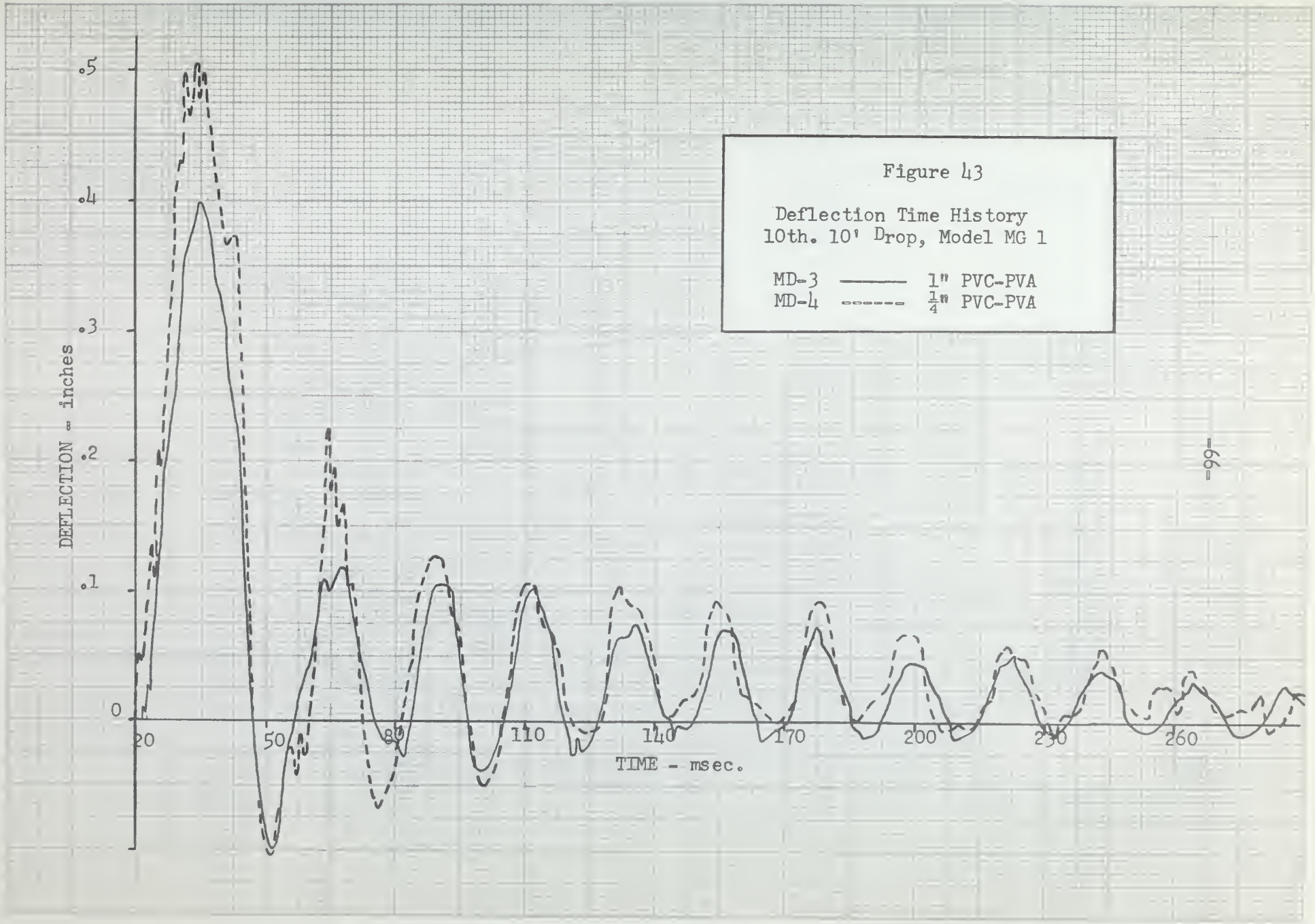

Figure 43

Deflection Time History
10th. 10' Drop, Model MG 1

MD-3 ——— 1" PVC-PVA
MD-4 - - - - - - $\frac{1}{4}$" PVC-PVA

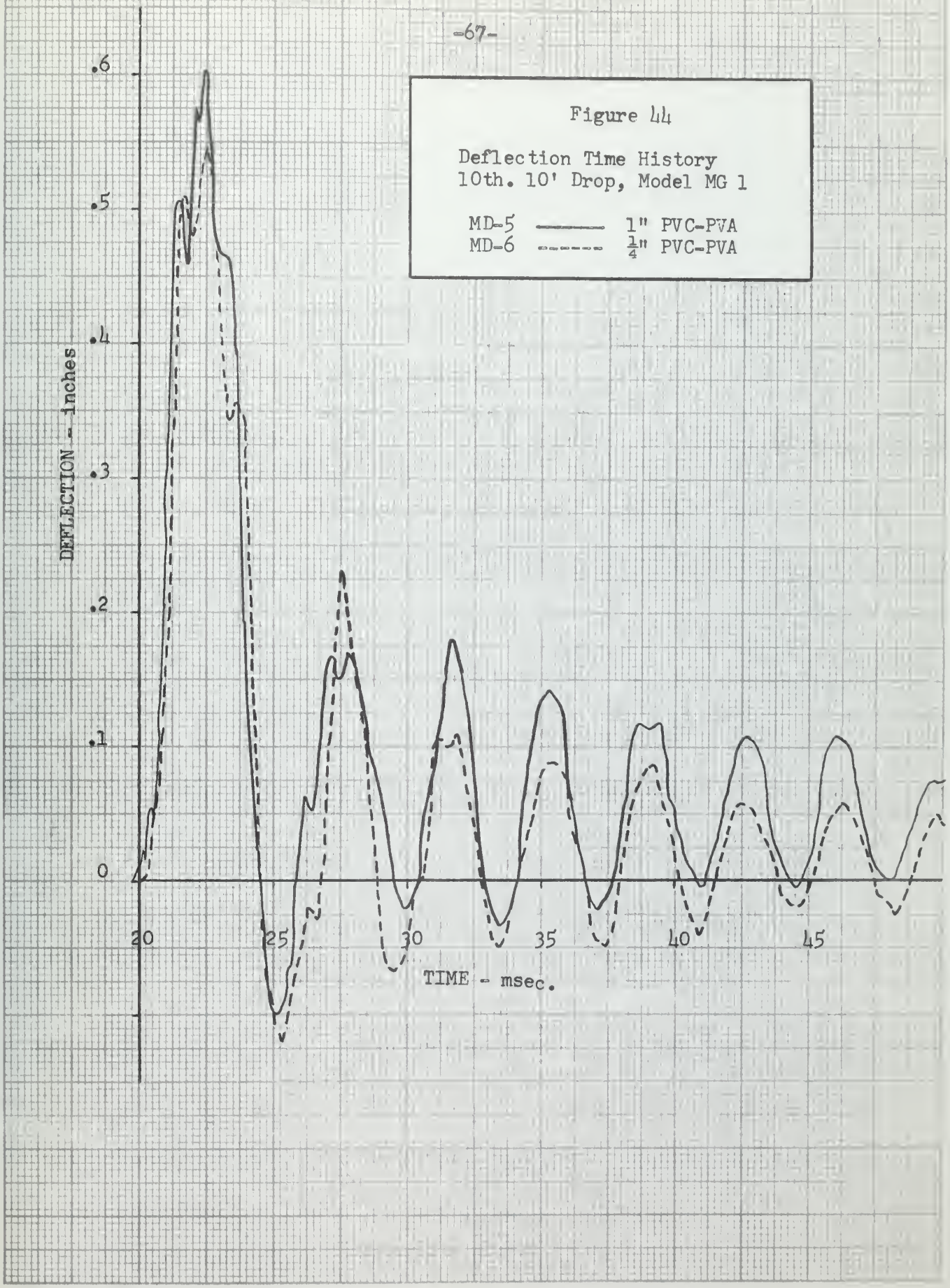

Figure 44

Deflection Time History
10th. 10' Drop, Model MG 1

MD-5 ——— 1" PVC-PVA
MD-6 - - - - - $\frac{1}{4}$" PVC-PVA

Figure 45

Strain Time History
10th. 10' Drop, Model MG 1

ST-5 ——— 1" PVC-PVA
St-6 - - - - - $\frac{1}{4}$" PVC-PVA

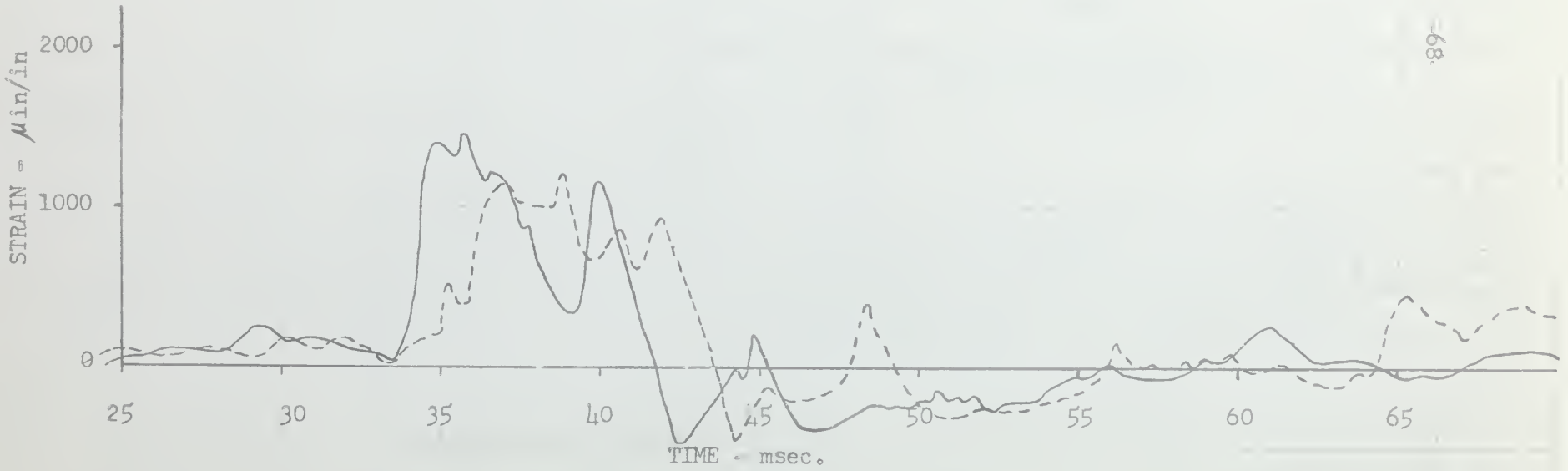

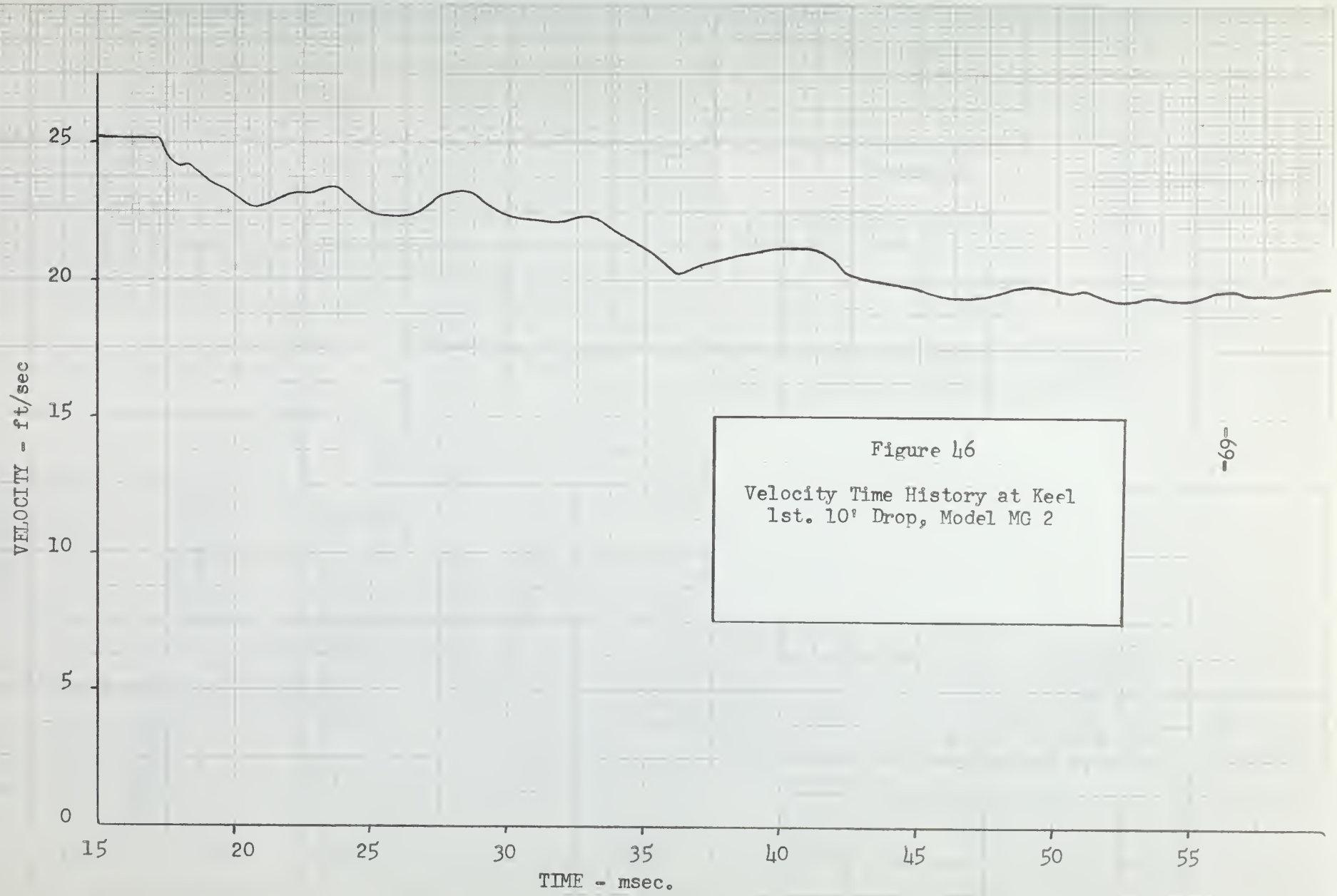

Figure 46

Velocity Time History at Keel
1st. 10' Drop, Model MG 2

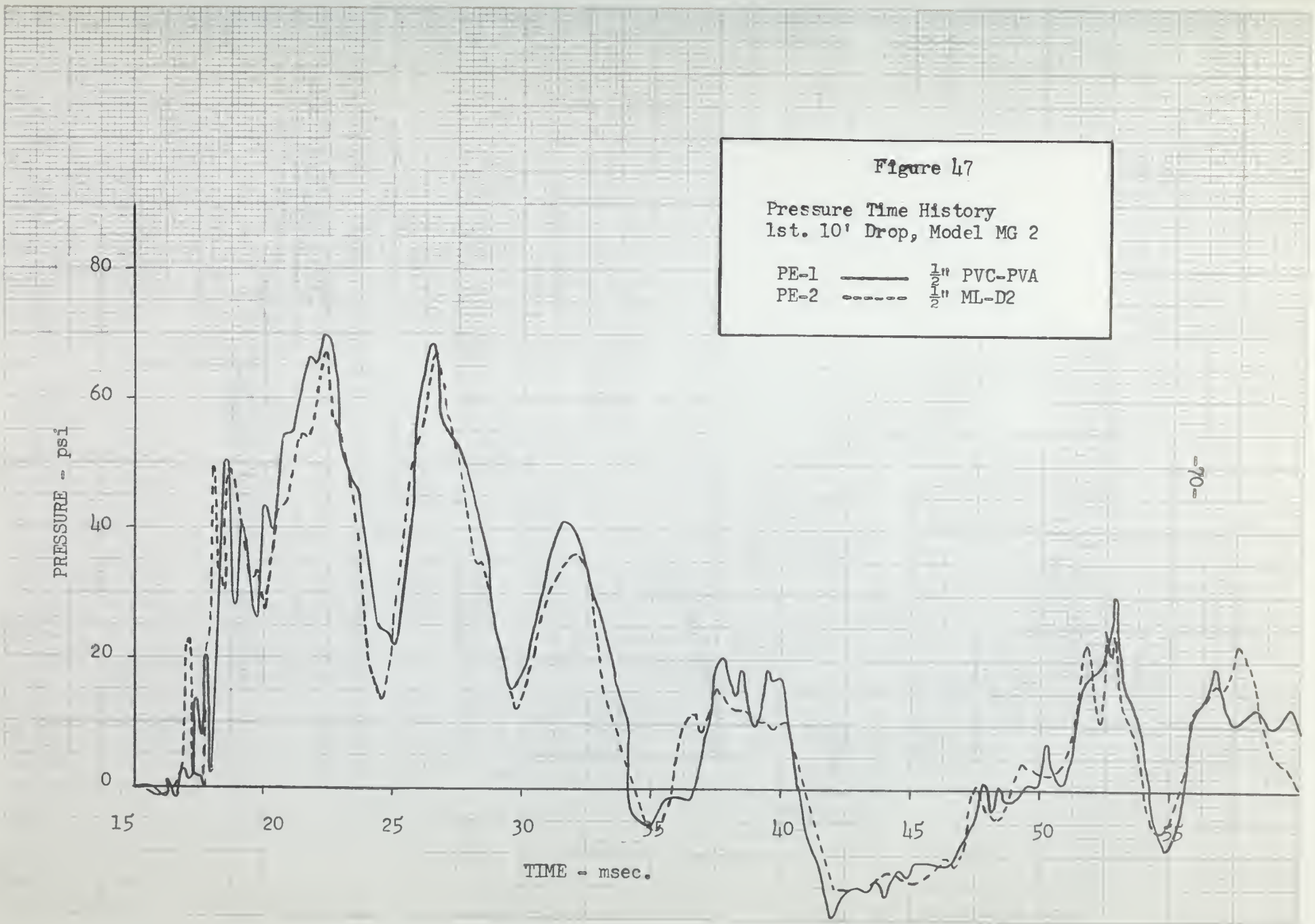
Figure 47
Pressure Time History
1st. 10' Drop, Model MG 2
PE-1 ——— ½" PVC-PVA
PE-2 - - - - - ½" ML-D2
PRESSURE - psi
80
60
40
20
0
15
20
25
30
35
40
45
50
55
TIME - msec.

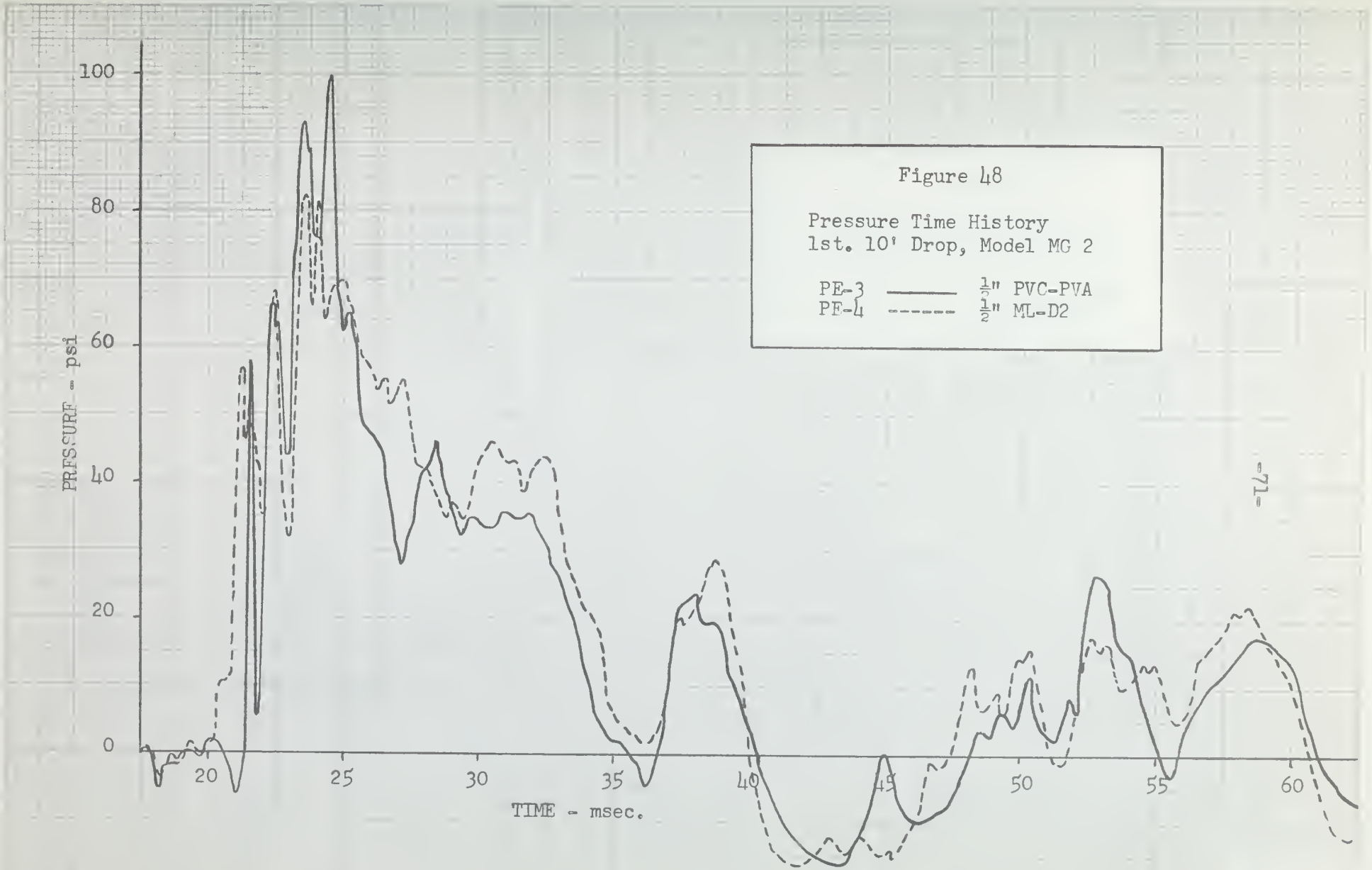

Figure 48

Pressure Time History
1st. 10' Drop, Model MG 2

PE-3 ——— ½" PVC-PVA
PE-4 ------ ½" ML-D2

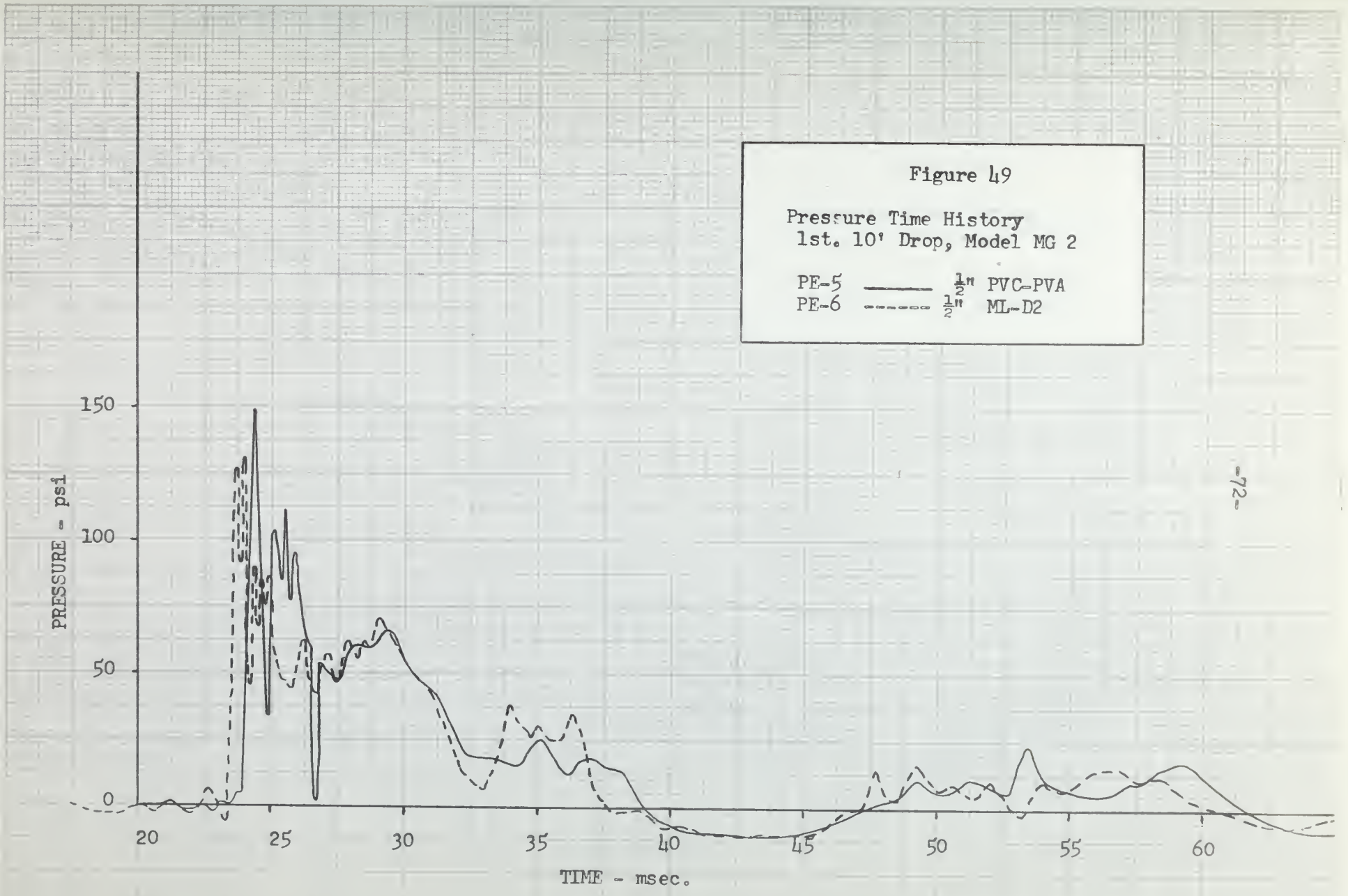
Figure 49
Pressure Time History
1st. 10' Drop, Model MG 2
PE-5 ——— ½" PVC-PVA
PE-6 ------ ½" ML-D2
150
100
50
0
PRESSURE - psi
20
25
30
35
40
45
50
55
60
TIME - msec.

Figure 50

Deflection Time History
1st. 10' Drop, Model MG 2

MD-1 ——— $\frac{1}{2}$" PVC-PVA
MD-2 - - - - - - $\frac{1}{2}$" ML-D2

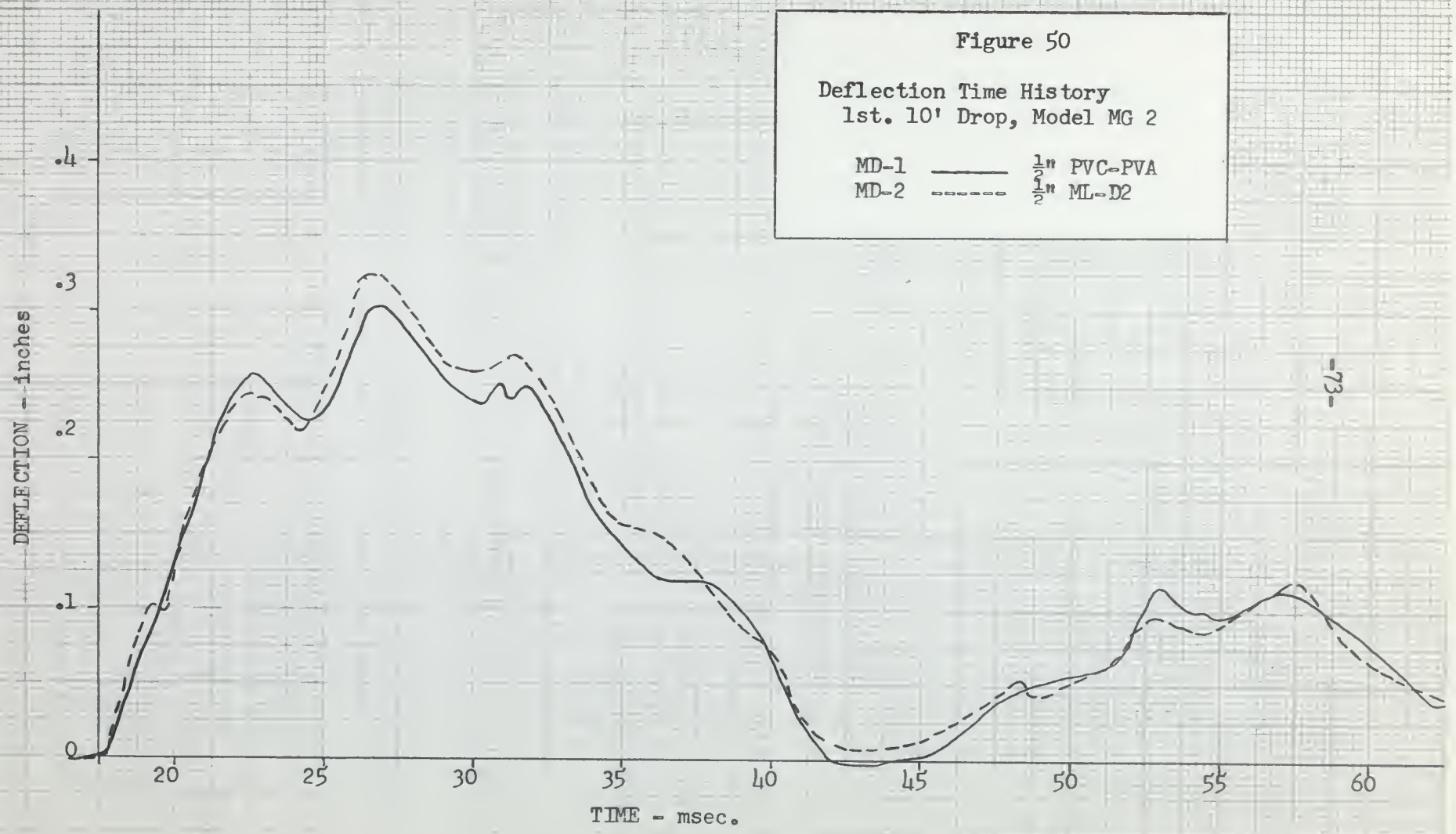

Figure 51

Deflection Time History
1st. 10' Drop, Model MG 2

MD-3 ——— ½" PVC-PVA
MD-4 - - - - - ½" ML-D2

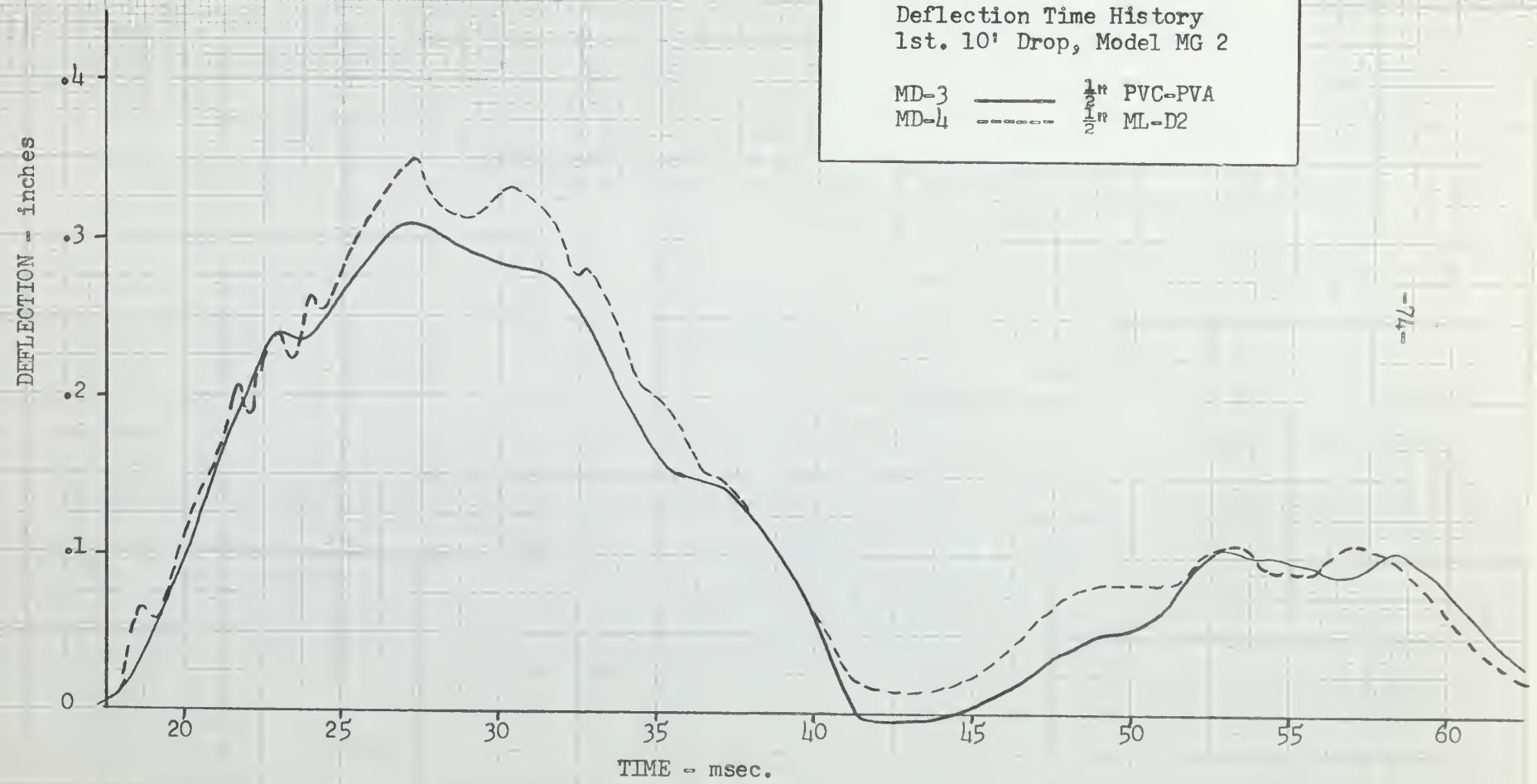

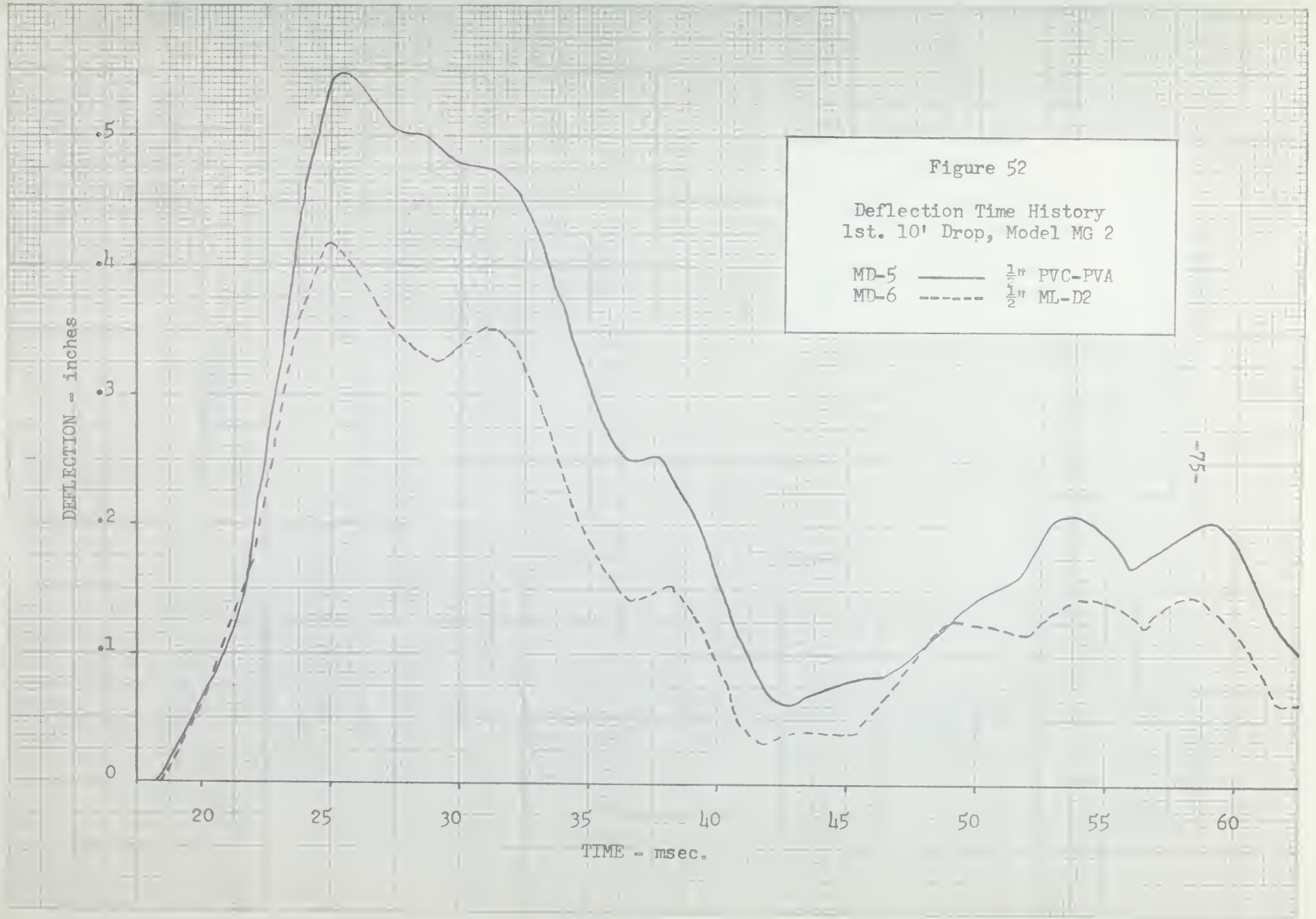
Figure 52
Deflection Time History
1st. 10' Drop, Model MG 2
MD-5 ——— ½" PVC-PVA
MD-6 ------ ½" ML-D2
DEFLECTION - inches
0
.1
.2
.3
.4
.5
20
25
30
35
40
45
50
55
60
TIME - msec.

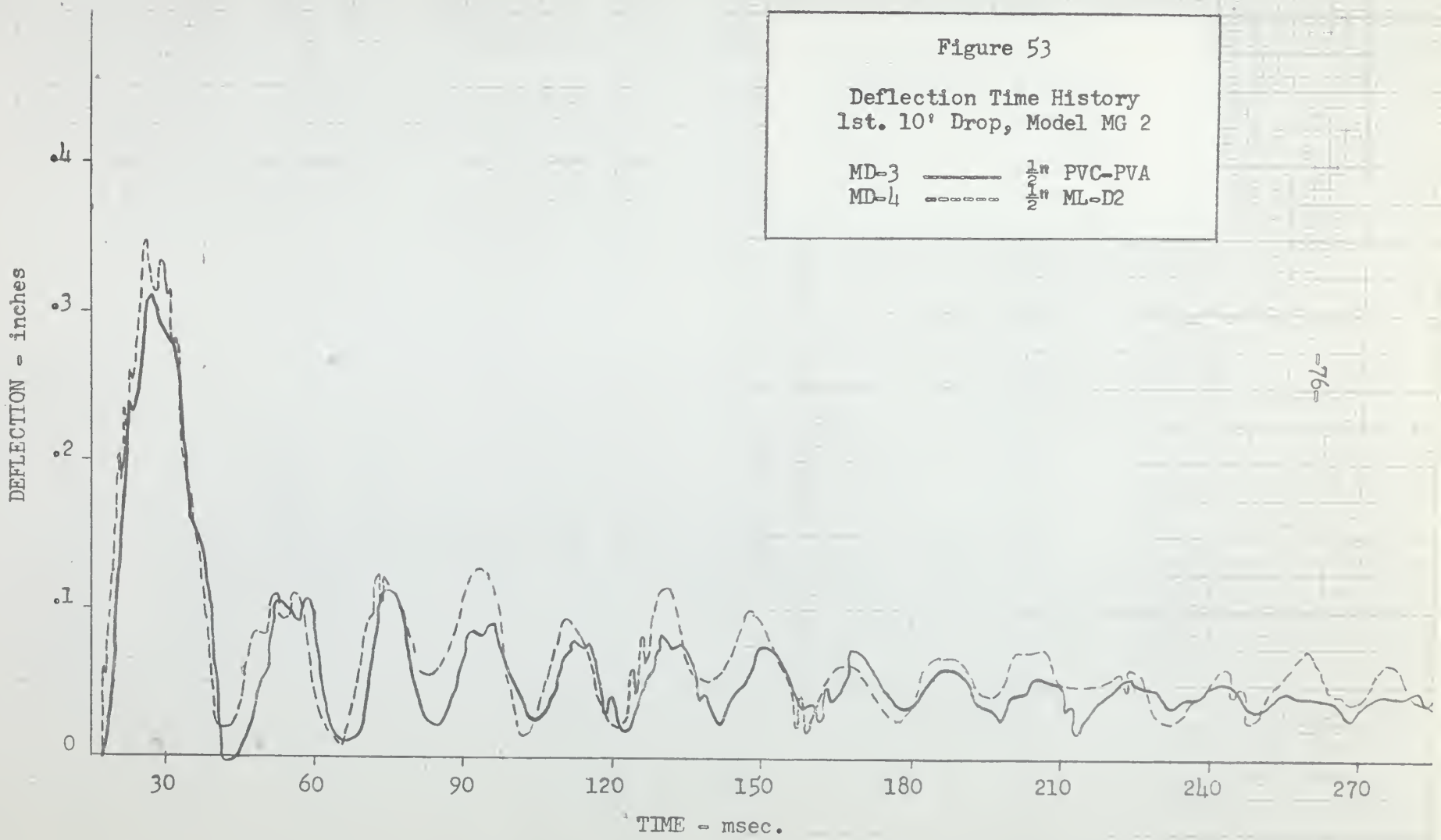

Figure 53

Deflection Time History
1st. 10' Drop, Model MG 2

MD-3 ——— ½" PVC-PVA
MD-4 - - - - ½" ML-D2

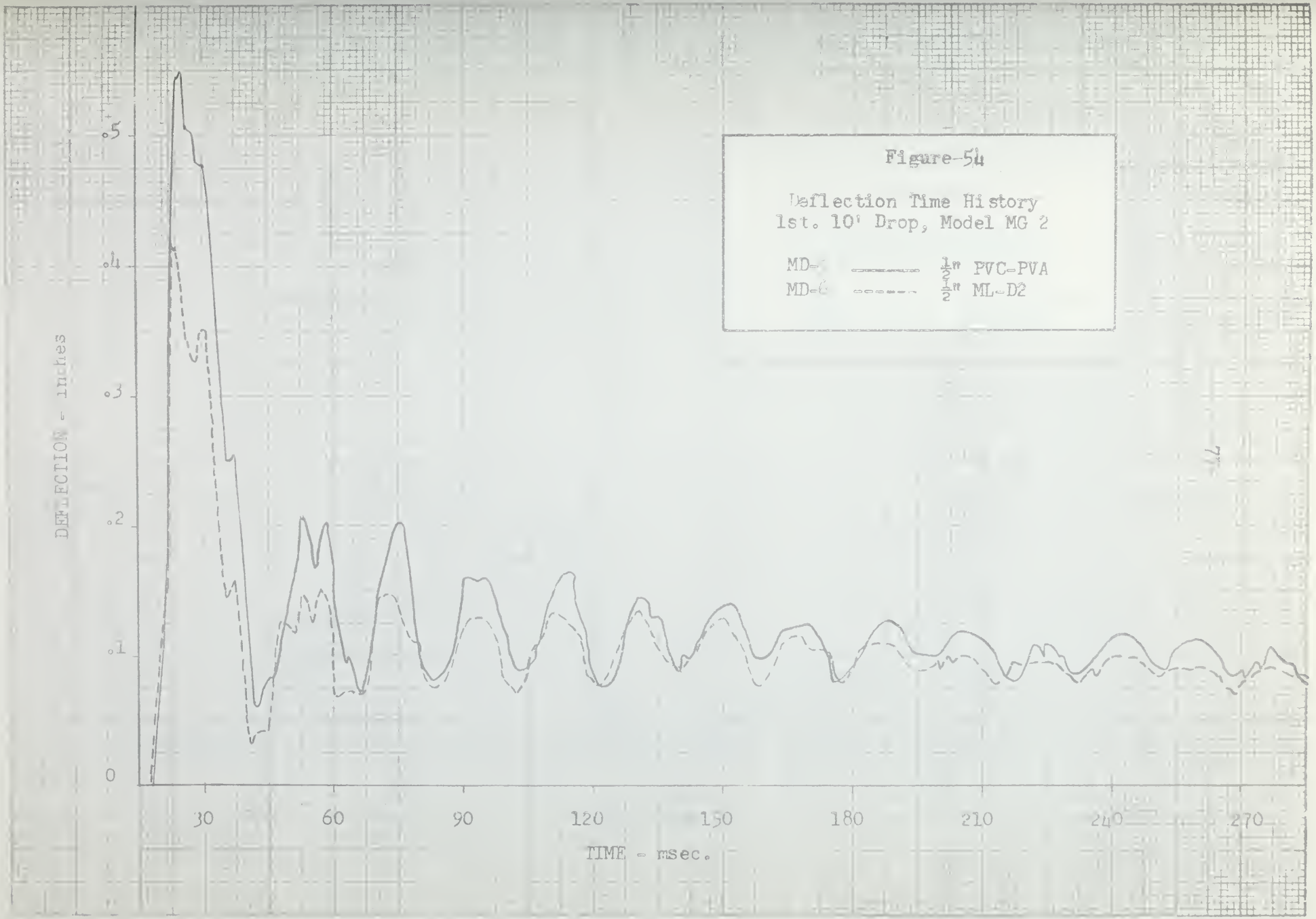
Figure-54
Deflection Time History
1st. 10' Drop, Model MG 2
MD-5 ——— ½" PVC-PVA
MD-6 - - - - ½" ML-D2
DEFLECTION - inches
.5
.4
.3
.2
.1
0
30
60
90
120
150
180
210
240
270
TIME - msec.

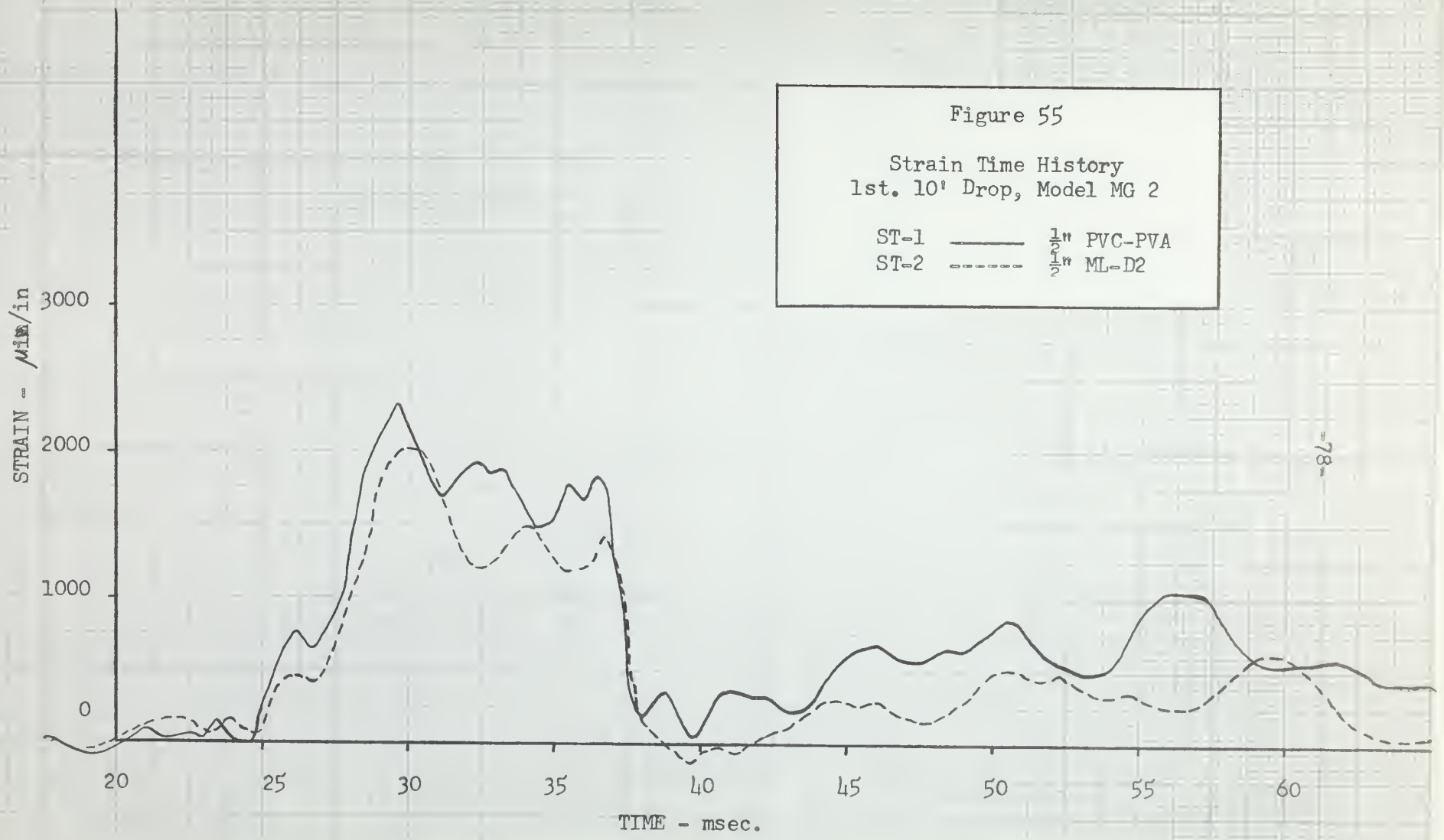
Figure 55
Strain Time History
1st. 10' Drop, Model MG 2
ST-1 ——— ½" PVC-PVA
ST-2 - - - - - - ½" ML-D2
STRAIN - μin/in
3000
2000
1000
0
20
25
30
35
40
45
50
55
60
TIME - msec.

Figure 56

Strain Time History
1st. 10' Drop, Model MG 2

ST-5 ——— $\frac{1}{2}$" PVC- PVA
ST-6 - - - - - - $\frac{1}{2}$" ML-D2

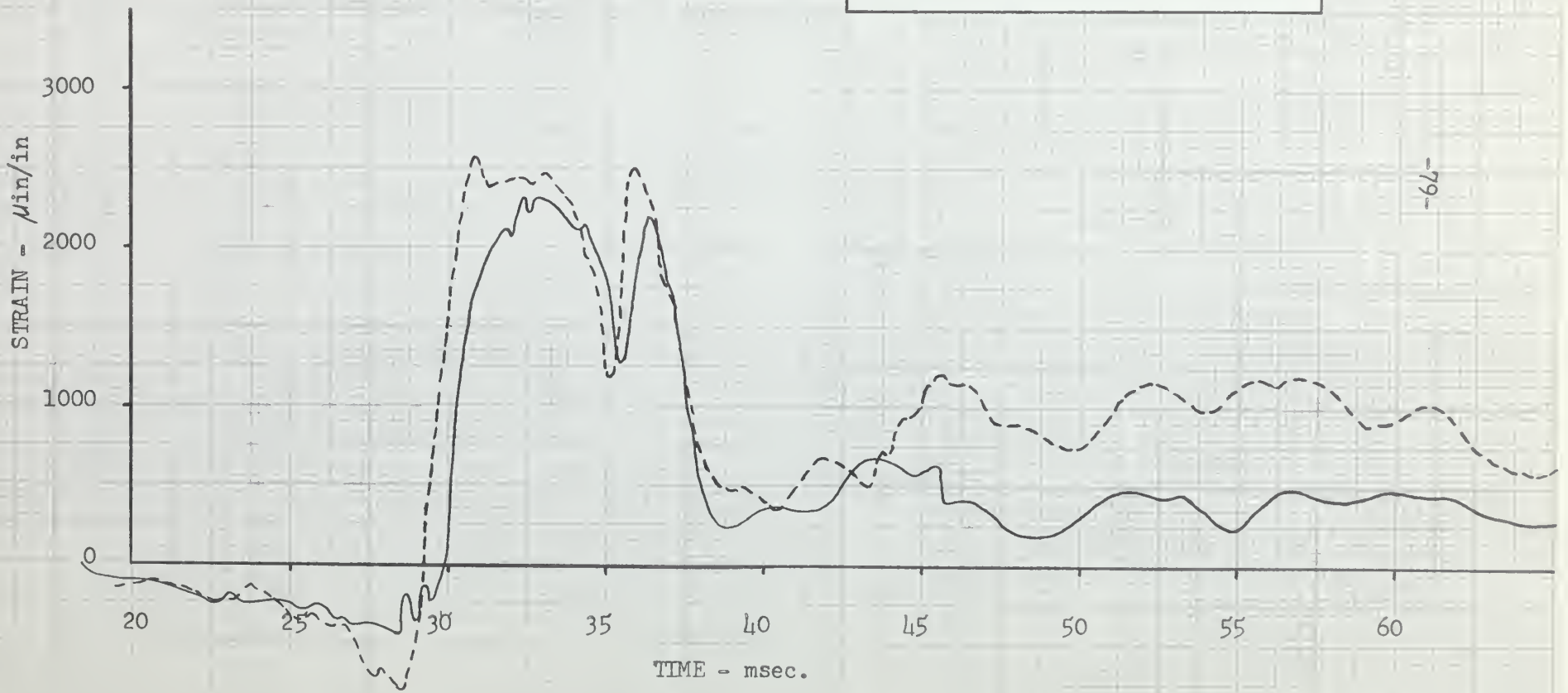

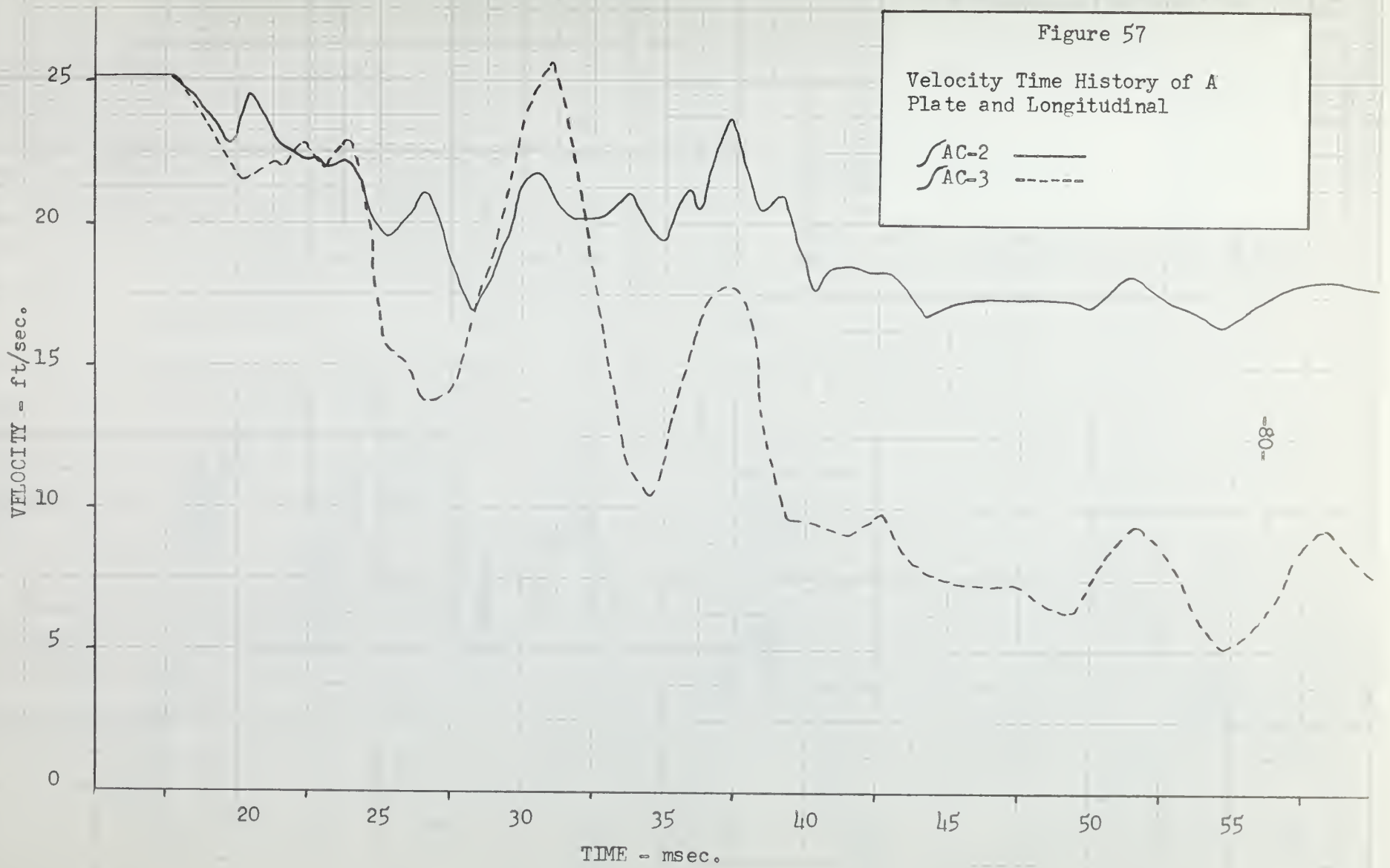
Figure 57
Velocity Time History of A Plate and Longitudinal
AC-2
AC-3
VELOCITY - ft/sec.
0
5
10
15
20
25
TIME - msec.
20
25
30
35
40
45
50
55

Figure 58

Pressure Time History
10th. 10' Drop, Model MG 2

PE-1 ——— ½" PVC-PVA
PE-2 -·-·- ½" ML-D2

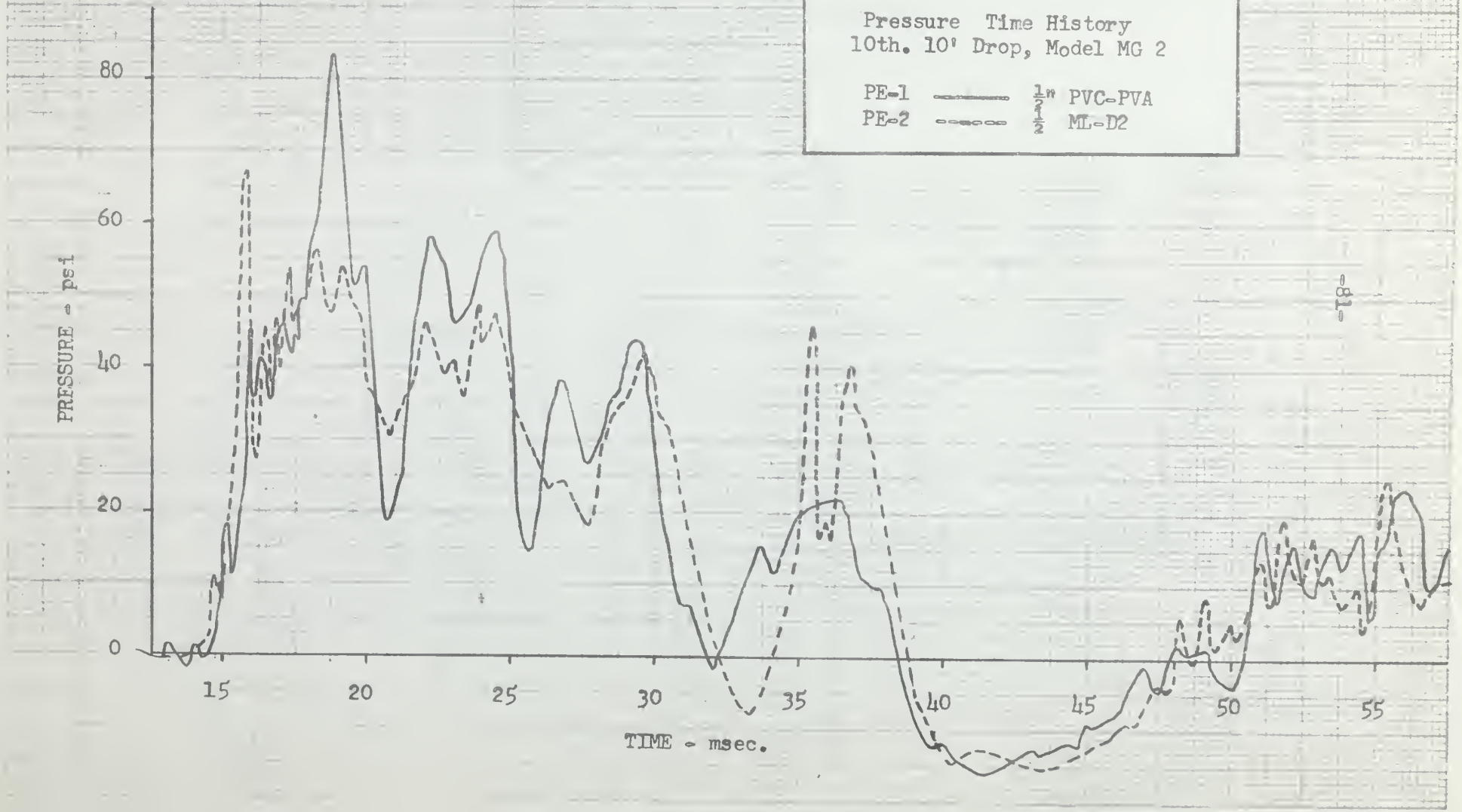

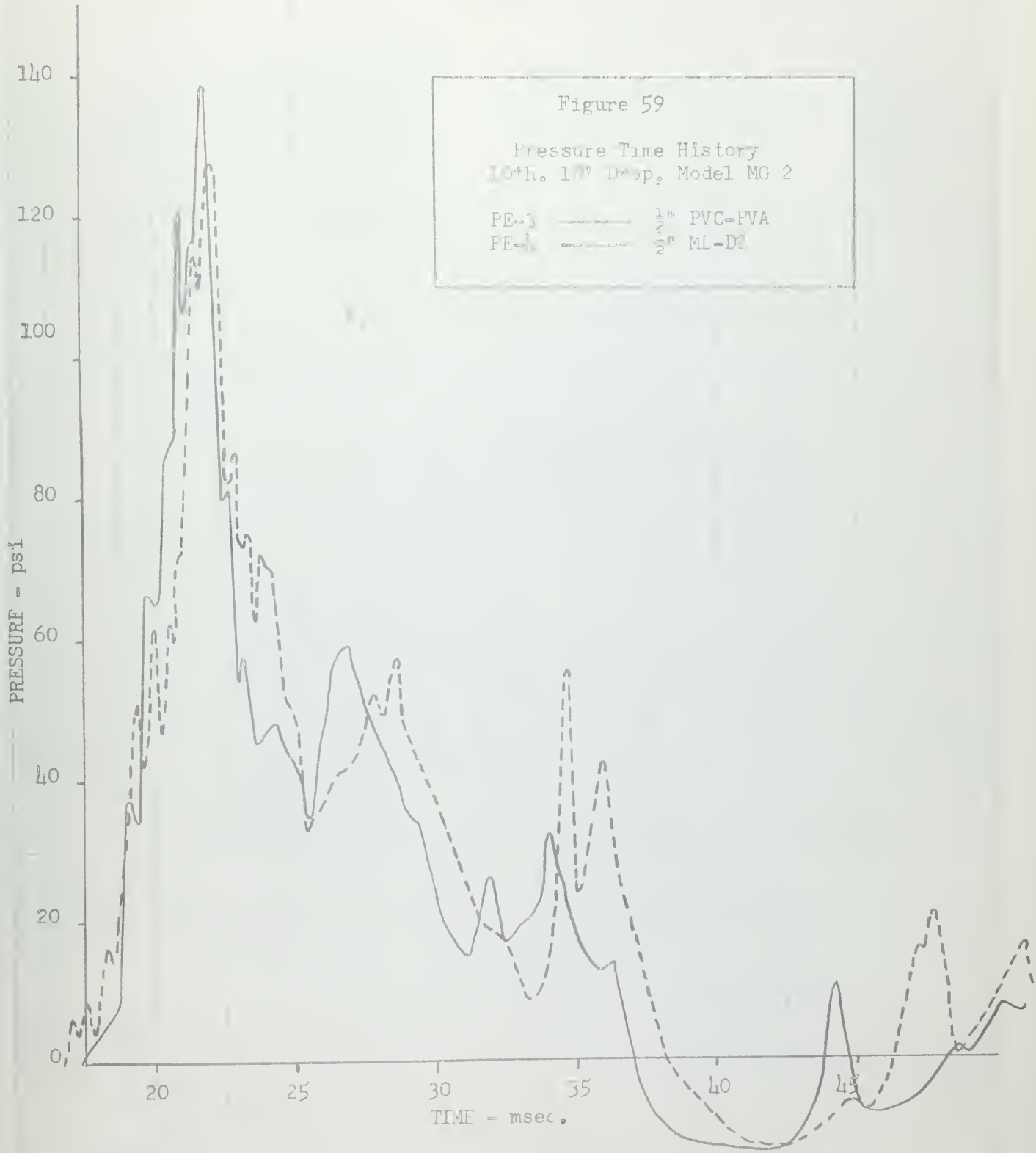

Figure 59

Pressure Time History
10'h. 17° Drop, Model MG 2

Figure 60

Deflection Time History
1st. 10' Drop, Unbacked Model
at Location $1\frac{1}{2}$-F Stbd.

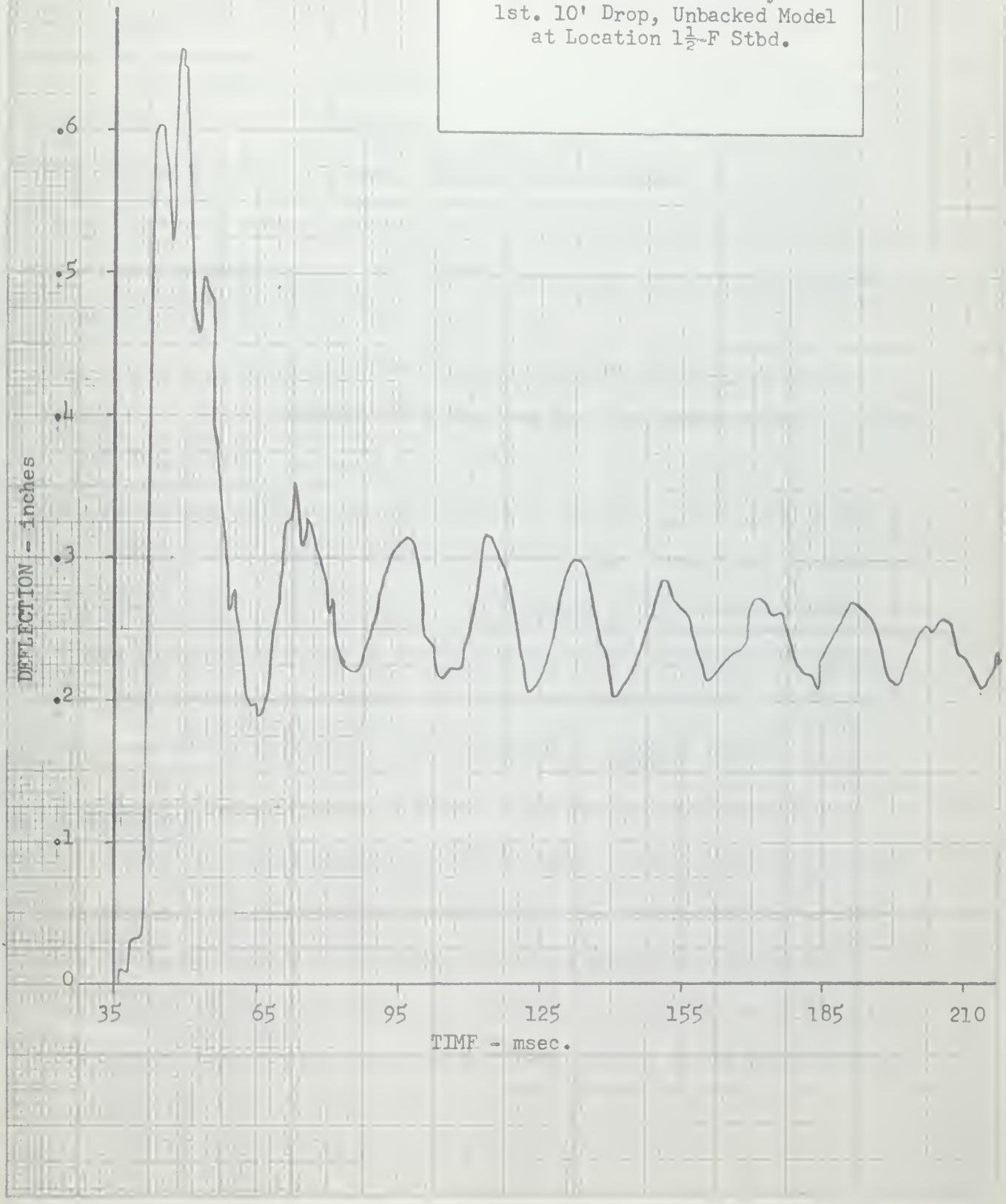

DISCUSSION OF RESULTS

A. General:

For purposes of this discussion only the 10 foot test drops of the models are to be considered. The loadings from the 3 foot test drops were such that the model remained in the elastic range; these test drops only served to eliminate the effects of "oil canning" of the model bottom plating. All further references concerning the model testing will be to the 10 foot test drops.

Before there can be any discussion of the time history plots of the models, it is necessary to state that the time scales of all of these plots start before the model hits the water. The actual time of impact of each model can be obtained from figures 33 and 46 which show the velocity retardation of the keel as the model impacts on the water. The time of impacting differs for each model. For a valid comparison between the sides of a model it is only necessary to compare the plots using the existing time scale. To make comparisons between the models it is necessary to allow for the difference in time of impact.

B. Pressures:

Before a valid comparison of the damage to each side of the model can be made, it must first be verified that the loading on the models was the same. The test drop height for both models was maintained constant at 10 feet, resulting in a velocity of 25.4 feet per second at the time of impact. The resultant pressure loading on the model bottom

is shown in figures 34, 35, 41, 42, 47-49, 58, 59. The pressures from identical locations on the port and starboard side of each model have been superimposed to facilitate the comparison of the loading on each side of the model. These plots show that the loading on each side of the model was essentially the same for each test drop. Comparison of the pressure plots obtained of models MG-1 and MG-2 indicate that the pressures on the models were the same. In addition, the pressures did not change appreciably from the first to the last 10 foot test drop. The pressure profiles of all the test drops show some random variation. These minor differences do not indicate a difference in the loading, but do indicate a difference in the response of the model to the loading. Therefore the loading on each side of a model was, in fact, the same.

The pressures are not uniform over the model bottom at any one time. The pressure peak is observed starting at the keel and increasing to a maximum somewhere between 15 to 30 inches outboard of the keel. Because of the pressure peaking near the center of each side of the model, it is not possible, with the instrumentation installed, to determine if the pressure at the more rigid portions of the model (stiffners) were larger than the pressures observed on the more elastic portions (plates). Additional pressure gages installed at each stiffner location would have clarified this point.

Cavitation is seen to exist at all gage locations. Of special note is the fact that the cavitation occurs at the same time at all gage locations. Thus cavitation occurs simultaneously over a large portion of the bottom of the model. The cavitation is caused by the

vibratory motion of the model, that is the plate stiffner combination, rather than by individual plate panel vibrations. This cavitation causes a reloading of the plate that will be discussed later.

The outboard pressure gages, PE-5-8, tended to break loose from the bottom of the model after one or more 10 foot drops. The gages were remounted using shock cord and tape to hold the gages to the bottom of the model. Because of this, some of the very high second pressure peaks observed during the later test drops are felt to be gage error.

C. Deflection and Deformation:

The total amount of permanent deformation at identical locations on each side of models MG-1 and MG-2 is shown in figures 26-29. These figures are plotted from the data obtained from the direct readings taken of the model bottom before and after the test drops. These plots show the general pattern of the permanent deformation in longitudinal and transverse directions. The relative standing with regards to the least amount of total permanent deformation after the ten test drops is, 1/2 inch ML-D2, 1/2 inch PVC-PVA, 1 inch PVC-PVA and 1/4 inch PVC-PVA. These relative standings are verified by figures 14-18 that show how the deformation progressed during the testing. Note that for the first half of the test drops of model MG-1, the 1/4 inch thickness of PVC-PVA gave better results than 1 inch thickness.

Figures 24 and 30 compare the total deformation received at identical locations on the side backed with 1/2 inch PVC-PVA and the two sides of model KG-1, the unbacked model. The figures indicate that no

substantial reduction of slamming damage was obtained by backing the model with damping material.

Although the magnitude of the damage reduction to be obtained from an application of damping material could not be predicted before the investigation, it was anticipated that the more damping material applied the better the results would be. The poor performance of the 1 inch thickness compared to the 1/2 inch thickness or the 1/4 inch thickness for the first six test drops remains in part unexplained. A discussion of the deflections and deformations will help to better understand the variation of the test results.

The deflection time history plots, figures 36-38, 43, 44, 50-54 are very similar at identical locations on the model sides. These plots indicate the deflection of the bottom at each gage location and do not indicate the deflection of the plate relative to its adjacent stiffners or vice versa.

The peak deflection of each drop was compared with the deformation received during the drop at each gage location. It was found that maximum deformation and maximum deflection did not necessarily occur on the same test drop. No relationship between the amount of deformation and the magnitude of the deflection was found.

The permanent deformation per drop (deformation rate) at the deflection gage locations are shown plotted in figures 19-23. The trends of these plots are all basically the same. There is a large deformation on the first drop followed by a few drops of reduced deformation rate until about the sixth drop when the deformation rate

increases. The initial high deformation of the undeformed model is to be expected as the plating is initially plane and must undergo some deflection before it can develop membrane forces. On the second drop there is, in general, less deformation because the model has work hardened and membrane forces in the plating are of greater proportions than on the first drop. If the models were only a flat plate with rigid boundaries, the deformation per drop would continue to decrease until the plate could accept the load without further deformation[8,9] or until the plate ruptured. The actual model being a plate stiffner combination does not show a continued decrease of deformation rate, but instead the rate increases during the later test drops. This increase was due to the failure of the transverse floors of the model. The extent of these failures is seen in figures 26-28, 31, 32. The failure of the transverse floors makes a substantial difference in the amount of deformation in the model. Differences in construction leading to an early failure of the floors would result in increased total deformation.

An analysis of all the plots of deformation shows that the plots of the two sides of model MG-1 are grouped together and the plots of the sides of model MG-2 are grouped together. The assumption is made that the deformation observed may be more a function of the model than the backing material. It, therefore, seems more valid, in the case of deformation, to make comparisons of one side of a model to the other than to compare the results of one model to that of the other. Figure 25 shows the deformation of the keel of models MG-1, MG-2 and KG-1. The differences of the total deformation of the keel for unbacked and

backed models seems to be independent of the backing material.

Additionally data from repeated drop tests of similar unbacked models indicate that a variation of deformation at similar locations is to be expected in this model. Figures 24 and 30 indicate that a 20 to 25 per cent variation of permanent deformation exists between the port and starboard sides of the unbacked model, KG-1. The variation between models certainly is of this same magnitude. This variation is of the same order of magnitude as the differences in deformation between the sides of the models tested. Model construction is seen to be a large factor in determining the total deformation.

If we attribute part of the difference in deformation to model construction, this in no way limits the effectiveness of the model in determining the basic objective of this investigation. Any material that would substantially reduce slamming damage would produce results of greater magnitude than the expected differences in deformation due to construction and be readily observed.

D. Strain:

An analysis of the strain time histories associated with a slam, figures 39, 40, 45, 55, 56, leads to some interesting conclusions. These plots show the strains on the flange of a longitudinal stiffner and the strains on the inner surface of the adjacent plate. The strain in the plate barely exceeds the elastic limit, but the strain in the stiffner is well into the plastic range. This substantiates, in part, a previous conclusion[12] that the stiffness should be designed for a greater loading than the plate.

The strain time histories when compared with the deflection time histories reveal that the permanent deformation takes place entirely during the first half cycle of deflection of the plate from its equilibrium position. All of the remaining plate deflections are elastic and therefore cannot contribute to the deformation. It is not obvious from the strain time histories as plotted that the motions after the first deflection peak are elastic. However, a check of the strain time history for the whole drop reveals that the strain gage has been elongated permanently by the deformation of the member. This elongation shifts the axis of the strain gage by the amount of deformation received during the first deflection peak. When the axis is shifted the motion after the first deflection peak is seen to be elastic. The preceding argument is verified by the deflection time history plots, figures 43, 44, 53, 54, 60. Here the deformation is seen to occur during the first 1/2 cycle of the motion, and thereafter the model is seen to vibrate about the new equilibrium position.

As a consequence of the above facts two important conclusions can be reached. First, in order for a backing material to be effective in reducing slamming damage, it must be able to perform this reduction in the first half cycle of the model motion and not depend on several Cycles of motion to dissipate the energy of a slam. Second, the cavitation reloading discussed earlier in this paper is well within the elastic range and does not contribute to the damage as previously concluded.[11]

E. Damping Material:

The effect of the damping material in damping model vibrations was determined by assuming that the amplitude of the model vibrations decayed exponentially. Using the following:

$$C/C_0 = \frac{1}{2\pi} \frac{(X_n - X_{n+1})}{X_n}$$

where X_n is the n^{th} maximum amplitude during a vibration and X_{n+1} is the next maximum amplitude,[22] the per cent of critical damping was found for the models. The per cent of critical damping achieved was 3.1 and 3.5 per cent for the backed models and 3.6 per cent for the unbacked models. This indicated that the damping of the model was a function of the model and was not dependent on backing materials.

It was discovered during the testing of the first model that a few of the damping tiles became cracked and/or loosened from the bottom plating. A careful investigation of the second model tested indicated that some tiles started to loosen from the plate on about the 7^{th} test drop. The loosening was greatest in the 1-inch thick tiles and there was very little loosening in the 1/4 inch tiles. The damage to the tiles can be seen in Figures 31 and 32. In as much as the tiles are of dubious value in reducing deformation it is felt that this loosening of the tiles had little effect on the results.

VI. CONCLUSIONS

Slamming damage cannot be substantially reduced by backing the ship's bottom shell plating with a practical application of present day damping materials.

Adding mass to the ship's bottom shell plate of up to 1.75 times the weight of the plate will not lead to any substantial reduction of slamming damage.

The damage to the model occurs during the first half-cycle of the bottom vibratory motion, an interval of approximately 10 milliseconds.

In order for a backing material to be able to reduce slamming damage it must be able to dissipate a large amount of energy during the first half-cycle of bottom motion and not depend upon several cycles of bottom motion for energy dissipation.

Cavitation reloading of the bottom occurs after the initial slam loading but in no way contributes to the slamming damage.

With the model described herein it is not possible to differentiate between small reductions in damage resulting from the installation of a backing material and the expected variation of damage resulting from small differences in model construction.

VII. RECOMMENDATIONS

Future investigations into the reduction of slamming damage using models of ship form should compare the results of increasing the size, the number and the arrangement of the bottom shell stiffners.

Backing materials should be tested on flat plate models to determine their effectiveness in reducing damage due to impact loading before any attempt is made to determine their usefulness in reducing slamming damage.

APPENDIX A

TABLE I

UERD SHOT NO.	MODEL	TEST DROP HEIGHT
7051	MG 2	3
7052	MG 2	3
7053	MG 2	10
7054	MG 2	10
7055	MG 2	10
7056	MG 2	10
7057	MG 2	10
7058	MG 2	10
7059	MG 2	10
7060	MG 2	10
7061	MG 2	10
7062	MG 2	10
7076	MG 1	3
7077	MG 1	3
7078	MG 1	10
7079	MG 1	10
7080	MG 1	10
7081	MG 1	10
7082	MG 1	10
7083	MG 1	10
7086	MG 1	10
7088	MG 1	10
7089	MG 1	10
7090	MG 1	10

BIBLIOGRAPHY

1. Foster-King, J., "Heavy-Weather Damage," Northeast Coast Institution of Engineers and Shipbuilders Transactions. No. 51-1934-35.

2. Hansen, K. E., "Pounding of Ships and Strengthening of Bottom Forward," Ship Building and Shipping Record, Vol. 45, 1935.

3. Townsend, H. S. "Some Observations on the Shape of Ship Forebodies with Relation to Heavy Weather," New York Metropolitan Section, SNAME, April 28, 1960.

4. Ochi, M. K., "Extreme Behavior of a Ship in Rough Seas," Paper presented at the Annual Meeting of SNAME, 1964.

5. Ochi, M. K., "Experiments on the Effect of Bow Form on Ship Slamming," DTMB Report 1400, 1962.

6. Swaan, W. A., and Vossers, G., "The Effect of Forebody Section Shape on Ship Behavior in Waves," Transactions, Royal Institution of Naval Architects, Vol. 103, 1964.

7. Szeberhely, V. G., "Hydrodynamics of Slamming of Ships," DTMB Report 823, July 1952.

8. Nagi, T., "Permanent Set of a Bottom Shell Plate Due to Slamming Loading," University of California, Institute of Engineering Research, Series No. 186, Issue No. 2, August 1962.

9. Nagi, T., "Large Permanent Set of Ship Bottom Plating Due to Slam Loads," University of California, Institute of Engineering Research, Series No. 186, Issue No. 3, December 1962.

10. Leibowitz, R. C. and Greenspon, J. E., "A Method for Predicting the Plate-Hull Girder Response of a Ship Incident to Slam," DTMB Report 1706, October 1964.

11. Goodwin, J. J. and Kime, J. W., "Slamming of a Ship Structural Model with Backing Material," M.I.T. Thesis, 1964.

12. Clevenger, R. L. and Melberg, L. C., "Slamming of a Ship Structural Model," M.I.T. Thesis, 1963.

13. Bledsoe, M. D., Bussenaker, D. and Cummings, W. E., "Seakeeping Trials on Three Dutch Destroyers," Transactions SNAME 68, 1960.

14. Ungar, E. E., and Hatch, D. K., "Your Selection Guide to High-Damping Materials," Reprint from Product Engineering, April 17, 1961.

15. "Damping of Flexural Vibrations By Free and Constrained Visco-Elastic Layers," Bolt, Beranek and Newman, Inc., Technical Report 632.

16. Ross, D., Ungar, E. E., and Kerwin, E. M., Jr., "Damping of Plate Flexural Vibrations by Means of Viscoelastic Laminal," Reprint from Structural Damping, ASME, 1959.

17. Nolle, A. W., "Dynamic Mechanical Properties of Rubberlike Materials," Journal of Polymer Science, Vol. 5, 1950, pp.1-54.

18. Bourn, W. S., "Vibration Reduction Materials," Bureau of Ships Journal, October 1964.

19. "Development of Damping Treatments for Destroyer Hulls," Mare Island Naval Shipyard Rubber Laboratory Report 94-31, November 1961.

20. "Suitability of MIL-P-23653 Material for Damping Mechanical Vibrations in Light Steel Plates," Mare Island Naval Shipyard Rubber Laboratory Report 94-52, May 1964.

21. "Effects of Various Environments on the Vibration Damping Efficiency of Monsanto Treatment MRC-OG4," Mare Island Naval Shipyard Rubber Laboratory Report 94-43, January 1963.

22. Den Hartog, J. P., Mechanical Vibrations, Fourth Edition, McGraw-Hill, New York, 1956, p.40.

REVISIONS				
REV. NO.	ZONE	DESCRIPTION	APPROVED BY	DATE
B	7	GEN. NOTE "4 ALTERED, NOTE "6 ADDED, BOTTOM OF END BHD STIFFNRS TO BE WELDED AS NOTED IN SECTS AA & E-B'B', BHD. STIFFNR PL. 11 & 14 INC. CHANGED FROM PL. 8 TO PL. 7. SEE LIST OF MATL ALTERED. TRANS. WEB PL. 5 ALTERED AS SHOWN TO ALLOW ATTACHMENT TO CARRIAGE.	E.E.	8/6/64

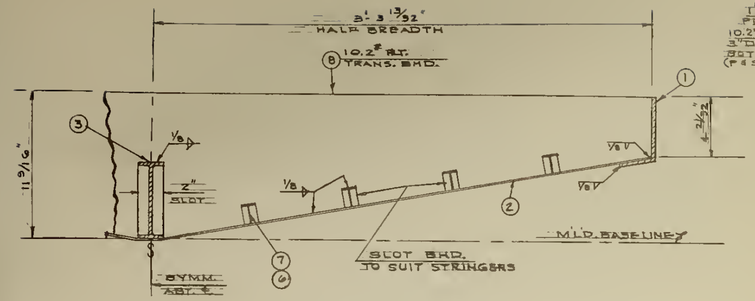

TRANSV. SECTION AT FR. 2 SHOWN
FR. 5 TO BE SIMILAR
FOR DETAILS NOT SHOWN SEE SECT. AT FR. 3
SCALE ~ 3" = 1'-0"

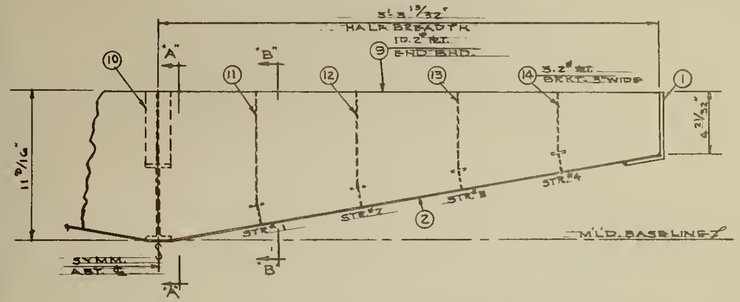

END BULKHEAD AT FR. 6 SHOWN
LOOKING FORD.
FR. 1 TO BE SIMILAR EXCEPT TO OPP. HAND.
SCALE ~ 3" = 1'-0"

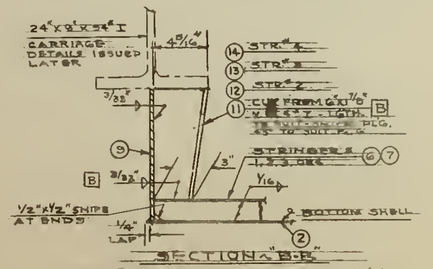

SECTION "B-B"
TYPICAL DETAIL OF END BHD. BRKTS.
SCALE ~ 3" = 1'-0"

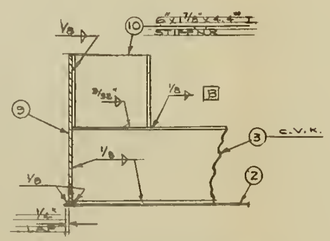

SECTION "A-A"
SCALE ~ 3" = 1'-0"

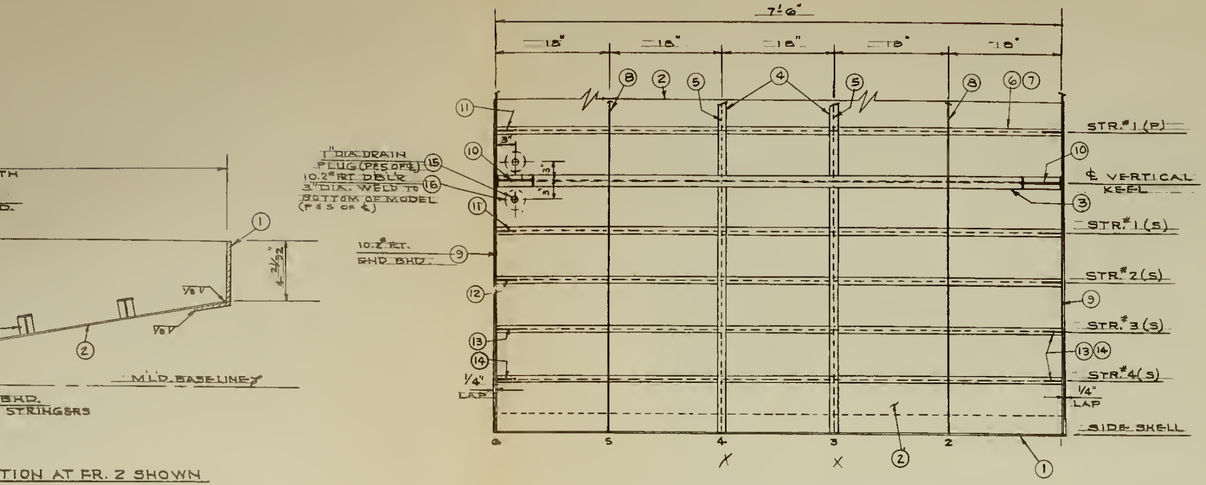

PLAN VIEW OF MODEL
STBD SIDE SHOWN, PORT SIDE SIM. TO OPP. HAND
SCALE ~ 1 1/2" = 1'-0"

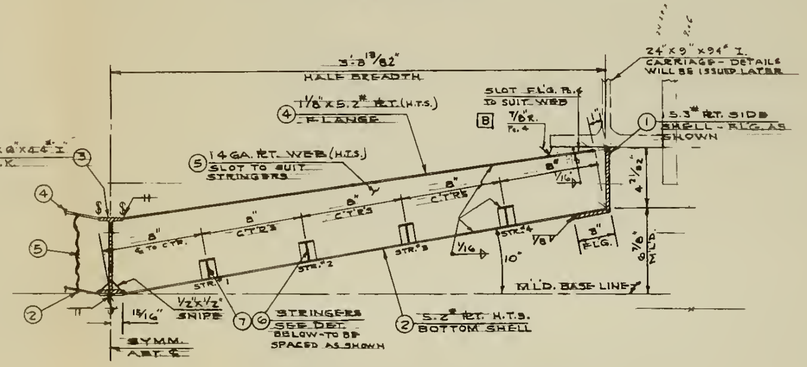

TRANSV. SECTION AT FR. 3 SHOWN
LOOKING FORD.
FR. 4 TO BE SIMILAR
SCALE ~ 3" = 1'-0"

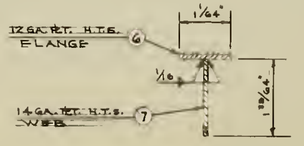

DETAIL OF STRINGERS
FULL SIZE

GENERAL NOTES

1. ALL THICKNESSES GO FORWARD OF THE MOLDED LINE.
2. MODEL TO BE PRIMED AND PAINTED ONE COAT OF HAZE GREY, IDENTIFY STRENGTH MEMBERS AS DIRECTED.
3. ALL MATERIAL TO BE CONSERVED AND UTILIZED (SO FAR AS POSSIBLE) FOR THE MANUFACTURE OF SMALLER STRUCTURAL MEMBERS, AND ALSO FOR ADDITIONAL MODELS, (SEE GEN. NOTE 6).
4. TEST SPECIMENS (7" X 20") LONGL. & TRANSV. TO BE CUT FROM EACH (H.T.S.) MOTHER PLATE AND SENT TO M&T. LAB. FOR CHEMICAL AND PHYSICAL ANALYSIS. PLATES ARE NOW IDENTIFIED 1 THRU. 20. LAY-OUT SHEETS (FURNISHED BY CODE 783) SHOWS MODEL & PC. NOS. WHICH MUST BE CUT FROM EACH PLT. USED.
5. IMPORTANT:
   EXTREME CARE TO BE EXERCISED IN MAINTAINING FAIRNESS OF STRUCTURE.
6. BOTTOM SHELL PLATING, PL. NOS. 2, & STRINGERS, PL. 6 & 7 TO BE ORIENTED WITH THE ROLLED DIRECTION FORE AND AFT. THE TRANSVERSE WEBS & FLANGES, PL. 4 & 5 ROLLED DIRECTION TO BE ATHWARTSHIPS.
7. SCALE WT. OF MODEL 750 LBS.

11/10/64 LARRY

PRINTS ISSUED

DATE
11
17
23
28
31
38
41
51
55
58
64
67
69
71
72
74
124A
128
228
270
308A
310
336
338
340
343
350
354
720 2
721D 4

C.O.V.
BURRIS
BUDRO

PEARL R.
LORD K'R.
SAN FRAN.
MARE IS.
PUGET S.
CHARR.
NYK.
PHILA.
NORTON
PORTS.

TOTAL

PIECE NO.	NAME OF PIECE	NO. REQ.	MAT.	STOCK NUMBER	REMARKS OR SERVICE	ROUTING
16	DEL'R. RT.	2	M.S.	SHOP PROVIDES	10.2# RT. 3" DIA.	
15	DRAIN PLUG	2	STL.	SHOP PROVIDES	1" DIA. PIPE PLUG	
14	BHD. BR'KT	4	M.S.		3/16 X 4 4" I - 6 5/16" LG.	
13	BHD. BR'KT	4	M.S.		" " " - 8" LG.	
12	BHD. BR'KT	4	M.S.		" " " - 7 1/2" LG.	
11	BHD. BR'KT	4	M.S.		CUT FROM 12" X G 1/8" X 10.2# RT. - 8 3/4" LG.	
10	BHD. STIFF.	2	M.S.	SHOP PROVIDES	1 1/8 X G X 4.4" I - 5 11/16" LG.	
9	END BHD.	2	M.S.	SHOP PROVIDES	CUT FROM 12" X G 1/8" X 10.2# RT.	
8	TRANS. BHD.	2	M.S.	SHOP PROVIDES	CUT FROM 12" X G 1/8" X 10.2# RT.	
7	LONG'L. WEB	8	H.T.S.	SUBMITTED BY WEBB'S CARR	1 35/64" X 14 GA. RT. - 7'-6" LG.	
6	LONG'L. FLG.	8	H.T.S.	" "	1 7/64" X 12 GA. RT. - 7'-6" LG.	
5	TRANS. WEB	4	H.T.S.	" "	CUT FROM 8" X 3'-6" X 14 GA. RT.	
4	TRANS. FLG.	4	H.T.S.	SUBMITTED BY WEBB'S CARR	1 7/8" X 5.2# RT. - 5'-2 3/4" LG.	
3	KEEL	1	M.S.	SHOP PROVIDES	1 7/8" X 9" X 4.4" I - 7'-6" LG.	
2	BOTTOM SHELL	2	H.T.S.	SUBMITTED BY WEBB'S CARR	11'-4" X 7'-0 3/4" X 5.2# RT.	
1	SIDE SHELL	2	M.S.	SHOP PROVIDES	CUT FROM 5'-4" X 7'-6 3/4" X 15.3# RT.	

LIST OF MATERIAL QUANTITIES FOR ONE MODEL (1 OF 2)

DRAWN BY	
TRACED BY	[illegible] 7/20/64
CHECKED BY	W. G. BUTT 7/21/64
DESIGN SUPVD	[illegible]
ENGINEERING SUPVR.	E. Florentin Vasile
E.S. BRANCH SUPVR.	

SLAMMING MODEL
(1/4 SCALE OF PROTOTYPE)

U.E.R.D. OF STRUCTURAL MECHANICS LAB. D.T.M.B., PORTSMOUTH, VA. REV.

APPROVED [signature] 4/1/65
DIVISION HEAD — PROJECT OFFICER — DATE

W.P. 157 | R.U. NO. 757 | B

SCALE: AS SHOWN | SHEET 1 OF 1

REVISIONS				
REV. NO	ZONE	DESCRIPTION	APPROVED BY	DATE

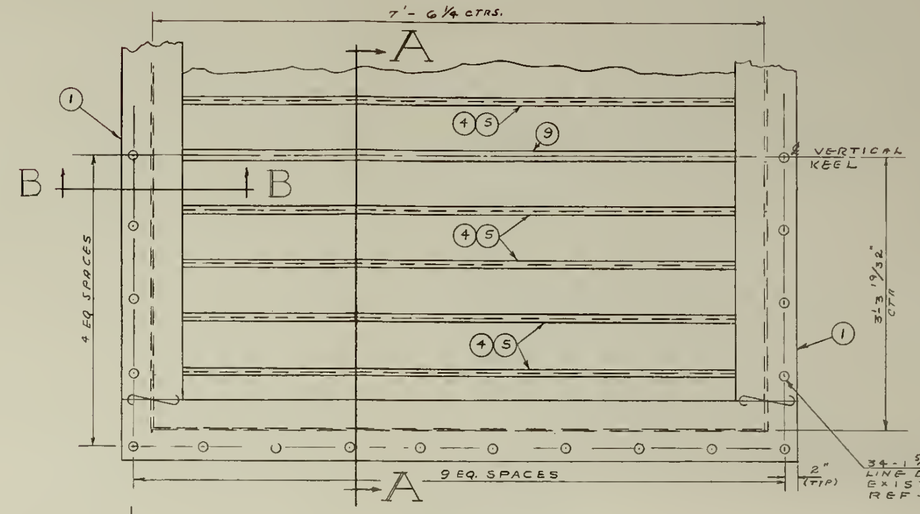

PLAN VIEW
1 1/2" = 1'-0"

NOTES
1. LINE DRILL PC #1 AND EXIST. CARRIAGE STRUCTURE
2. PAINT 1 COAT RED LEAD AND 1 COAT HAZE GREY

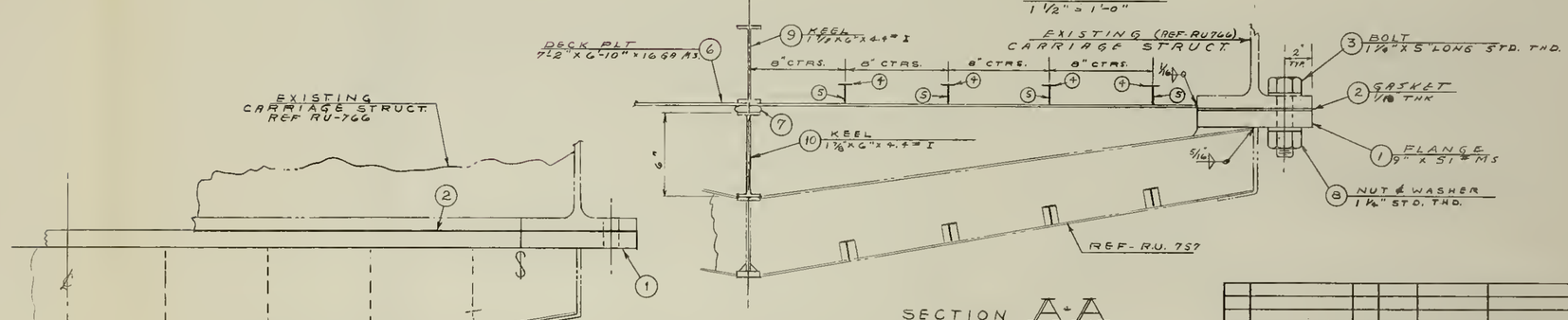

10	KEEL	1	MS	SHOP PROVIDE	1 1/8" X 6" X 4.4# I	11
9	KEEL	1	MS	" "	1 7/8" X 6" X 4.4# I	1
8	NUT & WASHER	34 EA	MS	" "	1 1/8" STD. THD.	11
7	GASKET	1	RUBBER	SHOP PROVIDE	1 THK X 2 WIDE X 7' LONG	11
6	DECK PLT	1	MS	" "	7'-2" X 6'-10" X 16 GA PLT.	17-11
5	WEB	8	HTS	CUSTODY X-11	1 9/16" X 14 GA HTS.	11
4	FLANGE	8	HTS	CUSTODY X-11	1 1/32" X 12 GA. HTS	11
3	BOLT	34	M.S.	" "	1 1/8" X 5" LONG M.S.	11
2	GASKET	1	FIBER	" "	1/16" THK. X 9" WIDE AS REQD.	11
1	FLANGE	4	MS	SHOP PROVIDE	9" WIDE X 51# M.S. PLT.	" A
PIECE NO.	NAME OF PIECE	NO. REQ.	MAT.	STOCK NUMBER	REMARKS OR SERVICE	ROUTING

LIST OF MATERIAL QUANTITIES FOR

CARRIAGE & SLAMMING MODEL MODIFICATION

WP-157

TYPICAL END BHD.
SCALE 3"=1'0"

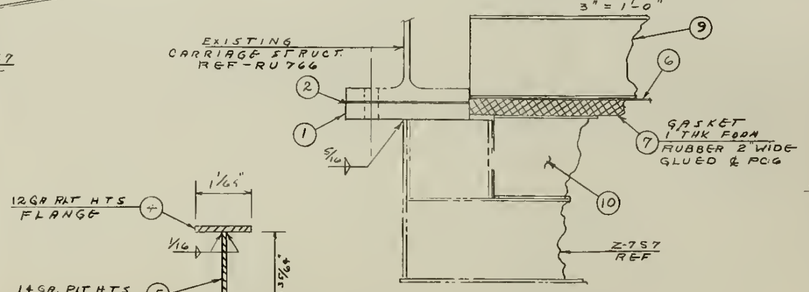

STRINGER DET.

SECTION B-B
SCALE 3"=1'0"

DRAWN BY		
TRACED BY	FOREMAN	
CHECKED BY	Norrell	
DESIGN NUPVA	F Howell 9/14/63	
ENGINEERING NUPVA		
BRANCH NUPVA	9/14/63	

NORFOLK NAVAL SHIPYARD PORTS., VA.

U.E.R.D. NO.	REV.
WP-157 R.U. NO. 804	A
SCALE: NOTED SHEET 1 OF 1	

APPROVED
DIVISION HEAD — PROJECT OFFICER — DATE 9/14/63